8-18-2016 12:00 AM

# Formulation and Process of Powder Coating for Solid Oxide Fuel Cell Interconnects

Yandaizi Zhou
*The University of Western Ontario*

Supervisor
Jesse Zhu
*The University of Western Ontario*

Graduate Program in Chemical and Biochemical Engineering
A thesis submitted in partial fulfillment of the requirements for the degree in Master of Engineering Science

# Abstract

Solid oxide fuel cell (SOFC) interconnects, which are made of chromia-forming ferritic stainless steels, are used to connect individual SOFCs in series to increase the overall cell voltage output. They are usually exposed to high operating temperature (around 800ºC) and both oxidative and reductive atmosphere. $Mn_{1.5}Co_{1.5}O_4$ (MCO) spinel is used for SOFC interconnect coating to decrease the oxidation rate and the chromium migration, and to increase the SOFC lifetime. The current preferred coating method is air-plasma spray (APS) which has transfer efficiency of only around 40%, and is relatively expansive. The objective of this project is to develop powder coating technology as an alternative in SOFC interconnect coating, given its environmental friendliness, recyclability and cost-effectiveness.

However, the key problems of powder coating techniques are how to make MCO powder well dispersed in polymer matrix (also known as coating binder, i.e. the resin and corresponding curing agent) and to form uniform film after binder burn off.

Four techniques of mixing and dispersing MCO powder were investigated in this project. Slurry powder coating showed a big tendency to form a good film, a further optimization is needed. Both thermally compacted and cold pressed powder coatings showed poor quality and severe defects of non-uniformity. The formed film by extruded powder coating exhibited excellent adhesion, moderate hardness and high gloss. This technique is the best of four and is used for SOFC interconnect testing.

For SOFC interconnects by extruded powder coating, thickness of the coating observed by cross-section analysis was fairly uniform, which is a key advantage of this technique. But a significant change in coating morphology was observed after thermal treatment, mainly due to the high dosage of binder used in the formulation. Extruded powder coating is promising but needs to be further optimized for SOFC application.



## Keywords

Powder coating, slurry, SOFC interconnect, $Mn_{1.5}Co_{1.5}O_4$, formulation, electrostatic spray, polyester/TGIC, epoxy

# Acknowledgments

Firstly, I would express my greatest gratitude to my supervisor, Prof. Jesse Zhu, who has 21 years' experiences in the research fields of particle fluidization and powder coating technology. I am very thankful for the opportunities he provided to me and I have learnt lots of experimental skills, abilities of thinking and problem solving, and also the enormous knowledge which will benefit me forever. His guidance and encouragement ensured the finish of this study, and I am very grateful to his help.

I also want to express my appreciation to my co-supervisor, Dr. Hui Zhang. He helped me overcome many challenges during this program. He is full of experience in powder coating technology and I will benefit from his instructions for the rest of my life.

In addition, I would also like to thank Mr. Shuai Yang, who have spent a lot of time on working with me and helped me a lot in the experiments. He is knowledgeable and helps me solve many problems. And also, much appreciation is extended to Danni Bao and Shan Gao for their suggestions and recommendations for my study.

Moreover, NSERC and Stackpole International (SI) also played important roles in this program. Without their strong financial and characterization technical support, this study would hardly be successful.

Finally, I want to thank my dear father Gaoping Zhou and my dear mother Qinxia Yan for their love and support during my study. And also I would like to thank my boyfriend Zhiwei Zhao for his understanding and contributions.

# Table of Contents

# List of Tables

# List of Figures

# List of Appendices

# Chapter 1

# 1 General Introduction

## 1.1 Introduction

Solid oxide fuel cell (SOFC) is a solid-state power generation system and is an increasingly attractive way for energy conversion because it is highly efficient and environmentally friendly [1-4]. In order to increase the overall cell voltage output, interconnects are used to connect individual SOFCs in series to create a stack. Chromia-forming ferritic stainless steels are considered among the most promising materials for interconnects due to their electrically oxide scale, thermal expansion matching with conventional SOFC components and low cost. However, the high oxidation rate and the formation of volatile gaseous Cr species such as $CrO_3$ (g) and $Cr(OH)_2O_2$ (g) at the operating temperatures (600~800 °C) of chromium based alloys will result in the degradation of SOFCs. Spinel coating, $Mn_{1.5}Co_{1.5}O_4$ (MCO), is the most effective way to solve this problem due to its excellent ability to reduce Cr volatility. The current preferred coating method is air-plasma spray (APS) which has transfer efficiency of only around 40%, and the APS equipment cost is relatively high. Therefore, there is a need to develop a more economical alternative. Powder coating is a promising technology as it is environmental friendly, recyclable and offering low cost.

Powder coating is an advanced technology, and it is directly coated onto substrates without using any organic solvent. It has some significant advantages over traditional liquid coating or conventional plasma spray. As the emission of the process is negligible, it is environmental friendly. Costs are also lowered because it cuts cost of solvent and has high transfer efficiency. Last but not least, most of the powder coating overspray can be collected and re-used.

However, there are several challenges that powder coatings and their application have faced. One of the challenge is the limitation of particle size. Particles with mean particle size above 30 μm are defined as coarse powder, which cause a relatively poor surface quality when being electrostatically sprayed. And also the film built with coarse powder

is normally over 60 μm. On the other hand, fine powder with average particle size below 30 μm allows a much smoother surface and a thinner film. But fine powders are not easy to utilize because of their cohesive nature. In fluidization process, the cohesiveness of the powder can create plugging or sever channeling [5], leading to non-uniform of powder deposition.

Another problem affecting the utilization of powder coating for SOFC interconnects is the limitation of pigment/binder ratio. The pigment volume concentration (PVC) is crucial to coating formulation, as it governs the dispersion of pigments in a polymer matrix [6] and affects melt viscosity of powder which further influences the finish quality of the coating. The inadequate flow of the coating with poorly dispersed pigment is accompanied by much higher viscosities, since in the case when the pigments are not completely wetted by the binder, the intermolecular attraction forces between the pigment particles will immobilize the system, leading to orange peel and other defects on the coating [7].

For SOFC interconnects, the coated interconnects will further experience oxidation and reduction processes at around 800 °C. Before sintering, the substrate coated by the “green coating” (thermally cured but not sintered coating on the substrate) should have some properties including: good adhesion, appropriate hardness, required film thickness and good film uniformity. To replace the conventional techniques by powder coating for SOFC interconnects, we have to develop new formulations that can fulfill all the requirements of SOFC interconnects. A comprehensive study on the new types of powder coating is undoubtedly needed.

## 1.2 Objectives

The research aims to use innovative powder coating approaches to replace the expensive plasma coating on SOFC interconnects. The objectives of this research are outlined as follow.

(1) Formulations of slurry powder coating

- To investigate formulations of slurry powder coating

- To optimize the formulation by changing pigment/binder ratio and adding PVA resins to enhance the film quality.

(2) Formulations of “thermally compacted” and “cold pressed” powder coatings

- To investigate formulations of thermally compacted powder coating
- To investigate formulations of cold pressed powder coating
- To optimize the formulation of cold pressed powder coating.

(3) Formulations of extruded powder coating

- To investigate formulations of extruded powder coating
- To study the effect of different voltages for electrostatic spray on film properties.

(4) Application of powder coating technology to SOFC interconnects

- To apply cold pressed powder coating to SOFC interconnects and to evaluate film quality by surface morphology, cross-section analysis and EDS analysis
- To apply extruded powder coating to SOFC interconnects and to evaluate film quality by surface morphology, cross-section analysis and EDS analysis.

## 1.3 Thesis structure

This thesis contains eight chapters and follows the “Monograph-Article” format as outlined in the Thesis Regulation Guide by the School of Graduate and Postdoctoral Studies of the University of Western Ontario. It is organized in the following structure.

- Chapter 1 gives a brief introduction to the background of this study and provides a research proposal. It states research objectives, thesis structure and the major contributions of the present study.

- Chapter 2 provides a detailed review of Solid Oxide Fuel Cell (SOFC) interconnects, current materials and techniques for coating SOFC interconnects and powder coating. The advantages and limits of powder coating technology are also discussed.

- Chapter 3 summarizes the experimental materials, equipment and methods that were used in this work. The operation of equipment, powder characterization and film quality evaluation techniques employed in the present study are detailed in the experimental section.

- Chapter 4 reports the formulation of slurry powder coating technique. Initial formulation is proposed and the optimization of the formulation are also investigated, including the effects of pigment/binder ratio and adding PVA resin on film quality.

- Chapter 5 discusses formulation of “thermally compacted” and “cold pressed” powder coating techniques. Formulations containing different types of resins and different particle sizes of MCO powder are investigated.

- Chapter 6 reports the formulation of extruded powder coating technique, and the effect of different voltages for electrostatic spraying is also discussed.

- Chapter 7 describes the application of powder coating techniques to SOFC interconnects. Techniques of cold pressed powder coating and extrude powder coating are discussed. Evaluations of finish quality are also conducted including surface morphology, cross-section analysis and EDS analysis.

- Chapter 8 summarizes the work, provides general conclusions and gives a list of recommendations for future work.

## 1.4 Major contribution

The present study explored the use of powder coating technology in SOFC interconnects, and a powder coating formulation and its manufacture method has been developed.

# Chapter 2

# 2 Background and literature review

## 2.1 Introduction of Solid Oxide Fuel Cell

Today the increasing concern about the environmental consequences of burning fossil fuels has initiated researchers to seek alternative technologies. As is pointed out, global warming is taking place due to effluent gas emission, mainly $CO_2$. During the past century, global surface temperature has increased at a rate near 0.6 °C per century [8]. Table 2-1 shows the total $CO_2$ emissions of the top 15 nations [9]. Global warming is not the only problem caused by energy supply, other environmental issues such as air pollution, ozone depletion, forest destruction and acid precipitation are also due to the use of fossil fuels and these all have attracted public attention.

Fuel cells are one of the most effective and efficient ways to solve the environmental problems that we face today. Electrical energy is produced by electrochemical reactions combining a fuel with an oxidant to produce power, heat, water and possibly carbon dioxide depending on the fuel [10]. Without the need of combustion as an intermediate step, fuel cells give much higher conversion efficiencies compared to conventional thermomechanical methods, and harmful emissions accompanied by burning of fossil fuels such as $NO_x$, $SO_x$ and $CO_2$ are greatly reduced.

**Table 2-1: Global emission of the top 15 nations by total $CO_2$ volume (billions of tonnes) [9]**

| Rank | Nation | $CO_2$ | Rank | Nation | $CO_2$ | Rank | Nation | $CO_2$ |
|---|---|---|---|---|---|---|---|---|
| 1 | USA | 1.36 | 6 | India | 0.19 | 11 | Mexico | 0.09 |
| 2 | Russia | 0.98 | 7 | UK | 0.16 | 12 | Poland | 0.08 |
| 3 | China | 0.69 | 8 | Canada | 0.11 | 13 | S.Africa | 0.08 |
| 4 | Japan | 0.30 | 9 | Italy | 0.11 | 14 | S.Korea | 0.07 |
| 5 | Germany | 0.27 | 10 | France | 0.10 | 15 | Australia | 0.07 |

A typical fuel cell consists of an anode, a cathode and an electrolyte, as shown in Figure 2-1 [11]. As most individual fuel cells are small in size and produce between 0.5 and 0.9 volts of DC electricity [12], they are typically connected in series by interconnect plates

to create a fuel cell stack to increase the overall fuel cell voltage. The interconnect plates contain flow channels for the purpose of the fuel supply on the anode side and air supply on the cathode side. Fuel cells are generally classified by the chemical characteristics of the employed electrolyte material, as summarized in Table 2-2 [11].

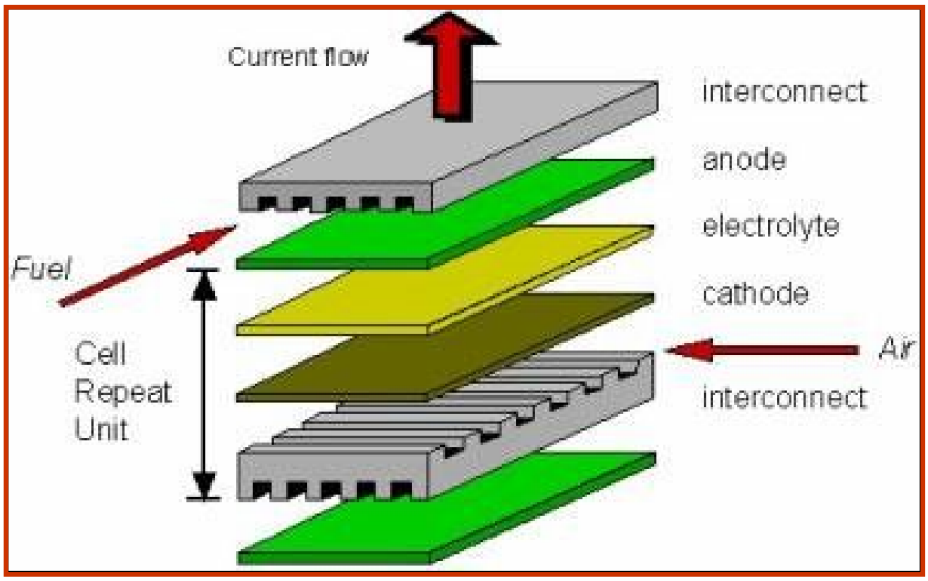


**Figure 2-1: Schematic representation of a Planar Fuel Cell [11]**

**Table 2-2: Types of fuel cells [11]**

| | PAFC | MCFC | SOFC | PEMFC |
|---|---|---|---|---|
| Electrolyte | Phosphoric Acid | Molten Carbonate Salt | Ceramic | Polymer |
| Operating Temperature | 375°F (190°C) | 1200°F (650°C) | 1830°F (1000°C) | 173°F (80°C) |
| Fuels | Hydrogen ($H_2$) Reformate | $H_2$/CO Reformate | $H_2$/CO/$CH_4$ Reformate | $H_2$ Reformate |
| Reforming | External | External/Internal | External/Internal | External |
| Oxidant | $O_2$/Air | $CO_2$/$O_2$/Air | $O_2$/Air | $O_2$/Air |
| Electrical Efficiency (HHV) | 40-50% | 50-60% | 45-55% | 40-50% |

Among the different types of fuel cells, solid oxide fuel cells (SOFCs) are attractive and promising which represent one of the most environmentally clean ways of energy generation. Table 2-3 shows a typical SOFC air emissions [13]. SOFCs have many benefits with respected to other fuel cells [10-12,14]. One of the most attractive

advantages is the high conversion efficiency with the ability to achieve up to 50% electrical efficiency and more than 80% total efficiency. In addition, they are flexible in choosing fuels such as carbon-based fuels including natural gas, liquefied petroleum gas, diesel and biogas. Moreover, they are more economical due to the simplified process and high conversion efficiency. Generally, they are made from available ceramic materials which do not present any moving parts or corrosive liquid electrolytes, and also SOFCs do not contain noble metals which are expensive and are not readily available. Because of their high operating temperatures (~1000 °C), high quality heat byproduct is produced for co-generation or combined cycle applications. And any CO produced is converted to $CO_2$ at the high operating temperature resulting in extremely low emissions. What is more, SOFCs have a theoretically longer life expectancy of more than 40000-80000 h.

**Table 2-3: Typical SOFC air emissions from one year of operation**

| Air emissions[a] | $SO_X$ | $NO_X$ | CO | Particles | Organic compounds | $CO_2$ |
|---|---|---|---|---|---|---|
| Fossil fuelled plant | 12,740 | 18,850 | 12,797 | 228 | 213 | 1,840,020 |
| SOFC system | 0 | 0 | 32 | 0 | 0 | 846,300 |

[a] kgs of emission per 1650 MWh from one year full operation

The operating principle of the solid oxide fuel cell is illustrated in Figure 2-2. A SOFC consists of two electrodes sandwiched around a dense oxygen ion conducting electrolyte. Hydrogen fuel is fed into the anode side and oxidized. Oxygen, from the air, enters the cathode side and is reduced. At the anode, oxygen ions leave the electrolyte and react with the fuel, releasing electrons ($e^-$). At the cathode, an oxygen concentration gradient is created across the electrolyte providing a driving force for the motion of oxide ions from the cathode to the anode. Also an electrical connection between the cathode and the anode allows electrons to flow from the anode to the cathode, maintaining overall electrical charge balance, thereby generating electrical power. The only product of this process is pure water and heat [12,14].

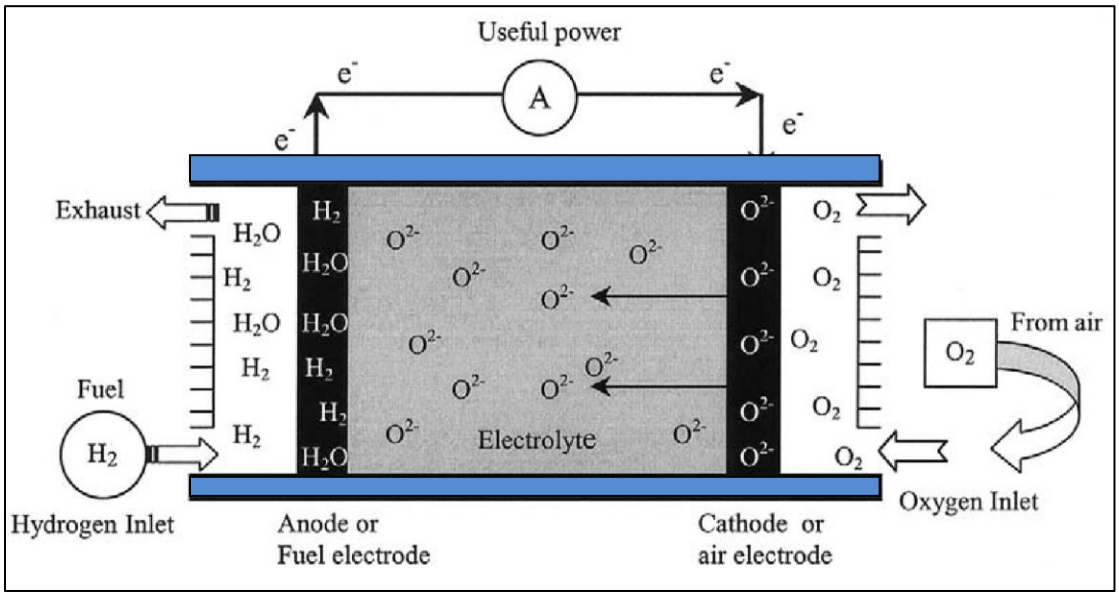


**Figure 2-2: Concept diagram of SOFC based on oxygen-ion conductors [12]**

The SOFC reactions include:

Anode side: $H_2 + O^{2-} \rightarrow H_2O + 2e^-,\ CO + O^{2-} \rightarrow CO_2 + 2e^-,$

$$CH_4 + 4O^{2-} \rightarrow 2H_2O + CO_2 + 8e^- \ (Fuel\ containing\ hydrogen)$$

Cathode side:$O_2 + 4e^- \rightarrow 2O^{2-}$

In order to lower the manufacturing cost of SOFCs, current research efforts have been focused on reducing the cost of each SOFC component. Figure 2-3 shows SOFC materials cost distribution, summarized by TIAX LLC in 2004 [15]. The anode and interconnect materials contribute to more than 90% of the total cost, so now more researchers are devoted to developing high-quality and low-cost interconnects in order to reduce the overall fabricating cost.

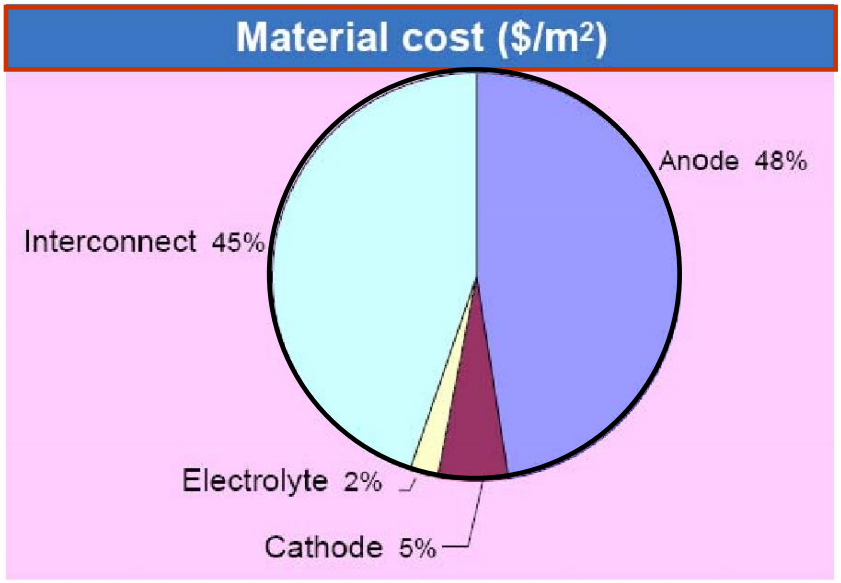


**Figure 2-3: SOFC materials cost distribution [15]**

## 2.2 Introduction of Solid Oxide Fuel Cell

### 2.2.1 SOFC interconnect materials development

Interconnects are used to connect individual SOFCs in series to create a stack that increases the overall cell voltage output, and they also protect the cathode from the reducing environment on the anode side. Moreover, they also have a structural role to keep the stack solid and transportable. As interconnects have multiple functions in the SOFC stack, the materials used for SOFC interconnects are required to have the following characteristics [16-18]:

- Interconnect must have excellent electrical conductivity which can reach nearly 100% electronic conduction at the high operating temperature and atmospheres. The extremely high electronic conductivity indicates that not only the electronic transference number should be high, but also the absolute magnitude of the electrical conductivity should be reasonably large. The acceptable area-specific resistance (ASR) level should be lower than 100 $m\Omega/cm^2$.
- Adequate stability in terms of dimension, microstructure, chemistry and phase at operating temperature around 800 °C in both reducing and oxidizing atmosphere are required for interconnect materials since they are exposed to air (or oxygen) on one

side and fuel on the other side.

- Interconnect should demonstrate excellent imperviousness for oxygen and hydrogen to prevent direct combination of oxidant and fuel during fuel operation.
- The thermal expansion coefficient (TEC) of interconnects should be compatible with electrolyte and electrodes, around $10.5\times10^{-6}$ /K, so that the thermal stress developed during stack startup and shutdown could be minimized.
- No reaction or inter diffusion between interconnect and its adjoining components is allowed to occur under operating conditions.
- Interconnect should exhibit fairly good thermal conductivity, around 5 W/(m.K), excellent oxidation, sulfidation, carburization resistance, adequate strength and creep resistance at elevated temperature.
- Interconnect should be easy to fabricate, and the cost of raw materials as well as fabrication processes for interconnect are also desired to be as low as possible so that they will be easy to commercialize.

(1) Ceramic Interconnects

Over the past several decades, ceramic interconnects with perovskite structure have been intensively studied. Lanthanum chromite ($LaCrO_3$), a kind of complex metal oxide, is currently the most common material used for SOFC interconnects, as it exhibits fairly high electronic conductivity in both reductive and oxidative atmospheres, suitable stability in the fuel cell environments as well as reasonably good compatibility with other cell components. Practically, $LaCrO_3$ is usually doped at lanthanum or chromium or both sites of perovskite block unit in industrial applications in order to improve the electrical conductivity and modify the TEC. It naturally turns out that the electrical conductivity of doped $LaCrO_3$ in reducing atmosphere like hydrogen is significantly lower than that in oxidizing atmosphere like air [19]. Fortunately, the overall conductivity of the doped $LaCrO_3$ is still sufficient when the operating temperature is above 800 °C [20]. As the temperature drops below 800 °C, the electrical conductivity of the doped $LaCrO_3$ is reported to experience a substantial decline [21]. Many researchers have studied on the effects of several dopants incorporated into the $LaCrO_3$ ceramic. Cobalt doping dramatically increases the electrical conductivity, however, the TEC also increases

significantly [22,23]; iron doping slightly improves the electrical conductivity while lowering TEC [24]; nickel doping shows a significantly increase in electronic conductivity and a transition to a metallic conductor typical for $LaNiO_3$, unfortunately, the stability and solid solution limit are considerably lower than cobalt and iron counterparts [25]; magnesium doping enhances electrical conductivity but hardly changes the TEC [26]; Copper doping improves both electrical conductivity and TEC [27]; strontium and calcium doping drastically enhance electrical conductivity, while TEC is also considerably increased [28,29].

However, the extremely inferior sintering behavior in air due to the easy volatilization of Cr species becomes a major problem to mass production of ceramic interconnects such as $LaCrO_3$ or doped $LaCrO_3$. The poor sinterability of $LaCrO_3$-based ceramics has been attributed mostly to the development of a thin layer of $Cr_2O_3$ at the interparticle neck at the initial stages of firing [30]. Moreover, chromium evaporation leading to chromium deficient composition will hinder sintering. Another problem that should be noted is the high cost and warping.

(2) Metallic Interconnects

Metal materials were initially proposed to replace ceramic interconnects in order to address the acute problems related to ceramic interconnects. Obviously, metallic interconnects have many advantages over ceramic interconnects [18]. Firstly, the electrical conductivities of metallic interconnects are generally several orders of magnitude larger than those of doped $LaCrO_3$ ceramics. Hence, the ohmic losses in metallic interconnects are small enough to be neglected. Secondly, the electrical conductivity of metallic interconnects is independent of oxygen partial pressure which is different with ceramic interconnects. The working temperature of metallic interconnects can be reduced to 600 °C ~800 °C, solving the problem of thermal expansion mismatch between metallic interconnects and the rest of ceramic SOFC components. What is more, because of their low cost, easy manufacture and good workability, metallic interconnects are more attractive than ceramic interconnects.

Currently, metallic materials can be divided into 3 groups:

- Chromium based alloys: they are attractive because they have moderate oxidation resistance and reasonably good corrosion resistance due to the formation of $Cr_2O_3$ scale. In addition, the binary metal oxide $Cr_2O_3$ has comparatively large electronic conductivity [31]. What is more, the thermal expansion behaviors of these alloys are similar to that of other ceramic components in the temperature range of 25 °C to 1000 °C. However, the drawbacks of chromium based alloys are their high oxidation rate and the formation of volatile gaseous Cr species such as $CrO_3$ (g) and $Cr(OH)_2O_2$ (g) at the operating temperatures [32,33]. These species have been shown to diffuse into and interact with electrodes due to their large vapor pressures, resulting in a change in the air electrode composition and formation of new phases [33].
- Iron based alloys: they are favored over chromium based ones because of their high ductility, low cost and easy machinability. Currently, there are two kinds of iron based alloys being explored due to their relatively low TECs, Fe/Cr/Mn and Fe/Cr/W. Chromium improve the formation of $Cr_2O_3$ scale while manganese addition enhance surface scales comprising the spinel $Cr_2MnO_4$ or a spinel layer on the top of an inner $Cr_2O_3$ layer. However, the major problem of iron based alloys is still chromium volatilization. Even newly developed ferritic alloys such as SS441 and Crofer 22 APU cannot completely eliminate the chromia scale growth and chromium evaporation into cells which leads to unacceptable degradation in the SOFC electrochemical performance [34,35].
- Nickel based alloys: they consist of nickel, chromium, iron and manganese which are resistant to high temperature. They have some apparent advantages such as slower oxidation kinetics and larger thermal expansion coefficients.

### 2.2.2 Coating materials for SOFC interconnect

Ferritic stainless steels (SS) are widely used as interconnects because of their reasonable electrically conductivity, good thermal expansion behavior and low cost [36-39]. However, the most important problem that should be handled is the degradation of the performance of SS interconnects due to evaporation of chromium species caused by reaction with water vapor and gradual oxidation [40-43]. In order to prevent the

chromium vaporization in the cathode side, as well as to reduce the rate of scale growth on the surface of chromium-forming alloys, coating technology has been proposed and presently is being extensively investigated.

Ceramic coating, particularly perovskite and spinel types, are commonly employed for surface protection. Perovskite materials deposition [44-50] has comparatively high conductivity with reasonably thermal expansion match. But their low thermochemical stability during thermal cycling caused by diffusion of chromium cations is challenging [38,51,52]. It has been determined that electronically conducting $LaMnO_3$ and $LaCrO_3$-based coatings are most stable, as they transport no oxygen ions to the metal surface, which accelerates corrosion [44-47]. In contrast, spinel coating with relatively good electrical conductivity has a low Cr migration rate. The family of materials, namely $(A,B)_3O_4$ oxides, has proven to be the spinel family which present reasonable CTE match to stainless steels (7~15 ppm/$^oC$), and also have limited electronic conductivity (3 mS/cm to 60 S/cm) [53,54]. Among different spinels, $(Mn,Co)_3O_4$ are the most promising due to their high electrical conductivity (60 S/cm at 800 $^oC$), low contact resistance, good CTE ($11.5 \times 10^{-6}$ /K, 20~800 °C) match with the cathode materials and ferritic stainless steel interconnects, and excellent ability to reduce Cr volatility [51,52,55].

Chen et al. [56] studied protective coating on stainless steel (SS) interconnect for SOFCs in 2004, and the coating is essentially a Mn-Co-O spinel. The research showed that the effective, dense and well adherent coating resulted in significantly reducing the oxidation rate of SS interconnect at elevated temperatures. The area specific resistance (ASR) was approximately 0.5 Ω $cm^2$ after 50,000h in air at 800 °C, and the Mn-Co spinel coating could greatly reduce the $Cr_2O_3$ sub-scale formation, lower the thermal expansion mismatch and increase the electronic conductivity of the scale. Yang et al. [57] showed that the $Mn_{1.5}Co_{1.5}O_4$ spinel barrier layer on ferritic stainless steel Crofer 22 APU stopped chromium migration and deceased oxidation, while promoting electrical contact and minimizing cathode/interconnect interfacial resistance. Hall et al. [10] demonstrated that $(Mn,Co)_3O_4$ spinel was shown to be sufficient to mitigate chromia diffusion and oxidation. Mirzaei et al. [58] utilized nanostructure $MnCo_2O_4$ powder with average crystallite size of 60 nm and studied the effects of the coating on SOFC interconnects.

The results showed that improved oxidation resistance and better electrical conductivity of the stainless steel substrate were attained in the presence of electrophoretic deposited $MnCo_2O_4$ coating.

## 2.3 Current coating techniques for SOFC interconnect

### 2.3.1 Electrophoretic deposition

Electrophoretic deposition (EPD) is particularly an attractive method because it is a simple and inexpensive procedure with potential of precise adjustment of thickness and morphology of deposits [59,60]. The electrophoretic deposition of Mn-Co spinels has already been investigated in details [51-52,61-63]. Hall et al. [10] studied the effect of Mo-Co coating on stainless steel interconnect by electrodeposition method. CoMn alloy coatings were electrodeposited onto 5 cm x5 cm T441 stainless steel substrates. The coatings were electrodeposited in an electrochemical cell designed to facilitate uniform flow across the surface of a flat substrate. Mirzaei et al. [58] employed electrophoretic deposition method to prepare a Mn-Co spinel coating on ferritic stainless steel substrates. In the experiment, cathodic electrophoretic deposition was performed in a glass cell with 50 cc volume. The counter electrodes (SS) were inserted in parallel of the cathode at a distance of 10 mm. Ethanol (99.99%) with 10 g/l spinel powder was adopted as EPD suspension, then 0.15 g/l iodine was added into the suspension to increase the deposition rate. The EPD suspension was homogenized for 10 min in an ultrasonic bath. A DC voltage power source at two constant voltage of 30 V and 60 V were used. The deposition time varied in the range of 60 s to 360 s. The schematic diagram of EPD is shown in Figure 2-4.

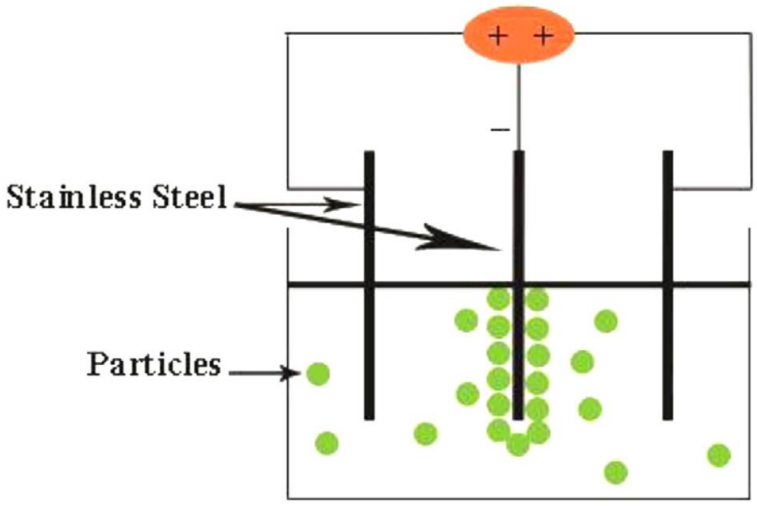


**Figure 2-4: Schematic view of EPD setup to prepare spinel coating on SS substrate**

### 2.3.2 Metal organic chemical vapor deposition

Piccardo et al. [64] employed Metal organic chemical vapor deposition (MOCVD) method to create coatings on substrates. This technique resulted in oxide films of about 100~200 nm thick [65-67]. MOCVD promotes formation of conductive perovskite oxides, and to retain chromium inside a mechanically and chemically resistant surface layer via reduced Cr surface diffusion [68-69]. Fontana et al. [70] deposited $La_2O_3$, $Nd_2O_3$ and $Y_2O_3$ coatings on different metallic alloys by MOCVD technique in order to form perovskite oxides at high temperature.

The multi-sources MOCVD apparatus is shown in Figure 2-5. It consists of:

- Three metal organic sources (A, B, C);
- A quartz reactor heated by infrared (IR) furnace;
- A vacuum system allowing the MOCVD process at low pressure;
- Mass flow meters to control $N_2$ (carrier gas for precursors) and $O_2$ flow rates.

The samples are placed horizontally on a metallic sample holder inside the cold-wall reactor. In the IR-heated reactor, precursors are pyrolyzed inside a small volume, just above the heated substrate. Nitrogen gas is used as carrier gas for metal organic precursors. Oxygen is used as oxidant and is incorporated to the main flow via an

intermediate mixing chamber. The gaseous mixture is then directed to the reaction chamber through a nozzle. The precursor delivery lines are heated and maintained at a temperature higher than the source evaporation line, to prevent condensation of the metal–organic vapor phase [70].

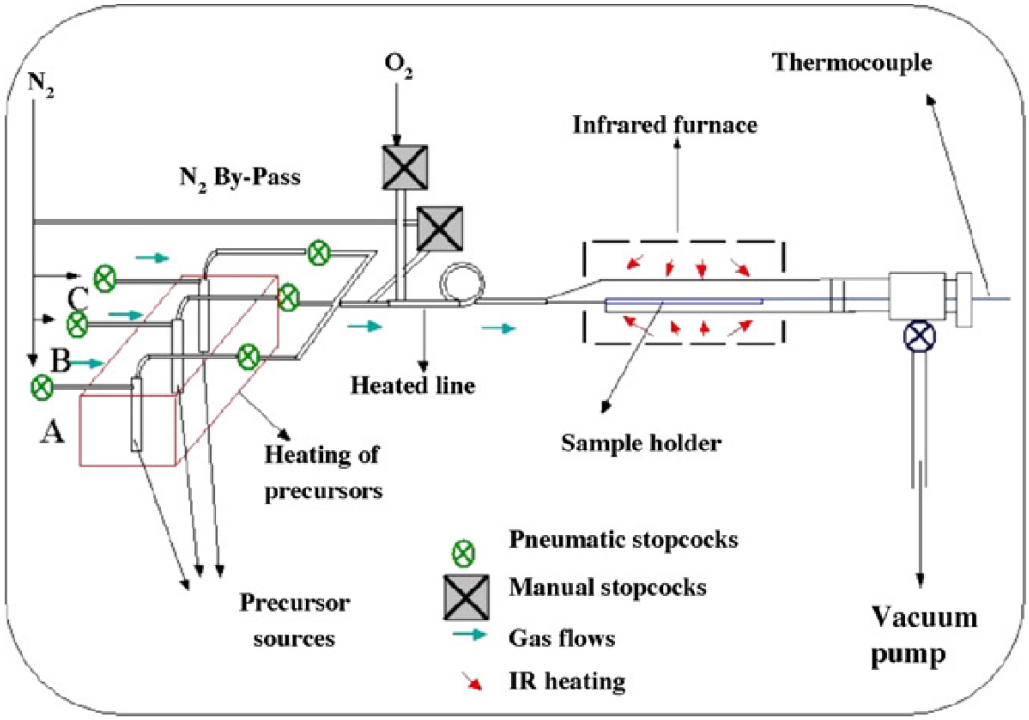


**Figure 2-5: Diagram of the MOCVD apparatus**

### 2.3.3 Air plasma spray

Air plasma spray (APS) is the most widely used method of applying perovskite coatings [46,71-74]. It can be widely used for commercial coating applications, including thermal barrier coatings as well as powder metallurgy derived SOFC interconnects. APS technique has already been investigated to apply the MCO protective coating layer onto metallic substrates [75].

Air plasma spray is a promising method, offering scalability and cost effective manufacturing for SOFC applications. Plasma spray is a direct melt-spray-deposition process in which powdered feedstock is injected into high temperature thermal plasma

and propelled towards a prepared substrate at high velocity. The coating is built up by successive impingement and rapid solidification of the impacting droplets (splats). The process allows significant material versatility and application flexibility as wide ranging alloys and oxides can be deposited on to numerous substrate and component types. The inherent scalability of the process, along with the ability to apply coatings at near ambient substrate temperatures, has enabled plasma spray to be a highly competitive and cost effective materials manufacturing technology [76]. The schematic diagram of APS is shown in Figure 2-6.

The coatings by APS are reasonably dense, and very stable, showing almost no degradation with time. But the film is very thick, and the overspray consideration makes the process expensive. So this technique should be further developed to be able to achieve thinner layers and overcome line-of-sight deposition issues.

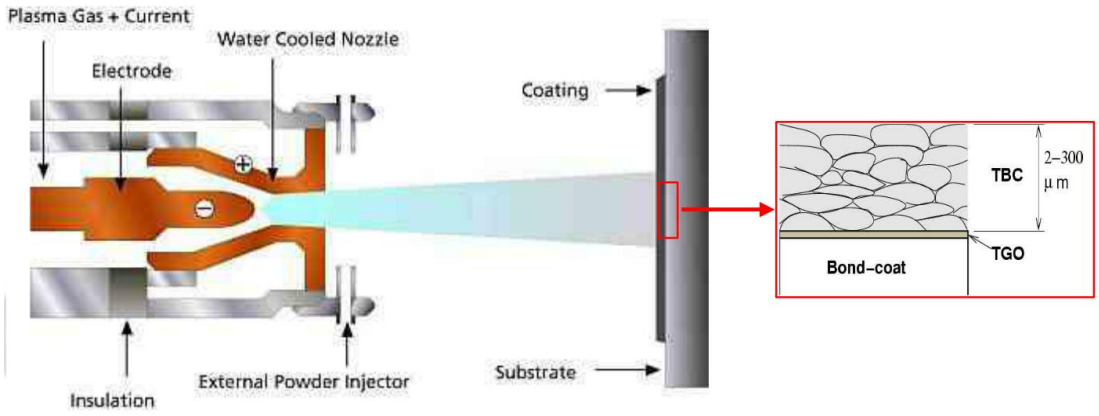


**Figure 2-6: Schematic diagram of APS**

## 2.4 Powder coating

Powder coating is a novel and attractive technology which has already attracted much attention. It is much favored over traditional liquid coating as it is an environmentally friendly method by which powder is directly coated onto a substrate without using any organic solvents, thereby this process does not emit any polluting volatile organic compounds into the atmosphere. In addition, the processes like venting, filtering and solvent recovery which are necessary with liquid coating are not required for powder

coating, so it is easy to operate and manufacture. Moreover, it is recyclable since the over-sprayed powder can be easily collected and re-used. Thus it is more cost-effective compared to liquid coating [77,78].

Powder coating technology originated in the 1950s. The coating application methods can be divided into two groups: powder is sprayed electrostatically onto a substrate; the substrate is dipped into a fluidized bed of suspended powder. In the spray process, powder adheres onto the substrate by electrostatic force, while in the fluidized bed process, powder adheres onto a preheated substrate. During the further curing process in an oven, particles flow to form a strong and adhering film [78].

During the past two decades, applications associated with powder coating have experienced a significantly growth and this new technology has been widely used both in industrial and consumer related markets. Both ecological and economic advantages result in the success of powder coating. The development of new formulations and the improvement of advanced equipment and application processes create many new market opportunities for powder coating technology [79]. Presently, it has been applied into many fields, including furniture, architectural, building materials and even automotive industry.

In general, materials used for powder coating are divided into thermoplastic and thermosetting. Both of them melt and flow to form a film when being heated. The thermoplastic powders persist in same chemical composition after cooling [80], which means that they can be re-melted if exposed to heat again. However, the thermosetting powders will be subject to the cross-linking reaction within themselves or other reactive components, resulting in much higher molecular weight products [81]. And they cannot be re-melted as the thermoplastic ones.

### 2.4.1 Thermoplastic powder coating

Generally, thermoplastic powders are high molecular weight polymers which can be manufactured relatively simply and do not involve complex curing mechanisms. However, they have some weaknesses such as high temperature of fusion, low

pigmentation level, poor solvent resistance and bad adhesion on metal surface. These problems were successfully overcome later on by the thermosetting powders which replaced the thermoplastic powder coating and quickly took the largest part (90%) of the market [82]. Thermoplastic materials for powder coating include polypropylene, nylon, vinyl, polyvinyl chloride (PVC), polyethylene, thermoplastic polyester and polyvinylidene fluoride (PVDF). Characteristics of some typical thermoplastic powders are shown in Table 2.4.

**Table 2-4: Characteristic of various thermoplastic powders [83]**

| | Vinyl | Polyester | Nylon | Polyethylene |
|---|---|---|---|---|
| Exterior Durability | Excellent | Very Good | Good | Excellent |
| Hardness | Excellent | Good | Excellent | Fair |
| Flexibility | Excellent | Fair | Very Good | Excellent |
| Corrosion Protection | Excellent | Good | Very Good | Good |

Thermoplastic polyester powder coatings [82] using thermoplastic polyesters as binders are prepared from linear high molecular weight polymers produced by polycondensation of dibasic acid and diols. There are two methods to produce high molecular weight polyesters: direct esterification and transesterification. The equations are shown in Figure 2-7.

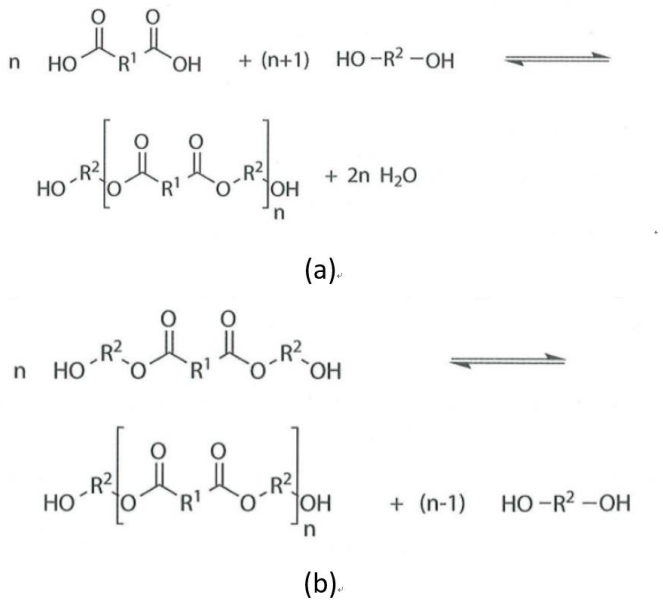


**Figure 2-7: Chemical reaction equations of high molecular weight polyester formation: (a) direct esterification; (b) transesterification**

Since the film forming process of thermoplastic polyester coatings does not involve any additional increase in molecular weight, in order to obtain a coating with good mechanical properties, it is necessary to start with a polyester resin with a relatively high molecular weight. For such applications typical molecular weights are higher than 15,000 g/mol.

The ability to crystallize is another important characteristic of thermoplastic polyester resins, since it is related to melting point, which determines the stoving temperature range of the coating during application. For example, the melting point of crystalline polyethylene terephthalate is 256 °C, however, polyethylene isophthalate with much lower degree of crystalline has a melting point of 108 °C, while the fully amorphous polyethylene orthophthalate melts at a temperature of only 63 °C [84].

When thermoplastic polyester resins are used as binders alone, they have poor adhesion to the substrate, leading to crack formation upon rapid cooling or bending and matt gloss. So thermoplastic polyester resins should have a certain degree of crystallization when cooled down to room temperature, after the fusion of powder particles has been

completed. The degree of crystallization is important to obtain surface hardness and a reasonably high service temperature of the coating. Oppositely, too high a crystallinity will reduce adhesion to the substrate due to an increase in the cohesion energy during crystallization.

### 2.4.2 Thermosetting powder coating

Generally, thermoplastic powder coatings have very poor adhesion on metal surfaces in spite of using high molecular weight resins. This problem can be solved by the thermosetting polymers. During the film forming process based on thermosetting polymers, crosslinking reactions take place, leading to the increase of molecular weight. Therefore, polymers with much lower molecular weights and consequently lower melt viscosities can be used. The cured film after crosslinking reactions exhibits exceptional resistance to solvents and good mechanical strength. The resins used to make thermosetting powders are epoxy, polyester and acrylic. There are generally five types of powder coating materials derived from these three resins: epoxy, epoxy-polyester, polyester-TGIC (Triglycidyl isocyanurate), acrylic-urethane and polyester-urethane [83]. Characteristics of some typical thermosetting powders are show in Table 2-5.

**Table 2-5: Characteristic of various thermosetting powders [83]**

| Properties | Epoxy | Polyester-Urethane | Polyester-TGIC | Acrylics |
|---|---|---|---|---|
| Exterior Durability | Poor | Very Good | Excellent | Excellent |
| Hardness | Excellent | Very Good | Excellent | Excellent |
| Flexibility | Excellent | Very Good | Excellent | Fair |
| Corrosion Protection | Excellent | Very Good | Excellent | Fair |

The low molecular weight binders are transformed into crosslinked polymers via crosslinking reactions during film forming process. The crosslinked polymers exhibit desirable physico-chemical and mechanical properties. In fact, the uncured thermosetting powder coatings with low flexibility, poor impact resistance and solvent resistance are far below the standard levels o industrial coatings. The main purpose of crosslinking reactions is to increase the toughness and chemical resistance of the coatings.

(1) Thermosetting epoxy powder coating [82]

Epoxy coatings were introduced in the market in the late 1950's as the first thermosetting powder coatings. Epoxy resins can be divided into two types: bisphenol A and novolac. The overall reaction for the manufacture of bisphenol A epoxy resins can be presented in a simplified way in Figure 2-8.

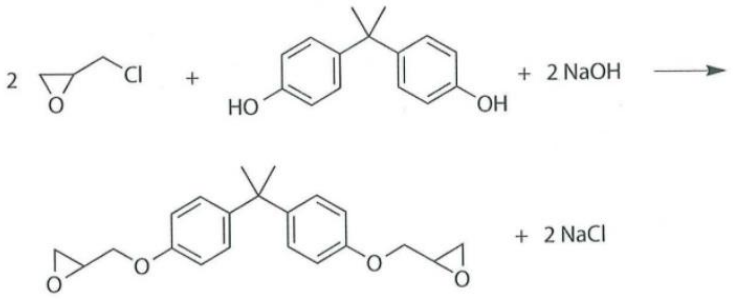


**Figure 2-8: Formation of bisphenol A epoxy resins**

In the mid 1960's new multifunctional resins of the epoxy-novolac type were introduces in the market. The chemistry of this resins is very similar to that of bisphenol A type. They are obtained by condensation of phenol, bisphenol A or cresol with formaldehyde in acidic media, followed by hydrohalogenation with epichlorohydrin and subsequently dehydrohalogenation with solidium hydroxide.

(2) Thermosetting polyester powder coating [82]

Polyester powders dominate the powder coatings markets worldwide. A big advantage of the polyester resins is the possibility of adjusting the place of functional groups in the polymer chain to a desired position which has an enormous influence upon the mechanical properties of the cured films, leading to superior mechanical properties. Thermosetting polyester resins are produced on the same equipment for production of high molecular weight polyesters.

Polyester-TGIC is good for outdoor applications because of good gloss retention and yellowing resistance. The glass transition temperature of polyester resins for TGIC

containing powder coatings should be at least 60 °C in order to achieve good storage stability. Table 2-6 presents a typical formula of polyester resins for TGIC.

**Table 2-6: Polyester resins for TGIC [85]**

| Ingredient | Parts by weight |
|---|---|
| Water | 30 |
| Neopentyl glycol | 530 |
| Terephthalic acid | 711 |
| Isophthalic acid | 88 |
| Adipic acid | - |
| Pelargonic acid | 58 |
| Trimellitic anhydride | 43 |
| “Fascat 4201”(1) | 5 |
| Final characteristics: | |
| Acid value (mg KOH/g) | 35±5 |
| Melting range (°C) | 100 to 110 |

(1) Catalyst (Elf Atochem S.A.)

### 2.4.3 Particle size limitation

Powder coating generally has a thicker and rougher film than traditional liquid coating. Normally, powder consists of particles of different shapes and sizes, which can be characterized by particle size distribution. $D_{50}$ values are the most widely used parameter of describing average particle size. The $D_{10}$, $D_{50}$ and $D_{90}$ are commonly used to represent the particle size distribution (PSD) of a given sample. $D_{50}$ is the medium particle size, and $D_{10}$ and $D_{90}$ are used to depict the broadness of particle size distribution. The closer $D_{10}$ is to $D_{90}$, the narrower the particle size distribution. Generally, a narrow particle size distribution is favorable for industrial applications.

According to the particle size, powder can be divided as coarse powder and fine powder. Particles with mean particle size above 30 μm are defined as coarse powder, which cause a relatively poor surface quality when being electrostatically sprayed. And also the film built by coarse powder is normally over 60 μm, which is much thicker than that of liquid coating. On the other hand, fine powder with average particle size below 30 μm allows a much smoother surface and a thinner film. The comparison of coating film thickness between fine powder and coarse powder is shown in Figure 2-9. However, fine powders are not easy to utilize because of their cohesive nature. In fluidization process, the

cohesiveness of the powder can create plugging or sever channeling [5]. Moreover, fine powders are found to have less particle deposition on the target measured by transfer efficiency (TE) during electrostatic spraying under normal coating condition [86].

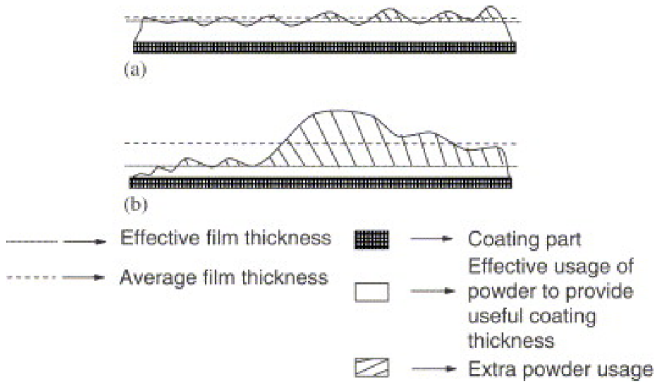


**Figure 2-9: Schematic of coating film thickness for the definition of effective thickness factor: (a) fine powder; (b) coarse powder [78]**

### 2.4.4 Pigment-to-binder ratio

The pigment volume concentration (PVC, total volume of pigments and fillers etc. divided by total volume) is crucial to coating formulation, as it governs the dispersion of pigments in a polymer matrix [6]. The strong pigment/polymer interaction results in the formation of a thin polymer layer around the particles, reducing the interparticle interaction, leading to a reduced melt viscosity of the powder [82].

Nix and Dodge [7] have shown that the degree of dispersion of the pigment in an acrylic powder coating has a considerable influence on the orange peel effect. The inferior flow of the coating with poorly dispersed pigment is accompanied by much higher viscosities, since in the case when the pigments are not completely wetted by the binder, the intermolecular attraction forces between the pigment particles build up reversible internal structures immobilizing the system.

Schellenberger, Thometzek et al. [87] investigated the optical effects of pearlescent pigments in β-hydroxyalkylamide based polyester powder coatings. The pigments close to the surface play a decisive role on the optical effects. The hardener had a positive

effect on the desired horizontally orientation of these pigments. This effect might be attributed to the differences of the wetting properties between the monomeric hardener and the polymeric resin.

Dullaert et al. [88] explored the influence of the pigment loading on the gloss of powder coatings. They found that the combination of short wave and long way patterns determine the optical properties of the coating. The pigment loading has an effect on the long wave roughness, in particular over 45 wt%, whereas the short wave roughness is predominantly influenced by the pigment particle size.

## 2.5 Comparison of powder coating approaches

### 2.5.1 Electrostatic dry powder coating

Electrostatic spray is the most common process used for application of powder coatings in metal finishing. The basic principle is that the dry powder flows through a spray gun by means of compressed air, where it becomes electrically charged. When the particles leave the charged gun and are applied to the substrate, the movement of the particles is governed by two forces: electrical force and mechanical force. The electrical force attributes to interaction between the charged powder particles and the electric field between the substrate and the gun, while the mechanical force is the result of the air that blows the powder through the gun. There are two types of powder coating spray gun in terms of the way to charge particles: corona gun and tribo charging gun.

(1) Corona charging guns

The most common type of corona guns is called external charging guns, which have a single short pointed electrode at the gun nozzle. The electrode is located at the center of the powder diffuser at the front of the spray gun [89]. These guns generate high voltage, low amperage electrostatic fields of 30 to 100 kV between the electrode and the workpiece. A typical corona powder coating gun is shown in Figure 2-10.

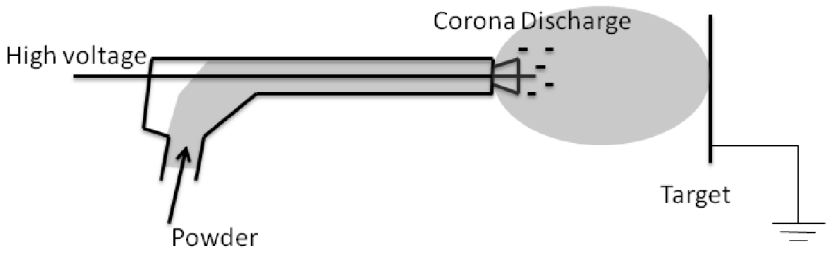


**Figure 2-10: Corona powder coating gun**

In general, not all powder particles leaving the gun nozzle are charged. Typically, only 0.5% of the ions produced by the corona are associated with powder particle charging. The remaining 99.5% exist as free ions in the powder cloud, which means that the powder leaving the electrostatic powder spray gun is composed of negatively charged powder particles, uncharged particles and negative ions [90]. The different mobility among the three types of particles results in an additional motion of air, which is called ion-wind [91]. Because of this, the electrostatic spray technique is possible to coat shadow areas which are not directly exposed to the air stream leaving the gun, as shown in Figure 2-11.

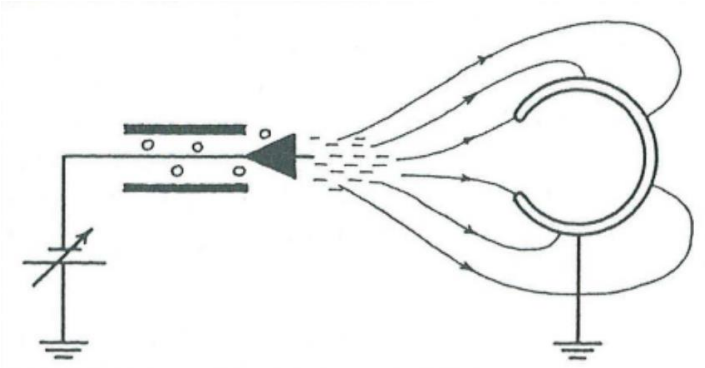

**Figure 2-11: Typical flow pattern for corona charged guns [91]**

Another problem with this type of gun is the Faraday Cage effect. If the air velocity is low, the particles will follow the field line pattern that does not penetrate the inside surface of the workpiece (Figure 2-11). Because of the electrostatic forces, powder flows into an opening to a depth equal to the minimum internal dimension of that opening.

Another phenomenon related to electrostatic spraying is back-ionization [92-94]. Figure 2-12 shows the accumulation of a powder coating layer on the substrate. The growth of the powder layer results in accumulation of charged particles and ions on the coated surface, leading to the increase of the potential across its thickness. At a certain moment the breakdown potential is exceeded and sparks occurs on the surface or within the layer. While the negative ions are retained by the substrate, the positive ions will drift away towards the gun, creating the phenomenon known as back-ionization.

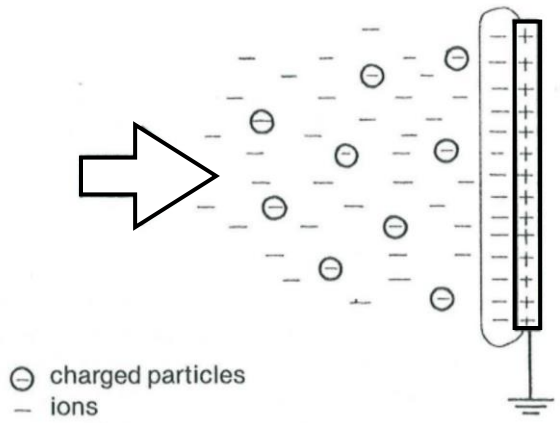


**Figure 2-12: Back-ionization in the powder layer [91]**

(2) Tribo charging guns

A typical tribo charging gun is shown in Figure 2-13. The only difference between corona charging guns and tribo charging guns is the charging method. The tribo charging guns charge the particles by friction between particles and the inner gun wall instead of external high voltage, as a result, the Faraday Cage effect is almost completely eliminated. Because of the very weak electric field between the workpiece and the charged powder cloud, the flow pattern of the powder is directed by the air stream rather than the weak electric field, and this makes it possible to coat objects having cavities and convex shape. However, previous studies indicated that the tribo charging gun is sensitive to spraying conditions such as humidity, substrate surface, shape of contact and powder properties [95-97]. Consequently, the application of tribo charging gun cannot surpass that of the corona gun.

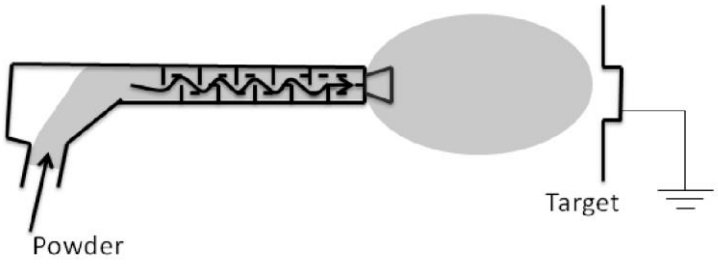


**Figure 2-13: Tribo charging powder coating gun**

### 2.5.2 Aqueous slurry powder coating

The aqueous slurry powder coatings are specialty powder coatings different from conventional dry powder coatings. This method uses water as dispersing medium to suspend dry powder coating particles. There are several subcategories within this method:

- Semi-wet method: a finished powder coating product is dispersed with the aid of water, dispersing agent, rheological modifier, etc. to formulate liquid coating. The mixture is wet milled (ground) to suitable particle size and water is used to adjust the viscosity, then standard air spray of liquid coatings is used subsequently.
- Wet method: the components inside the powder coating, i.e. resin, curing agent, pigment, fillers and various additives are dispersed into water. The mixture is ground to suitable particle size, and water is used to adjust the solid content and viscosity.

Amongst these two methods, the first one is more straightforward and efficient. Comparing with waterborne coatings, this slurry process has its own advantages as follows：

- One coat of 70~100 μm can be achieved.
- Water evaporation is faster, so the air drying time before baking can be shortened.
- Additives dosage can be smaller than waterborne coatings, and coating performance can be better.
- Water soluble content in the formula is lower, and there are no hazardous chemicals such as amines used, so no wastewater treatment is needed. The over-sprayed coating can be recovered and reused.
- When applying the coating, the effect of relative humidity on wet coating is less than

waterborne coatings. There is no pollution in the spray booth and it is easier to maintain the cleanness.

- The spray production line of liquid coatings can be readily used with minimal modification

Comparing with “regular” dry powder coatings, this slurry method’s advantages include:

- The commonly used and well accepted applying methods of liquid coatings can be used, e.g. spraying, dip coating and casting, etc.
- The dry film thickness (DFT) can be as low as 15~20 μm, and it is possible to achieve good smoothness at a DFT of 40 μm.
- Cleaning and color changing are easier than dry powder coatings.
- When applying the coatings, there is no potential risk of particulate pollution and explosion.

Whereas its shortcomings include higher manufacture cost due to the higher complexity, and the curing temperature is higher due to the high water content, and there is also a bigger tendency of blistering in the coating film. And if dispersing agents are used to stabilize the system, the laboratory screening requires large amount of work hours and experiences. Another potential problem with this method is that the resin is prone to hydrolyze if polyester resin is used [98].

## 2.6 Summary

A background review of current coating techniques and materials for SOFC interconnects and powder coating technology has been finished in this chapter. SOFC is an environmentally friendly and attractive technology for energy supply, and in order to increase the voltage of SOFC, individual fuel cells are connected in series by SOFC interconnects, which is currently made of ferritic stainless steel. However, the most important problem that should be solved is the degradation of the performance of SS interconnects due to evaporation of chromium species caused by reaction with water vapor and gradual oxidation. So coating is proposed to solve this problem. Presently, $(Mn,Co)_3O_4$ spinels are the most promising coating materials due to their high electrical conductivity, low contact resistance, good CTE match with the cathode materials and

ferritic stainless steel interconnects, and excellent ability to reduce Cr volatility. The current coating techniques for SOFC interconnects includes electrophoretic deposition (EPD), metal organic chemical vapor deposition (MOCVD) and air plasma spraying (APS). But these techniques are complex to manufacture and operate, as well as expensive. Powder coating is a possible alternative way to coat SOFC interconnects. It is favored because it is environmental friendly, easy to operate and recyclable. But the challenges of powder coating are the limitation of particle size and pigment-to-binder ratio. A comprehensive study about the powder coating used in the field of SOFC interconnects is important and desired.

# Chapter 3

# 3 Experimental methodologies

## 3.1 Experimental materials

This work focuses on new powder coating formulations for SOFC interconnects. The ingredients and resins used in the experiments are list in Table 3-1.

**Table 3-1: Materials used in the tests**

| Materials/Chemicals | Supplier | Grade name | Remark |
|---|---|---|---|
| $Mn_{1.5}Co_{1.5}O_4$ ($D_{50}$: 0.8 μm) | Praxair | - | MCO-1 |
| $Mn_{1.5}Co_{1.5}O_4$ ($D_{50}$: 6 μm) | Metco | XW0317 | MCO-2 |
| Solid epoxy resin | Olin Epoxy | D.E.R.™ 661 | Epoxy |
| Solid polyester | Allnex | CRYLCOAT™ 2845-0 | - |
| Polyester/TGIC-1 | DuPont | - | - |
| Polyester/TGIC-2 | TCI Powder Coatings | 9910-01289 | - |
| Polyvinyl alcohol (Mw 89,000-98,000) | Sigma-Aldrich | 1788 | PVA |
| Surfactant | - | Alkyl benzenesulfonate | - |

## 3.2 Experimental equipment and methods

### 3.2.1 Fine powder preparation

Fine powder preparation includes several processes. The most important processes are good mixing of fine powder and the acquirement of powder with suitable particle size. In the experiments, various methods are applied to mix resins and MCO powder well, including high shear mixing, ball milling, manual pressing and extrusion.

(1) High shear mixing

High shear mixing is a very effective mixing method for preparation of fine powder, simultaneously, it is also a good way to reduce particle size of powders and obtain powder with appropriate particle size. A typical item is shown in Figure 3-1. The mixer is designed for quick mixing of powders, pellets and viscous liquids with fillers, pigments

or other additives, normally between 10 seconds and 10 minutes. The mixing rotor operates at 25000 r/min rotation speed. It can break down particle size into a desirable range, from 30 mesh to 300 mesh. One distinguishing feature of this machine is the very short mixing time accompanied by extremely high mixing efficiency. However, the high workload of this machine can cause overheating. Since the softening temperatures of the resins used in the experiments are not very high, the operating time adopted in the experiments are below 10 seconds/once.

**Figure 3-1: A typical high shear mixing**

(2) Roll milling

Roll mill is a kind of fine mill, and is the key equipment for mixing and grinding powder. Figure 3-2 is a roll mill used in the experiments. In the experiments, the resins and MCO powder were mixed and co-ground in a roll mill filled with stainless steel balls of 5mm n, in diameter, occupying 60% of the mill chamber. After continuous milling of 48 hours, a desirable particle size is obtained.

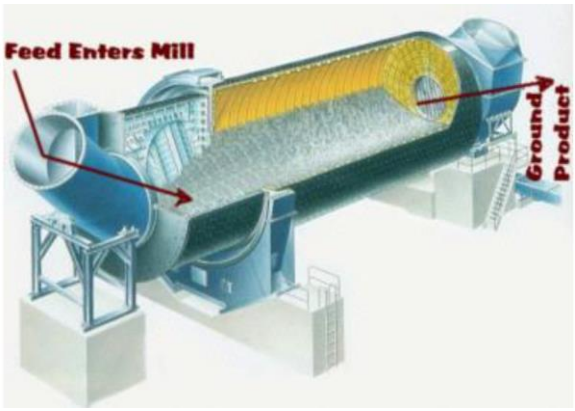


**Figure 3-2: A typical roll mill**

(3) Manual pressing

In laboratory this method utilizes a hydraulic press to compress dry powder mixture in an enclosed cell to form thin chips of 2~3 mm, which can be further thermally or mechanically processed. For industrial scale production, a tablet press can be used for continuous production. Then the formed cake is broken into particles by conventional methods in the powder coatings industry such as air classifying mills (ACM), high shear mixing etc. A typical laboratory manual press is shown in Figure 3-3.

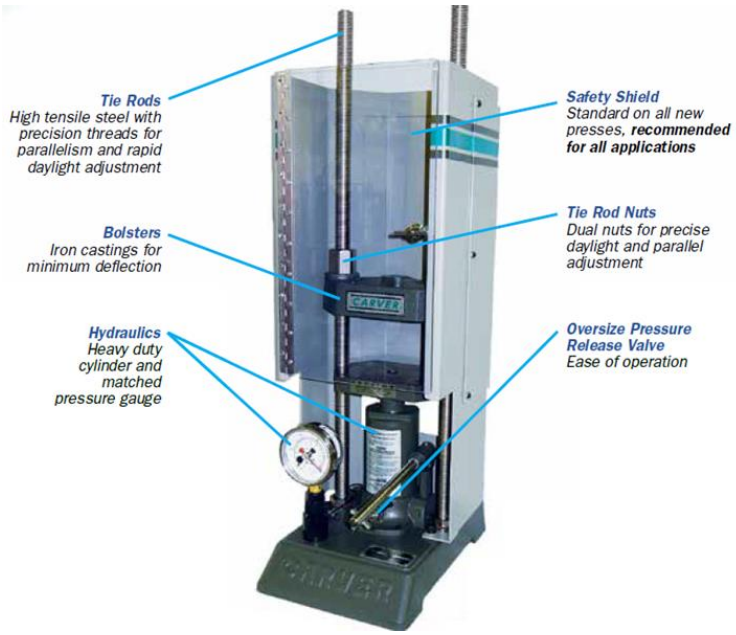


**Figure 3-3: Laboratory manual press**

(4) Extrusion

This is the most widely used method in the powder coatings industry. The resins, hardeners (curing agent), pigments, fillers and various additives are pre-mixed and fed into a twin screw extruder.

In the screw barrel the mixture is melted at a set temperature, and the residence time can be controlled by the rotation speed of the co-rotating screws. The vigorous blending provides excellent de-gassing and dispersion. After the hot melt compounding, the viscous “liquid” leaves the barrel, and is cooled down to room temperature in a chill roll which is attached to the extruder and powder coating chips are produced. A typical extruder is presented in Figure 3-4.

The chips are then ground down by air classifying mills (ACM), which can control the particle size and particle size distribution. Particles under a set value is allowed to leave the mill and collected by a cyclone, and big particles are trapped inside the mill for further breakdown.

The extrusion process allows a continuous operation and with decades of development, both the operating and capital costs are favorable in powder coating industry. However, one big challenge of using it for the current purpose is that the high pigment concentration, especially the highly abrasive particles such as ceramic microbeads would quickly wear out the components of the extruder. In particular, the delicate twin screws can be easily damaged due to high torque and abrasiveness of the pigment.

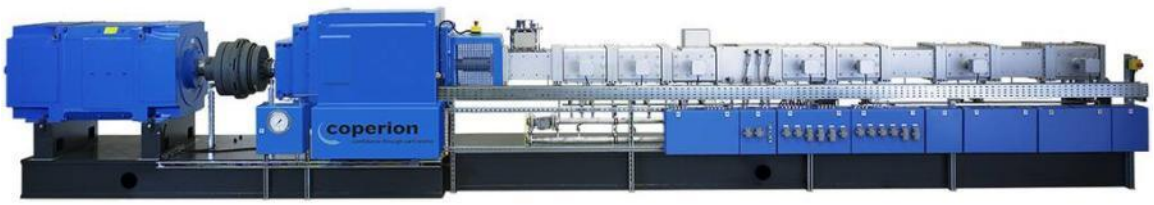


**Figure 3-4: ZSK 125 MEGA volume PLUS for powder coating**

### 3.2.2 Measurement of particle size

(1) Sieve analysis

Sieving or screening is one of the oldest known process techniques for classification still used in current practice in the production of powder coating. A vibratory sieve with 325 meshes (45 μm) is adopted in the experiments. Vibratory sieves are suitable for removal of oversized particles from fines, the so-called “scalping”. A vibratory tumbler screening machine is illustrated in Figure 3-5.

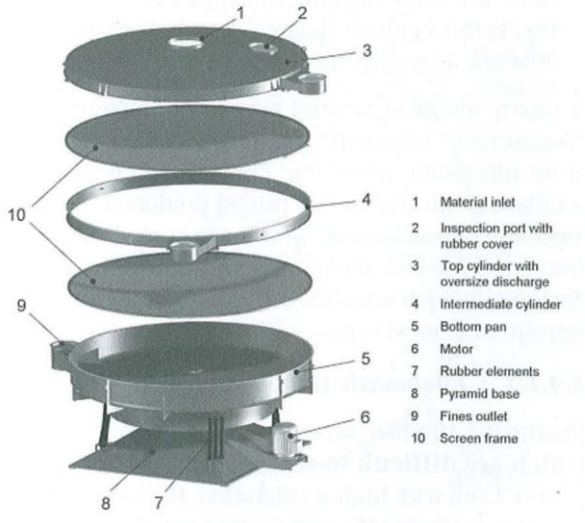


**Figure 3-5: Vibratory tumbler screening machine [82]**

(2) Particle size and particle size distribution

The particle size distribution is obtained by laser diffraction measurement BT-9300S Laser Particle Size Analyzer (BRTTER BAITE INSTRUMENTS LTD.) following standard test procedures. The results are reported by giving the values of $D_{10}$, $D_{50}$ and $D_{90}$ based on volume fraction and the specific surface area. $D_{10}$ is defined as a diameter where 10% of the particles of the powder are less or equal to the diameter by volume. $D_{50}$ represents the medium particle size of the powder samples, which is widely used to describe the mean particle size of powder, while $D_{10}$ and $D_{90}$ are the popular parameters used to determine the amount of fine and coarse particles. The particle size analyzer can

measure particle sizes ranging from 0.02 to 2000 μm, with fairly high reproducibility. The system deviation was reported as 0.3% (in June 2009).

### 3.2.3 Spraying of powder

(1) Electrostatic spray

The spray booth is 2 feet in all dimensions and attached to a vacuum system (Nilfish-GM80) to provide air flow. An ITW Gema manual spray guan as shown in Figure 3-6 was used to spray powder on to substrates from a distance of 20 cm. The voltage and air flow rate were set at the certain values, and the powder was fed in batch. The operating conditions varied when we investigated the effects of voltage and air flow rate on the surface quality.


**Figure 3-6: Gema manual spray gun**

(2) Slurry spray

The slurry was manually air sprayed using a standard IWATA gun LPH50 Gravity, as shown in Figure 3-7. By keeping fluid output as small as possible to an extent that the job is not hindered, it provides better finishing with fine atomization. The spraying distance from the gun to the workpiece is set within the range of 150~200 mm (6~8 in). The gun should be held perpendicular to the surface of the workpiece at all times. Then, the gun

should move in a straight and horizontal line. Arcing the gun causes uneven painting, as shown in Figure 3-8.

**Figure 3-7: IWATA manual air spray gun**

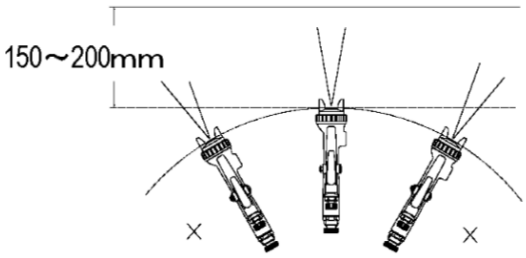


**Figure 3-8: The right operation of the air spray gun**

### 3.2.4 Curing of powder coating

The curing process is conducted in a SHELLAB SL bake oven (Sheldon manufacturing INC) at a certain temperature for a certain length of time in order to reach full cure and achieve the full film properties. When powder on the panel is exposed to an elevated temperature, it begins to melt, flows out and then chemically reacts to form a higher molecular weight polymer which is called crosslinking reaction (for thermosetting polymers). Usually the powders in this experiments are cured at 160~180 °C for 15min. The curing temperature varied when different resins were used.

### 3.2.5 Evaluation of surface quality

(1) Film thickness

DeFelsko PosiTector 6000 as shown in Figure 3-9 was used to measure the dry film thickness in a non-destructive way, coating thickness on both ferrous and non-ferrous metals can be measured. However, this method cannot replace the result from metallography, which is more accurate to measure the film thickness.


**Figure 3-9: DeFelsko PosiTector 6000 dry film thickness gauge**

(2) Coating film defects

Defects or faults on the coating film include pin holing, cratering and fish eye, etc. A paper with five holes was used to evaluate defects on the coating film (as shown in Figure 3-10). Five criteria, including very good, good, fair, poor, very poor, were used to evaluate the quality of the film. The film quality in each hole was recorded.

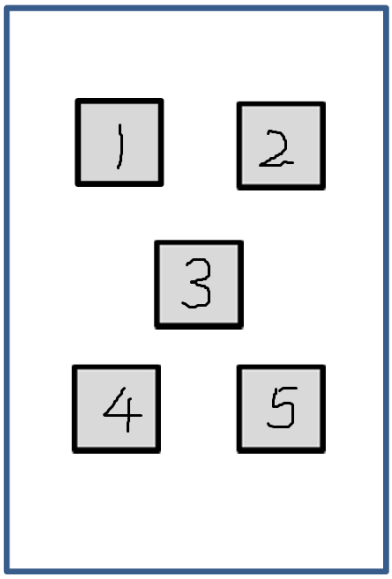


**Figure 3-10: The template for measuring defects on coating film**

(3) Film surface smoothness

Film appearance was assessed using DOI (Distinctiveness of Image), which is defined as a measurement of how clearly a reflected image appears in a reflective surface and was measured using a Gloss Haze and DOI Meter manufactured by Rhopoint Instruments Ltd following ASTM standard D5767 [99]. Measurement scale is 0-100 and 100 is a perfect smooth surface. Symptoms of poor DOI includes orange peel, brush marks, waviness or other structure visible on the surface, which are caused by application problems, insufficient coating flow, coating viscosity too high/low, sag or flow of coating before curing, incorrect particle size/distribution, overspray, improper flash/recoat time, inter coat compatibility, incorrect cure times and cure temperature. All coating films were measured three times, and the DOI reported in this thesis was the average of each measurement.

(4) Measurement of gloss

Gloss is measured by shining a known amount of light at a surface and quantifying the reflectance. The angle of the light and the method of measurement are determined by the surface. Gloss was measured using a Gloss Haze and DOI Meter (manufactured by

Rhopoint Instruments Ltd) following ASTM standard D523 [100], which directs a light at a specific angle to the test surface and simultaneously measures the amount of reflection. In order to obtain a clear differentiation over the complete measurement range from high gloss to matte, 3 different ranges, are defined using a 60° gloss meter (as shown in Table 3-2). If the gloss is >70GU when measured at 60°, a 20° gloss meter is used to improve accuracy and resolution. All coating films were measured three times, and the gloss intensity reported in this thesis was the average of the three.

**Table 3-2: Three different ranges defined used a 60º gloss meter**

| Gloss Range with 60º Gloss Meter | Measure with: |
|---|---|
| If Semi-Gloss - 10 to 70 GU | 60º |
| If High Gloss > 70 GU | 20º |
| If Low Gloss < 10 GU | 85º |

(5) Measurement of haze

Haze is an optical effect caused by microscopic textures or residue on a surface. Visible symptoms of high haze includes milky finish appearance on surface, loss of reflected contrast, halos and patterns that can be seen around reflections of high intensity light sources. These symptoms are due to poor pigment dispersion, raw material incompatibility, additive migration, stoving/drying/curing conditions, fine scratches, oxidization, poor cleanliness/surface residue etc. Its measurement unit is LogHU. This was measured by a Gloss Haze and DOI Meter produced by Rhopoint Instruments Ltd following ASTM standard E430 [101]. All coating films were measured three times, and the haze reported in this thesis was the average of the three.

(6) Measurement of adhesion

The adhesion of the coating was conducted by cross hatch test following ASTM D3359 - 09e2 “Standard Test Methods for Measuring Adhesion by Tape Test” [102]. A minimum of 4B is needed for a coating film. The method is based upon the control of the possible detachment of the trim submitted to cut by means of squaring-off device or dermographic blades. The smooth cut edges and small percentages of detached paint fragment mean a good cohesion.

(7) Measurement of hardness

The hardness of the coating was measured by Elcometer 501 Pencil Hardness Tester following the ASTM D3363-92a [103]. A coated panel is placed on a horizontal surface and the pencil is held firmly against the coating, point away from the operator, at $45^{o}$ angle. The pencil is then pushed away from the operator. The hardness of the pencils is increased until coating is marked by the tip, and hardness of the pencil denotes the coating's hardness.

(8) Optical microscopy

Optical microscope uses visible light and a system of lenses to magnify images of small samples. Surface and shape characteristics were examined by optical microscope with magnification values are 50x, 200x and 500x.

(9) Metallography of coating surface

Metallography is the study of the physical structure and components of metals, typically using microscopy. This is an accurate way of measuring the dry film thickness of organic coatings, together with epoxy mounting and precision sectioning. The cured epoxy composite wrapped up the delicate specimen for the cutting, and then the cross-section was observed under scanning electron microscope (SEM) for measuring the thickness and smoothness (evenness of film thickness across the substrate). This method can give an accurate measurement of coating dry film thickness and smoothness, and was conducted at Stackpole's research facility.

# Chapter 4

# 4 Slurry powder coating technique

## 4.1 Introduction

Powder coating is favored in comparison with traditional liquid coating because it is recyclable and environmental friendly. It contains no solvent and the emission of the process is eliminated. In addition, powder coating process does not require venting, filtering, or solvent recovery which are necessary in liquid coating process [104,105]. However, it is prone to form thick film when cured to form smooth, texture-free coating, thus it is not as easy to achieve smooth thin films. As the film thickness is reduced, the film becomes more and more orange peeled in texture due to the large particle size and high glass transition temperature (Tg) of the powder. Powder coatings of less than 30 μm or with a Tg below 40 °C can be used to produce smooth thin films, but they need specialized operations because they are very cohesive and hard to be fluidized.

Slurry powder coating, which is a technique in between is investigated in this part. This method combines the advantages of powder coatings and liquid coatings by dispersing very fine powders of 1~5 μm particle size into water, which then allows very smooth, low film thickness coating to be produced. As a result of capillary forces of the wet film with water evaporation, slurry powder coating can become dense and compact spontaneously compared to dry powder coating. Moreover, slurry powder coating is also environmental friendly and recyclable as it does not use any solvents and the overspray can be collected and dispersed in water to reuse.

## 4.2 Initial formula

MCO-2 powder and a commercially available full gloss powder clearcoat from TCI Powder Coatings 9910-01289 (polyester/TGIC-2) were adopted in this test. In order to improve the substrate wetting, a typical surfactant alkyl benzenesulfonate was added into the slurry. Dosages of 0.05%, 0.1%, 0.5% and 1% were compared. The properties of polyester/TGIC-2 is shown in Table 4-1. The formula is shown in Table 4-2.

**Table 4-1: Properties of polyester/TGIC-2**

| | |
|---|---|
| Hardness | Very Good |
| Flexibility | Excellent |
| Overbake Stability | Excellent |
| Exterior Durability | Excellent |
| Corrosion Protection | Very Good |
| Chemical Resistance | Very Good |
| Application Properties | Excellent |

**Table 4-2: Formula of slurry powder coating**

| Materials | Mass ratio |
|---|---|
| MCO-2 | 1 |
| polyester/TGIC-2 | 1 |
| D.I. Water | 1 |
| Surfactant | 0.05%-1% (percent in mass) |

## 4.3 Slurry powder coating process

The MCO-2 powder, polyester/TGIC-2 and D.I. water were blended at a mass ratio of 1:1:1, the surfactant was then added into the slurry under stirring. The slurry was ground by roll mill into a medium particle size of 5.3 μm ($D_{50}$), and then manually air sprayed using a standard IWATA gun (as shown in Figure 3-7). The slurry was evaluated on a standard Q-Lab aluminum panel. After spraying, the slurry coating was air-dried for 24 hours at 25 °C and cured at 190 °C for 15 minutes in convection oven. The process is illustrated in Figure 4-1.

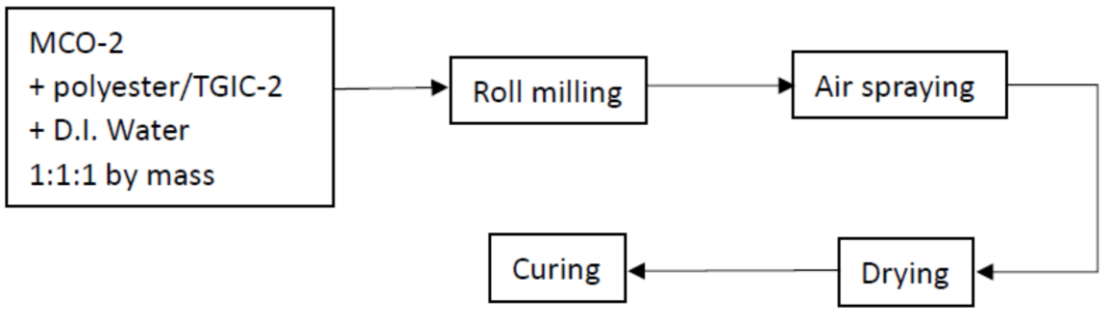


**Figure 4-1: Block diagram of slurry powder coating**

## 4.4 Results and discussion

A dry film thickness (DFT) of 50 µm was obtained. The coated panel is shown in Figure 4-2. Microscopy of 200x magnification (as shown in Figure 4-3) showed inadequate smoothness of the dry film. Most of the substrate was not covered and the powder sprayed onto the panel could not form a continuous film. Severe cracking was observed on Q-Lab standard aluminum panels, possibly due to too high pigment/binder ratio and poor dispersion of the pigments (MCO). Nix and Dodge have shown that the degree of dispersion of the pigment in an acrylic powder coating has a considerable influence on the orange peel effect typical for these coatings, indicating the importance of good wetting of the particles during dispersion of the pigments [7]. The good wetting of the particles gives a strong pigment/binder interaction, resulting in the formation of a thin polymer layer around the particles, and thus reducing the interparticle interaction in this way, as which leads to a reduced melt viscosity of the powder [82]. The reduced melt viscosity can create a better levelling property and improve film forming.

**Figure 4-2: Panel visual appearance of slurry powder coating**

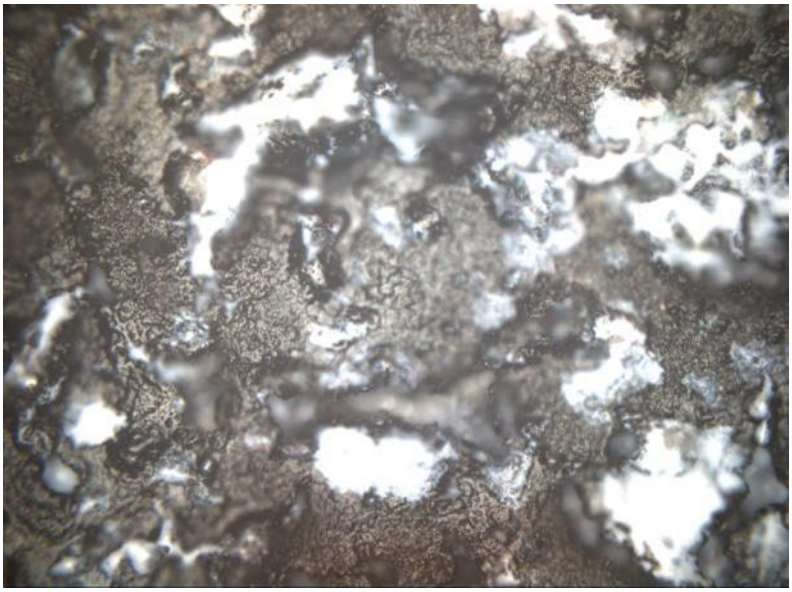

**Figure 4-3: $200_X$ optical microscopy of slurry powder coating**

In order to improve the wetting of the particles, a typical surfactant alkyl benzenesulfonate was added into the slurry. Dosages of 0.05%, 0.1%, 0.5% and 1% were compared, but the results showed that adding surfactant had no effect on improving film quality.

## 4.5 Optimization of slurry powder coating formula

### 4.5.1 Effects of different pigment-to-binder ratios

As discussed above, the inferior quality of the coating was possibly due to high pigment/binder ratio. In order to solve this problem, we proposed a new formula (as shown in Table 4-3), where MCO-2 powder, polyester/TGIC-2 and D.I. water at a mass ratio of 1:2:1 were used instead. The coating process was the same with mentioned above.

**Table 4-3: Formula with lower pigment/binder ratio**

| Materials | Mass ratio |
|---|---|
| MCO-2 | 1 |
| polyester/TGIC-2 | 2 |
| D.I. Water | 1 |

Although the pigment/binder ratio was significantly decreased, the same severe cracking was still observed at a dry film thickness of 50 μm (as shown in Figure 4-4). This

phenomenon may be caused by the residual tension and surface tension. Thin films deposited on a substrate are usually subject to residual stress, with a misfit strain. If the thermal expansion coefficient of the film differs from that of the substrate, the misfit strain is biaxial (thin film cracking), resulting in film cracking. Some researchers proposed that high surface tension promotes better flow of the powder coatings during the film forming process [7,106]. On the other hand, it was shown that low surface tension facilitates the wetting process. It lowers viscosity of the coating, and thus improves the flow of the material and prevents the formation of craters during curing. As a result, in order to obtain a powder coating with good flow and without surface defects, a compromise must be achieved to fulfill these two contradictory requirements.

Melt viscosity is also an important factor with respect to film forming. It influences the possibility of coating flowing during the second stage of the film forming process, after sintering has been finished. Orchard has found that a low melt viscosity create good levelling properties of powder coating, which is also desirable and results in fast coalescence of particles for film forming [106]. However, a too low viscosity leads to bad edge coverage and even sagging on vertical surface [82]. Walz and Kraft have suggested that a good compromise should be within a viscosity range of 6000 and 10,000 mPa.s [107].

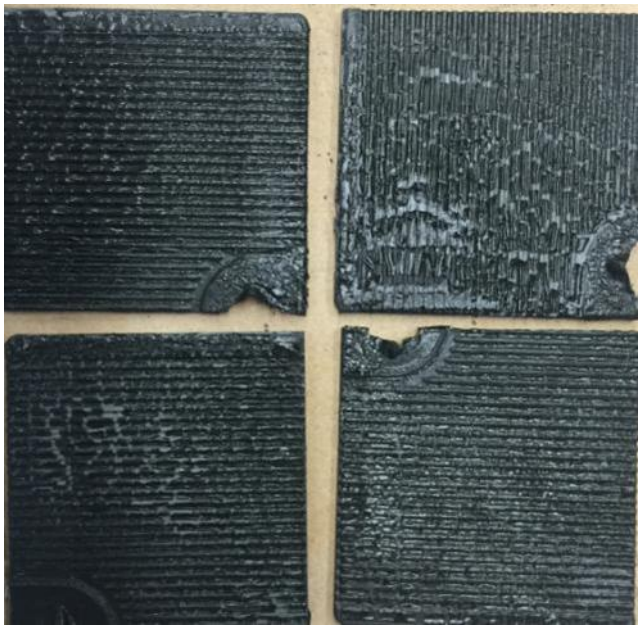

**Figure 4-4: Panel visual appearance of slurry powder coating with lower pigment/binder ratio**

### 4.5.2 Effects of adding polyvinyl alcohol

Polyvinyl alcohol (PVA) is high molecular weight polymer with excellent characters to dissolve easily in water but not to dissolve in common organic solvent or organic acids, and with excellent film-forming property, and also good oil resistance, chemical-resistance [108]. It can react with formaldehydes to form polyvinyl acetal. It is usually used for coatings, adhesives, dispersing agents, textile sizing materials, sensitize coatings and so forth. Figure 4-5 shows the structure of PVA. The -OH functional group in PVA structure can react with the ester link -COO- in polyester resins, as increases the molecular weight and thus improves the adhesion of the film. In this test, PVA 1788 was added into the formula to solve the problem of severe cracking. The properties of PVA 1788 and a new formula are described in Table 4-4 and Table 4-5.

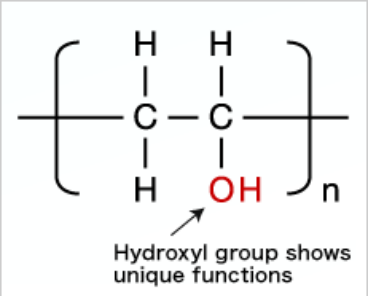


**Figure 4-5: Structure of PVA**

**Table 4-4: The properties of PVA 1788**

| | |
|---|---|
| Appearance | White crystalline powder |
| Degree of alcoholysis (mol/mol) % | 86.0-90.0 |
| Viscosity mpa.s | 20.0-28.0 |
| Volatiles (%) max | 5.0 |
| Sodium Acetate(%) max | 2.5 |
| PH value | 5-7 |

**Table 4-5: Formula (a) with added PVA**

| Materials | Mass ratio |
|---|---|
| MCO-2 | 6 |
| polyester/TGIC-2 | 12 |
| D.I. Water | 6 |
| PVA 1788 | 1 |

The coating process was the same with slurry powder coating as described in Section 4.3. The slurry was sprayed by the same gun as shown in Figure 3-7 to get a dry film thicknesses of 50 μm. With the wet film, the flow and leveling was unacceptable, and the cured film still cracked (as shown in Figure 4-6) and was not uniform. However, there was some improvement comparing to the formula without PVA. Although being with existing film cracking problem, most of the substrate was covered. This formula showed a bigger tendency to form a good film. We added more PVA into the formula, which were 1.5, 2, 2.5 and 3 times more than initial PVA content, respectively, but increasing amount of PVA did not promote the film forming process.

**Figure 4-6: Panel visual appearance of formula (a) with added PVA**

After several trials, we finally adopted a formula as illustrated in Table 4-6. These materials were blended and roll milled for 48 hours, an average particle size ($D_{50}$) of 5.5 μm was obtained. Then the slurry was air sprayed onto the substrates.

**Table 4-6: Formula (b) with added PVA**

| Materials | Mass ratio |
|---|---|
| MCO-2 | 6 |
| polyester/TGIC-2 | 6 |
| D.I. Water | 6 |
| PVA 1788 | 1 |

Dry film thicknesses of 65 μm was obtained and the visual appearance was good, and no cracking was observed. The panel visual appearance is shown in Figure 4-7, and optical microscopy of the coating using this new formula is shown in Figure 4-8. Under optical microscopy, the surface showed a high roughness, and the film was still not continuous. Gloss value of the film was almost 0, and measurements of adhesion and hardness were also conducted. The adhesion was only 1B and the hardness of the film was only HB, which meant inferior adhesion and poor hardness were got.

However, comparing to the films using previous formula, the film showed a significant improvement. As the phenomenon of film cracking disappeared and the film showed relatively uniform. Compared to extruded powder coating method, the coating was still of

a bad quality. Further investigation should be conducted to improve the adhesion, hardness and continuity of the film.

**Figure 4-7: Panel visual appearance of formula (b) with added PVA**

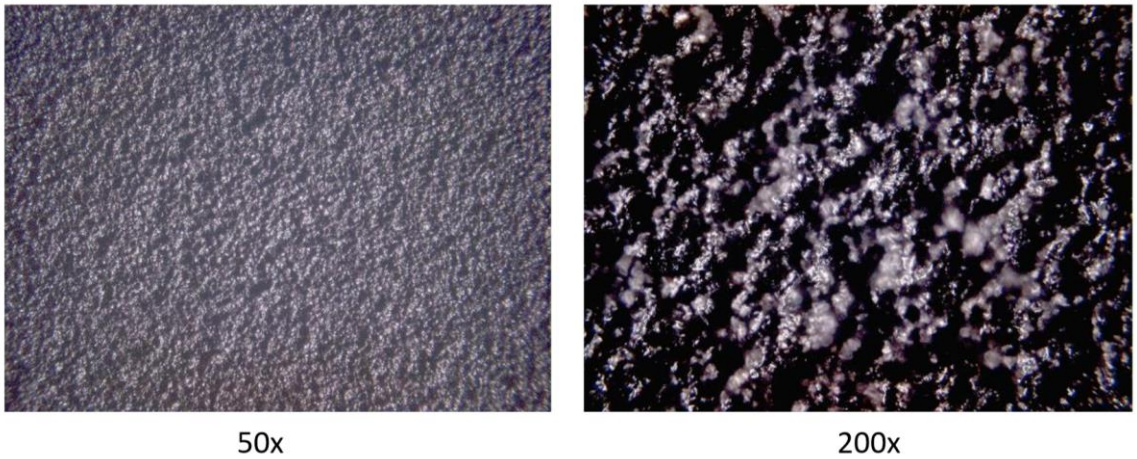


**Figure 4-8: Optical microscope images of formula (b) with added PVA**

## 4.6 Conclusions

The slurry powder coating technique was described in this part. The purpose of this part was to investigate the formulation of slurry powder coating:

(1) An initial formula was proposed, which consisted of polyester/TGIC-2 resin and MCO powder mixed by 1:1 mass ratio. It was found that the quality of the coating was not satisfactory, with respect to film smoothness and substrate coverage. Severe cracking of the coatings on aluminum panels was observed, possibly due to too high pigment/binder ratio and poor dispersion of MCO powder in resins. A typical surfactant of which dosages were 0.05%, 0.1%, 0.5% and 1% was adopted to improve the wetting property and dispersion of MCO particles. The results showed that the surfactant almost has no effect on improving film quality.

(2) A lower pigment/binder ratio (MCO: polyester/TGIC=1:2 by mass) was employed to investigate its effect on film quality. Although the pigment/binder ratio was significantly decreased, the same sever cracking was still observed, which may be mainly due to the surface tension, residual tension and melt viscosity. The difference of thermal expansion coefficient between the film and the substrate also contributed to film cracking. In addition, an appropriate surface tension and melt viscosity can lead to good levelling properties.

(3) The effect of polyvinyl alcohol (PVA) on film forming was also studied in this chapter. For the formula with MCO powder, polyester/TGIC and PVA mixed by mass ratio of 6:12:1, there was an improvement on film forming, although there was still existing film cracking phenomenon. For the formula with MCO powder, polyester/TGIC and PVA mixed by mass ratio of 6:6:1, the cracking phenomenon disappeared, and the panel visual appearance was much better than before, mainly attributing to the function of PVA, which has excellent film-forming property. However, the adhesion and hardness of the film were not very good, so further optimization of the formulation is necessary.

# Chapter 5

# 5 Compacted and pressed powder coating techniques

## 5.1 Introduction

Powder coating is an attractive technique that has already drawn many researchers' attentions. It is favored as there are several distinguishing advantages. Firstly, it is an environmentally friendly method which uses no organic solvents that are harmful to health and environment, and also it is cost effective as less coats are needed for high film thickness and over-sprayed powder can be collected and re-used easily. What is more, without the solvent or water evaporation stage, the production rate of powder spraying can be very high compared with waterborne coatings.

In this study, an electrostatic spray gun was adopted to spray powder onto the substrates. While depending on different methods for fine powder preparation, the powder coating techniques are divided into two groups: thermally compacted powder coating and cold pressed powder coating.

## 5.2 Thermally compacted powder coating

### 5.2.1 Powder coating formula

MCO-1 powder $Mn_{1.5}Co_{1.5}O_4$ by Praxair was used in the test. The original MCO-1 powder size is measured as $D_{50}$=0.8 μm, $D_{10}$=0.31 μm, $D_{90}$=1.53 μm. Olin Epoxy's D.E.R.$^{TM}$ 661 solid epoxy resin was used as binder. The solid epoxy is a standard low molecular weight, solid reaction product of liquid epoxy resin and bisphenol-A, and it can be used in applications where cure must be achieved at room temperature. It is used to formulate high quality chemical resistant coatings, automotive, can, coil, marine, protective and industrial maintenance coatings. Being cured with polyamine or polyamide, solid epoxy resin provides outstanding resistance properties, hardness, very good adhesion and flexibility. Epoxy powder coatings usually provide smooth finish with low risk of having defects such as pinholes and craters due to their low viscosity while melting [109]. However, because of their poor resistance to UV exposure, they are

usually limited for indoor applications or as primers for outdoor applications [110]. The properties of this epoxy is shown in Table 5-1. The formula is illustrated in Table 5-2.

**Table 5-1: Properties of D.E.R. 661 solid epoxy resin**

| | |
|---|---|
| Epoxide equivalent weight | 500-560 g/eq |
| Viscosity@25°C | 165-250 $mm^2/s$ |
| Colour, Platinum Cobalt | <100 |
| Melt viscosity @150°C | 400-800 mPa.s |
| Softening point | 75-85 °C |
| Water content | <5000 ppm |
| Shelf life | 24 months |

**Table 5-2: Formula of thermally compacted powder coating**

| Materials | Mass ratio |
|---|---|
| MCO-1 | 1 |
| D.E.R. 661 solid epoxy resin | 1 |

### 5.2.2 Powder coating process

The solid epoxy resin and MCO-1 powder were dry blended by high shear grinder/mixer foe 30s at 1:1 by mass ratio, and then the powder mixture was then melted at 100 °C in a convection oven for 15 min, in order to release the entrapped air in the powder. This also results in the consolidation of the powder. Then the formed chunk was pulverized by the same high shear grinder. The ground powder was sifted by a 45 μm vibratory sieve, and the particle size of the mixture after sieving was measured as $D_{50}$=26.15 μm, $D_{10}$=7.29 μm, $D_{90}$=60.13 μm.

The produced powder coating was then manually dry electrostatic sprayed at 25 °C, relative humidity 50% at 30 kV and 70 kV, with a 30 μA charging current. The powder output is set to be 60% and the total air volume is 6.0 $m^3/h$. A typical Gema corona gun was used for the manual dry electrostatic spray (as shown in Fig. 3-6). The substrates adopted in this test were Q-Lab flat aluminum panels.

The voltage of 30 kV showed inferior transfer efficiency, because it was not high enough to charge the powder, so the powder could not be electrostatically adhered on to the substrates. Then the increased voltage of 70 kV showed a better result. After that, the

sprayed panels were cured at 110 °C for 15 min. The block diagram of this method is shown in Figure 5-1.

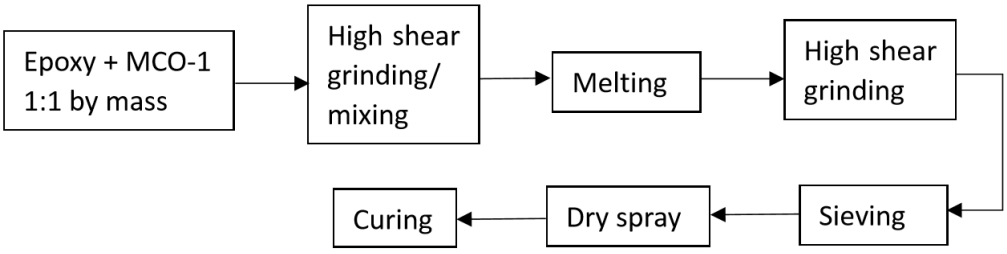


**Figure 5-1: Block diagram of thermally compacted powder coating**

### 5.2.3 Results and discussion

The panel appearance after curing is shown in Figure 5-2, with a dry film thickness (DFT) of 50 µm. As shown in Figure 5-2, the film quality was fairly poor and had severe defects of non-uniformity. The formed film was not continuous and exhibited lots of pinholes. This inferior film is mainly due to the fact that when melting the epoxy and MCO-1 powder mixture, air bubbles are trapped inside the chunk, resulting in the large distance between particles. During the film-forming process, resins cannot merge together to form a continuous film.

The adhesion of the coating onto the aluminium panels was only 2B by ASTM D3359-09e2. The coating was easily peeled off from the substrate as the resin used is thermoplastic and is not coupled with a curing agent, leading to a poor adhesion. Overall, this method has many problems and is not suitable for coating SOFC interconnect.

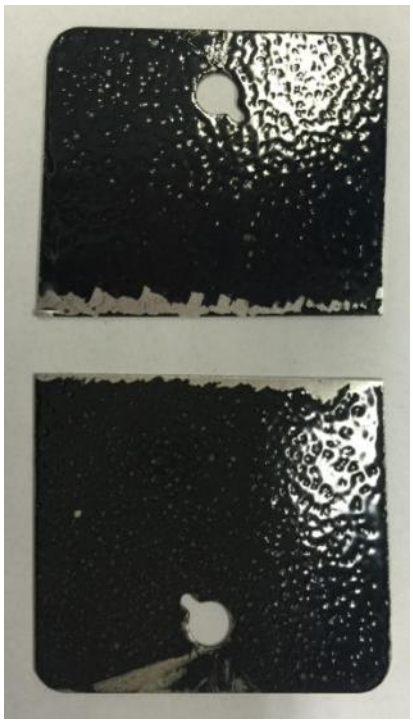

**Figure 5-2: Panel visual appearance of thermally compacted powder coating**

## 5.3 Cold pressed powder coating

### 5.3.1 Powder coating formula

In this test, MCO-1 powder and a typical solid polyester resin Allnex CRYLCOAT$^{TM}$ 2845-0 was used. CRYLCOAT$^{TM}$ 2845-0 is a hydroxyl functional polyester resin. It is well known that polyester resins are easy to use and have lowest cost, as well as excellent weatherability. As they contain polar groups, they can react with many substances and show a good adhesion on the substrate. Polyester powder coating usually offers better coating performances than others [110]. In addition, they can provide better film quality with higher gloss and less yellowing [111]. As a result, they are favorable for applications on outdoor articles such as air conditioner and bicycle frames. The properties of this polyester is shown in Table 5-3. The formula is illustrated in Table 5-4.

**Table 5-3: Properties of CRYLCOAT 2845-0 polyester resin**

| | |
|---|---|
| Appearance | Pale granules |
| Hydroxyl value (mg KOH/g) | 30-40 |
| Brookfield Viscosity @200°C, mPa.s | 6400-7800 |
| Color, b-value | Max. 15 |
| Acid value (mg KOH/g) | ≤5 |
| Glass transition °C | Approx. 57 |

**Table 5-4: Formula of cold pressed powder coating**

| Materials | Mass ratio |
|---|---|
| MCO-1 | 1 |
| CRYLCOAT™ 2845-0 polyester resin | 1 |
| D.I. Water | 1 |

### 5.3.2 Powder coating process

To overcome bubble formation in the method of thermally compacted powder coating, a water-based approach was conducted. In this process, the powder was pressed in order to release the air inside the powder and to make it compact. The polyester was blended with MCO-1 powder at a ratio of 1:1 by mass, and the almost same weight of water as the resin was used as grinding medium. The mixture was co-ground in a rolling mill filled with stainless steel balls of 5 mm, occupying 60% of the mill chamber, the equipment was equivalent to sand mill in liquid coating manufacture. After continuous milling of 48 hours, an average particle diameter of 8 μm ($D_{50}$) was obtained. Then the liquid paste was transferred to a flat plate and air dried at 25 °C in a fume hood with strong ventilation for 48 hours.

A chunk was formed in the flat plate and compressed by a hydraulic press at 50,000 N. Then the pressed cake was pulverized by a high shear grinder for 30 seconds and sifted by the 45 μm vibratory sieve. The average particle diameter was measured to be 14.6 μm ($D_{50}$).

The powder coating was dry electrostatic sprayed onto a standard Q-Lab flat aluminum panel at 70 kV voltage and the sprayed panel was cured at 160 °C for 15 min in a convection oven. In this test, the same parameters for evaluation were used in order to compare with the method of powder coating thermally compacted. The block diagram of this method is shown in Figure 5-3.

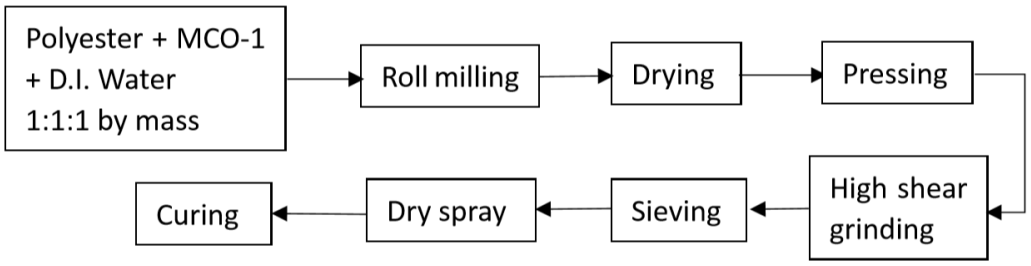


**Figure 5-3: Block diagram of cold pressed powder coating**

### 5.3.3 Results and discussion

The cured panel with a dry film thickness (DFT) of 65 μm is displayed in Figure 5-4. Compared to the panel by method of thermally compacted powder coating, the continuousness of the film was better. However, there were still some defects on the surface such as pinholes. Figure 5-5 shows the 50x and 200x optical microscope images of the coating. The substrate was not fully covered and the color of the coating was different which meant that the film was not uniform. As MCO-1 powder is black, the part of deep color in the coating contains more MCO-1 powder while the light part is mainly composed of polyester resin.

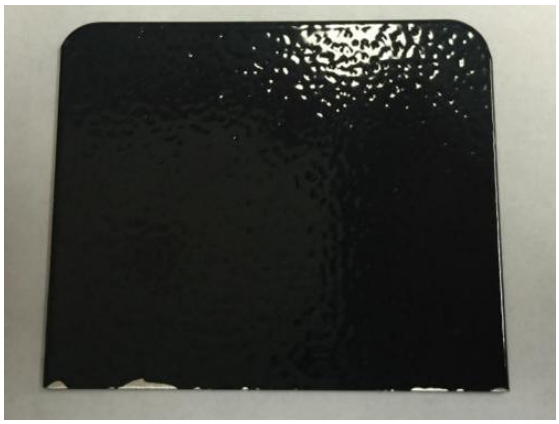

**Figure 5-4 Panel visual appearance of cold pressed powder coating**

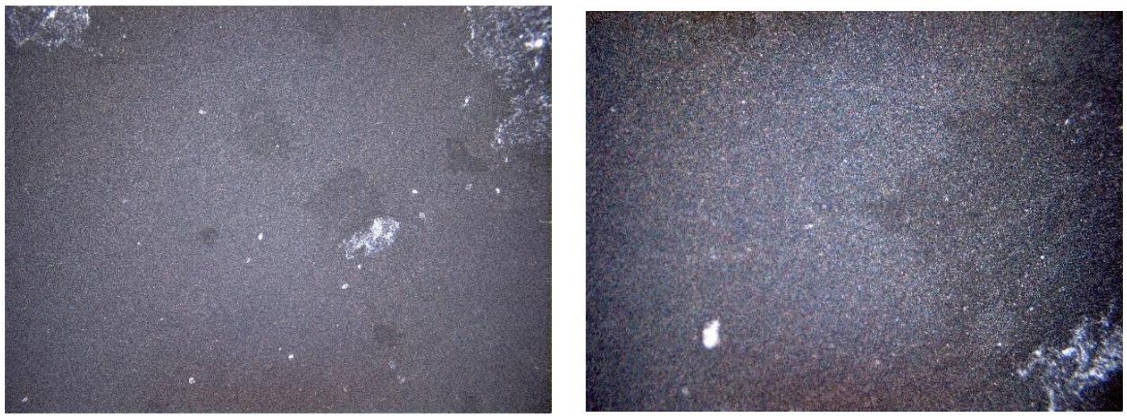


**Figure 5-5: Optical microscope images of cold pressed powder coating**

The adhesion of this film was 3B, which means that it was easily cracked and peeled off the substrate. The hardness of the film is not strong, only achieving 3B. The poor adhesion and hardness is due to the lack of crosslinking reaction. Since the polyester used is thermoplastic and in order to solve this problem, thermosetting polymer should be adopted.

The gloss, DOI and haze values of the coating is described in Table 5-5. It can be seen from the table that the film was semi-gloss and the DOI was very low, meaning that the coating was not smooth. As shown in optical microscope images, there were some visible holes and marks on the surface. The haze value was also high, leading to halos and patterns around reflections of high intensity light source. The low DOI, high haze value and non-uniformity of the film are caused by poor dispersion of the pigment (MCO-1), raw material incompatibility and incorrect particle size or distribution. The original average particle size ($D_{50}$) of MCO-1 powder was 0.8 μm, while after roll milling with polyester resin for 48 hours, the average particle size of the mixture was 8 μm. So the polyester resin is ground to around 8 μm while the MCO-1 powder is almost still 0.8 μm, resulting in the incompatibility of particle sizes. As the resin particles are much larger, bringing about big voids between them, MCO-1 particles gather together in the void. As a result, MCO-1 particles cannot be dispersed well in the resins. The state of the mixture can be illustrated in Figure 5-6.

**Table 5-5: Gloss, DOI and haze values of the coating**

| Gloss (GU) | | DOI | Haze (LogHU) |
|---|---|---|---|
| 20° | 60° | | |
| 26 | 65.2 | 13.3 | 28.5 |

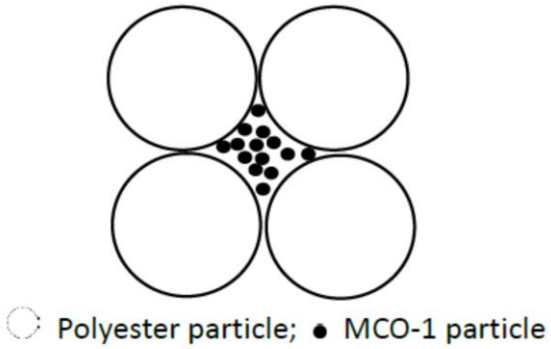


**Figure 5-6: Mixing state of polyester and MCO-1**

### 5.3.4 Improvement on powder coating formula

In order to solve the problems discussed above, including poor adhesion and hardness, big difference in particle size between materials, a new formula was proposed. MCO-2 powder by Metco has a different particle size distribution compared to MCO-1 powder. The original particle size of MCO-2 powder is measured as $D_{10}$=1.88 µm, $D_{50}$=6.74 µm, $D_{90}$=15.34 µm. Due to the fact that good adhesion and mechanical strength are required for metallographic analysis, a curable/crosslink-able binder system was used instead of the thermoplastic counterpart. In this test, a commercial available solid polyester/TGIC powder clearcoat from DuPont (polyeater/TGIC-1) was adopted.

Triglycidyl isocyanurate (TGIC) is one of the most important curing agents for carboxyl functional binders, specifically for carboxyl terminated polyesters [82]. It is the most popular crosslinker (curing agent) for polyester powder coatings for outdoor use. The chemical structure of TGIC is given in Figure 5-7.

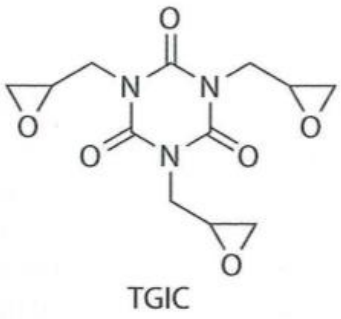


**Figure 5-7: Chemical structure of TGIC [82]**

It is well known that polyesters are unsaturated synthetic resins formed by the reaction of polyhydric alcohols, organic compounds with multiple alcohol or hydroxyl functional groups, with saturated or unsaturated dibasic acids. The crosslinking reaction of polyester/TGIC is described in Figure 5-8.


**Figure 5-8: Curing reaction in polyester/TGIC [82]**

In general, thermoplastic powder coatings have very poor adhesion on metal surface. However, for thermosetting powder coatings, the crosslinked nature of the cured film improves chemical resistance. The introduction or formation of polar groups and the increase of molecular weight also considerably improve the adhesion properties. Table 5-6 shows the difference among binder types in relation to various performance characteristics. The new formula is shown in Table 5-7.

**Table 5-6: Differences in performance characteristics among binder types**

| Properties | Epoxy | Hybrid | Urethane | TGIC-Polyester |
|---|---|---|---|---|
| Hardness | Excellent | Good | Good | Very Good |
| Flexibility | Excellent | Excellent | Excellent | Excellent |
| Overbake Stability | Fair | Very Good | Excellent | Excellent |
| Exterior Durability | - | - | Excellent | Excellent |
| Corrosion Protection | Excellent | Very Good | Good | Very Good |
| Chemical Resistance | Excellent | Good | Good | Very Good |
| Ease of Application | Very Good | Excellent | Very Good | Excellent |

**Table 5-7: New formula of cold pressed powder coating**

| Materials | Mass ratio |
|---|---|
| MCO-2 | 1 |
| polyester/TGIC-1 | 1 |
| D.I. Water | 1 |

The powder coating process was the same as mentioned above. After roll milling for 48 hours, the mean particle size of the mixture ($D_{50}$) was 5.33 μm. The slurry was air dried for 48 hours, compressed and pulverized to a powder of $D_{50}$=8.91 μm, $D_{10}$=2.2 μm, $D_{90}$=22.17 μm. Dry electrostatic spray under the same conditions was performed. The produced powder coating was sprayed onto both aluminum panel and SOFC interconnect.

The film thickness was 55 μm and inadequate uniformity after curing was observed (as shown in Figure 5-9). There was no coverage in the groove of the panel, possibly due to Faraday cage effect, and this was a great challenge with powder spraying onto substrate of irregular geometry. From optical microscope images (as shown in Figure 5-10), it can be observed that the coating was not continuous and did not form a compact film. The coverage of the substrate was poor and the coating also showed roughness. Moreover, the adhesion and hardness were not improved.

The inferior quality of the film may be due to the low curing temperature around 160 °C. In general, the curing temperature for polyester/TGIC is 190~200 °C. The curing temperature will affect the curing mechanism and crosslinking reaction. Five factors will

be considered during the crosslinking reaction, including rate determining step, rate of reaction, collision theory, activation energy and curing conditions. For powder coating, reactions take place as a result of particle colliding and a reaction is initiated. The particles must have sufficient kinetic energy and correct orientation with respect to each other to react [112]. The kinetic energy of particles is related to heat energy, higher heat means higher collision energy and lower viscosities for liquefied powder coatings, resulting in higher mobility of the resin molecules to create favorable conditions for collisions [113]. Increasing the temperature also increases the average speed of the particles and consequently more effective reactions. The adequate crosslinking reaction enhances the adhesion and hardness of the coating and also improve its chemical resistance.

In addition, although pressing was introduced in this process to escape the air inside the powder and to compact powder, the strength of the pressing was not enough to make MCO powder and resins to mix well, but the mixing is also a very important factor that influences the film-forming process.

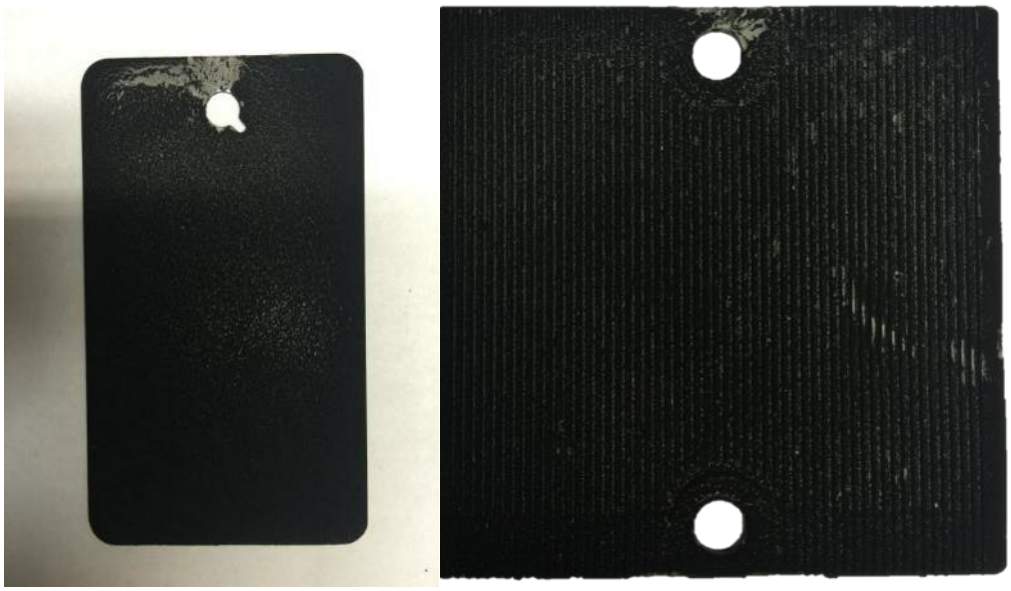

**Figure 5-9: Panel visual appearance of powder coating with improved formula**

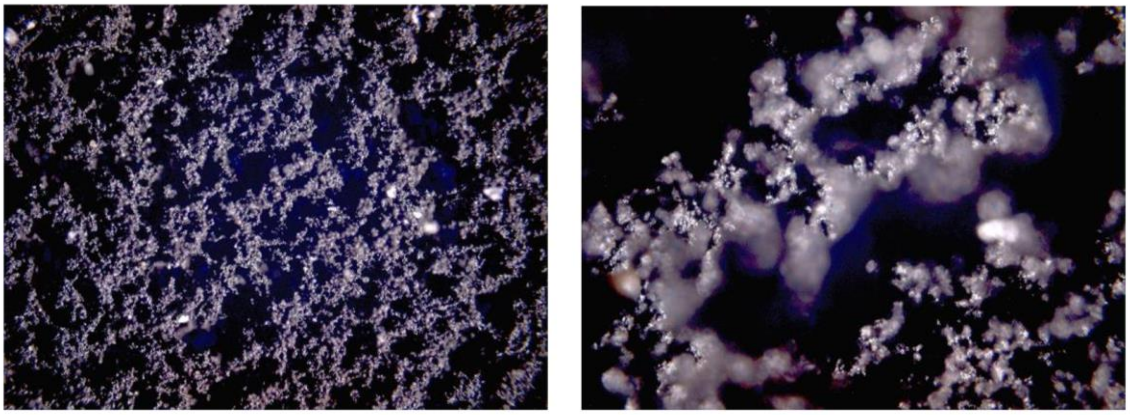


**Figure 5-10: Optical microscope images of powder coating with improved formula**

## 5.4 Conclusions

Dry powder coating techniques including thermally compacted powder coating and cold pressed powder coating have been discussed in this chapter. Formulas and processes of these two techniques were investigated.

(1) For thermally compacted powder coating, the formula of D.E.R.$^{TM}$ 661 solid epoxy resin and MCO powder with 0.8 μm ($D_{50}$) by mass ratio of 1:1 was proposed. The film obtained was fairly poor and had severe defects of non-uniformity, mainly due to too much air trapped in the powder, which results in the large distance between resin particles. As a result, resins cannot merge together to form a continuous film.

(2) For cold pressed powder coating, pressing was introduced in the process in order to let the air inside the powder escape and to compact the powder. A typical solid polyester resin was used to replace solid epoxy resin. It was found that this formula achieves a better film quality with respect to the continuity of the film. However, there were still some defects on the film, which are attributed to the incompatibility of particle sizes between resin and MCO powder. The adhesion and hardness of the film were not good, which are due to the lack of crosslinking reaction and can be solved by adding curing agent.

(3) An improved formula was studied for cold pressed powder coating in this chapter.

MCO powder with 6 μm ($D_{50}$) and polyester/TGIC were employed. But there was no improvement on the film quality because of the low curing temperature and the lack of high shear pressing. Increasing the curing temperature may create more effective crosslinking reactions, further leading to enhancement of adhesion and hardness of the film. In addition, particles under high shear press and high temperature can form a uniform structure, which benefits film-forming process. A further optimization of this method is necessary.

# Chapter 6

# 6 Extruded powder coating technique

## 6.1 Introduction

Extrusion is a classic mixing technique that has been used by the industry for over 70 years [114]. Comparing with other mixing techniques, it is able to mix materials on a much smaller scale due to its high-shear mixing characteristic. The application of extrusion process in polymer industry has a long history. By utilizing this process, polymer materials can be well mixed with additives and other ingredients into a nearly homogenous material with uniform density [115].

The formed uniformly chips are then ground down by air classifying mills (ACM), which can control the particle size and particle size distribution. Particles under a set value of particle size is allowed to leave the mill and collected by a cyclone, and big particles are trapped inside the mill for further breakdown.

The process allows a continuous operation and with decades of development, both the operating and capital costs are favorable now. However, one big challenge of using it for the current purpose is the high pigment concentration, especially the highly abrasive particles such as ceramic microbeads, which would quickly wear out the components of the extruder. In particular, the delicate twin screws can be easily damaged due to high torque and abrasiveness of the pigment.

## 6.2 Powder coating formula

MCO-2 powder and a commercially available full gloss powder clearcoat from TCI Powder Coatings 9910-01289 (polyeater/TGIC-2) were adopted in this test. The properties of polyester/TGIC-2 is listed in Table 4-1. The formula for this method is shown in Table 6-1.

**Table 6-1: Formula of extruded powder coating**

| Materials | Mass ratio |
|---|---|
| MCO-2 | 1 |
| polyester/TGIC-2 | 1 |

## 6.3 Powder coating process

A standard extruder for powder coating manufacture was used in this method. Figure 6-1 illustrates a typical extrusion process for powder coatings. At the beginning of the process, dry-mixed raw materials are fed into the extruder which has major components including the extruding screws, and the heating/cooling elements. Usually, there are twin-screw extruders with two to three temperature zones in the extruder. In the first zone, raw materials start to soften at elevated temperature (40~60 °C) and the twin screws within this zone have large helical treads that push the material forward. In the second zone, the actual mixing begins and the temperature is gradually increased to 100~130 °C. The shape of the screws in this zone becomes elliptical with positions shown in Figure 4.11b. In this zone, the softened materials are subjected to high shear mixing by the inter-meshing motion of the screws. There can be an optional third zone for ejecting the mixed material out from the extruder. It is important to control the temperature inside each zone in order to avoid pre-curing. The mixed material comes from the extruder is in a state of hot paste. It is then cooled and rolled into a solid thin sheet by two cooling drums followed by a long cooling belt. Finally, the sheet is crushed down by a pelletizer. The end material is called powder coating chips which are ready for grinding [110].

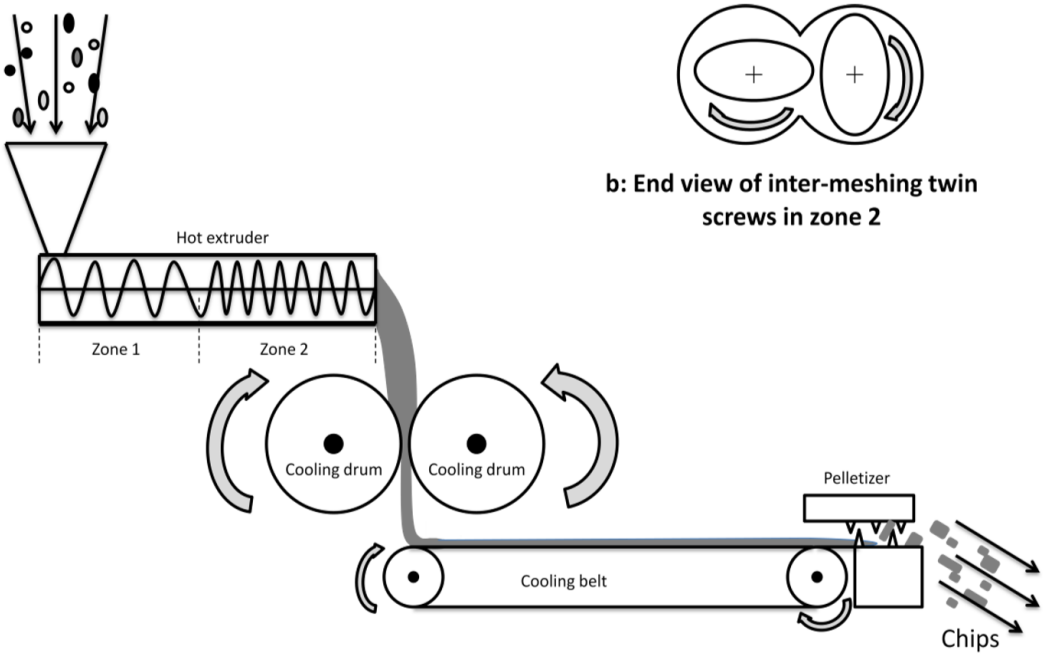


**Figure 6-1: A typical extrusion process**

In the test, MCO-2 powder and polyester/TGIC-2 were blended by high shear mixer at a ratio of 1:1 by mass. These materials were fed into the barrel by a screw feeder, and the barrel temperatures of infeed zone, plastification zone and homogenizing zone were set as 80 °C, 90 °C and 95 °C, respectively. For minimizing the pre-curing of the thermosetting powder coating, a high rotation speed of 350 rpm was used to keep a short average retention time. The hot material leaving the extruder was cooled down to 20 °C and collected as chips, which were pulverized by a high shear grinder for 5 s and sifted by a 45 μm vibratory sieve for 3 minutes, and then the mixing and sifting were repeated until enough powder was produced for electrostatic spraying. The mean particle size ($D_{50}$) was measured as 33 μm.

The powder coating was dry electrostaticallly sprayed onto both standard Q-Lab flat aluminum panel and SOFC interconnects. The conditions of the electrostatic spray gun were the same as those of spraying process in thermally compacted powder coating method. The charging current was 30 μA. The powder output was set to be 60% and the total air volume was 6.0 $m^3$/h. In this test, 3 different voltages were adopted, namely 30 kV, 50 kV and 70 kV, among which 30 kV was not effective. The 30 kV voltage was too

low to spray powder onto the substrate due to low transfer efficiency. The sprayed panel was cured at 190 °C for 15 min in convection oven.

## 6.4 Results and discussion

A continuous high gloss film was formed and the DFT of any value between 40 and 100 µm were produced. Figure 6-2 shows the visible surface appearance, Figure 6-3 and Figure 6-4 display the optical microscope images of the coatings electrostatic sprayed at 50 kV and 70 kV, respectively. While preliminary results were promising, the obtained panels still had defects of craters, pinholes and inadequate flow/levelling. The visual appearance of the panels was excellent, even though the pigment dosage was as high as 50% by mass, which depletes the presence of binder in the formula, so the free flow of the melted binder is severely restricted. The visual appearance might also be improved by using low molecular weight resins other than standard ones, as the molecular weights governs mainly the melt viscosity of the resin. Lower melt viscosity can help get better levelling and final smoothness of coating surface. When electrostatic spraying at 70 kV, the defects of the coating were more than that at 50 kV, the pinholes can be caused by a phenomenon called back ionization, which is attributed to a relatively high voltage.

From the optical microscope images, the substrates were not fully covered and coating deposited at 50 kV exhibited a smoother film and better coverage. The craters may also be caused by trace amount of contamination. The difference in surface tension deteriorate the smoothness, but this can be solved by adding acrylic additives. Compared to the former method of cold pressed powder coating, the extruded powder coating showed better quality, as the film was compact and continuous. This significant improvement is mainly due to the extrusion process. During the extrusion, resins melted and fused together with MCO powder to form a uniform structure under the high shear stress and temperature. So the air in the powder was released and the problem of incompatibility between resin and MCO powder was overcome. In addition, as MCO powder was well dispersed in resins, the color of the film was almost the same under optical microscopy, signifying the uniformity of the film.

**Figure 6-2: Panel electrostatically sprayed by extruded coating at 50 kV and 70 kV**

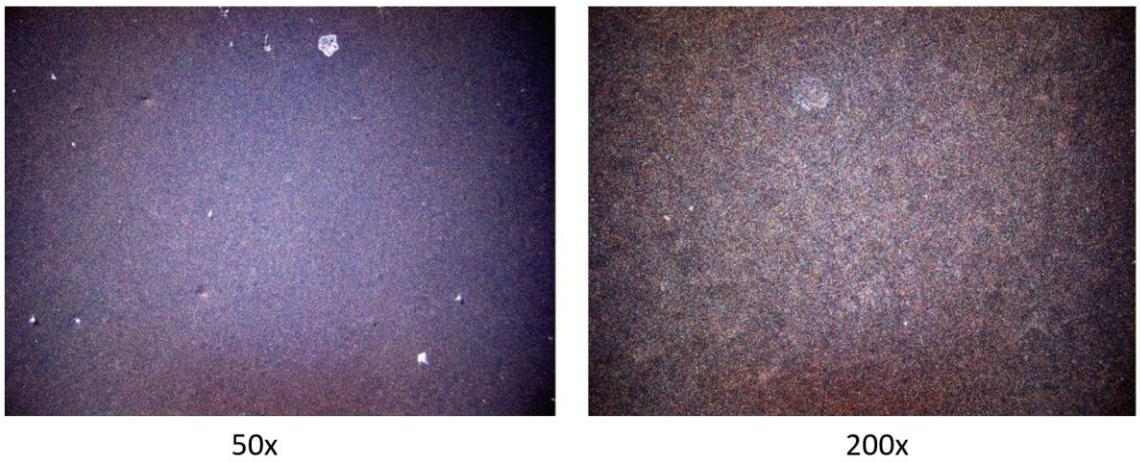


**Figure 6-3: Optical microscope images of extruded powder coating at 50 kV**

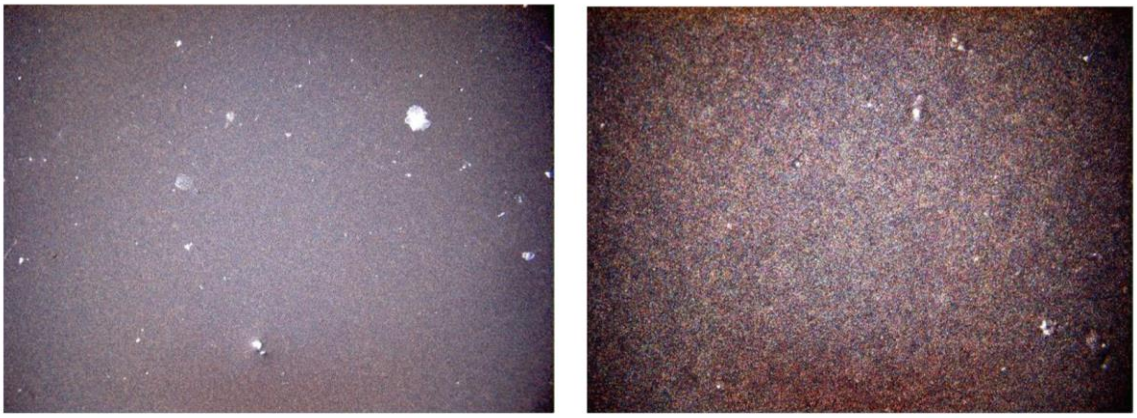


**Figure 6-4: Optical microscope images of extruded powder coating at 70 kV**

A paper with five holes was used to evaluate defects on the coating film (as shown in Figure 3-10). The surface qualities at the five locations are shown in Table 6-2. The quality of the film deposited at 50 kV was better than that at 70 kV. Table 6-3 illustrates gloss, DOI and haze values of coatings deposited at 50 kV and 70 kV, respectively. They both were high gloss at almost the same value. DOI of the coating electrostatically sprayed at 50 kV was larger which showed a better smoothness. And haze value of 50 kV was smaller than that of 70 kV, which also showed a better film property.

The measurements of adhesion and hardness were conducted to evaluate the film quality. For both coatings deposited at 50 kV and 70 kV, their adhesion was excellent, measured as 5B following ASTM D3359-09. And their hardness was HB, which showed moderate strength. The excellent adhesion is due to the good mixing of resins and MCO powder by extrusion and the crosslinking reaction during curing. Overall, this method can be applied to SOFC interconnect coatings in industrial production.

**Table 6-2: Surface qualities at five locations**

| Operating condition | Location 1 | Location 2 | Location 3 | Location 4 | Location 5 | Overall |
|---|---|---|---|---|---|---|
| 50kV | Good | Very Good | Fair | Fair | Very Good | Good |
| 70kV | Poor | Poor | Fair | Good | Good | Fair |

**Table 6-3: Gloss, DOI and Haze of the coatings**

| Operating condition | Gloss (GU) | | DOI | Haze (LogHU) |
|---|---|---|---|---|
| | 20° | 60° | | |
| 50kV | 37.3 | 80.3 | 9.6 | 22.8 |
| 70kV | 35.6 | 80.9 | 6.1 | 26.4 |

## 6.5 Conclusions

The extruded powder coating technique was investigated in this part. Extrusion is a conventional process in powder coating industry. By utilizing this process, ingredients can be well mixed into a relatively homogeneous materials with uniform density due to the high shear-mixing characteristics of the extruder. The good properties of produced powder show that it can improve the film-forming process and enhance film quality. The effects of voltages adopted for electrostatic spraying on film quality have also been discussed. Three different voltages, 30kV, 50kV and 70kV were employed and compared, among which 30kV voltage was too low for powder deposition on the substrate and was not effective. Both 50kV and 70kV voltages showed good film properties. The conclusions of this part are described in details as follows:

(1) For both 50 kV and 70 kV voltages, the films showed excellent adhesion, moderate hardness and high gloss intensity, due to the good mixing during extrusion process and crosslinking reactions during curing process. Under optical microscopy, both films showed defects, including pinholes, seeds and inadequate coverage which are caused by trace amount of contamination and the difference in surface tension.

(2) From panel visual appearance, it was found that the film electrostatically sprayed at 50 kV showed better smoothness than that sprayed at 70 kV. When electrostatic spraying at 70kV, the film formed had more pinholes which is caused by a phenomenon called back ionization. This technique is promising and can be used for the application of SOFC interconnects.

(3) The powder coating even showed great coverage at the thin edges of substrate which are perpendicular to the particle flow, as the electric field between the gun tip and workpiece guides the particles to wrap up the entire substrate. This is an unexpected benefit that is very important to future use, as it eliminates the need to spray

delicately onto the edges. A good coverage of the edges is required for the protection of the substrate in SOFC system, in this way the procedure can be greatly simplified and be much more economical.

# Chapter 7

# 7 Application of powder coating technology on SOFC interconnects

## 7.1 Introduction and objectives

This research project is funded by NSERC Engage Grant in collaboration with Stackpole International (SI). SI specializes in the manufacturer of powdered-metal (PM) components and has for many years received global recognition as a leader in the development and implementation of novel PM materials and manufacturing technologies.

The current project arises from initiatives at SI in the application and development of PM skills and manufacturing capabilities to other industries such as the “green-energy” sector. In collaboration with a leading SOFC system builder the volume manufacture of chromium-rich metallic interconnects by powder metallurgy processing has been successfully developed by SI. Consequently, the SOFC customer has requested the development of an industrial scale manufacturing method for the application of diffusion barrier coatings to the PM interconnects. The coatings for SOFC must inhibit outward diffusion of chromium and provide high electrical conductivity at the SOFC operating temperature, which is around 800 °C.

The current preferred coating is lanthanum-strontium-manganite (LSM) perovskite applied by air-plasma spray (APS) methods. APS has transfer efficiency of only around 40% and the APS equipment cost is relatively high. Therefore, there is a need to develop a more economical alternative. New research has shown that cobalt–manganese-oxide (MCO) spinel coatings meet or exceed LSM functionality and are compatible with the SOFC environment. The MCO coatings can be applied by a variety of methods, such as APS, electroplating and ultrasonic spray deposition. Subsequent further thermal processing might be necessary to achieve specific preferred microstructural condition. Each coating processes has certain advantages and disadvantages. Relative to APS, ultrasonic spray equipment is lower in cost and deposition efficiency is expected to be ~80%. However, a key disadvantage of using ultrasonic spray deposition is the need for

use of volatile organic compounds (VOC's) as a carrier. Some of the better performing VOC's such as acetone pose significant HSE (health, safety and environment) considerations. Thus, a novel economical method, such as electrostatic spray deposition, which eliminates the need for use of VOC's and can deposit MCO coatings with high transfer efficiency will have a significant practical value.

This research aims to use innovative powder coating approaches to replace the expensive air-plasma coatings on the substrate. Cold pressed powder coating and extruded powder coating are both investigated. In both methods, the VOCs (Volatile Organic Compounds) and energy consumption will be eliminated, and they can also help reduce the cost of the whole manufacture process.

## 7.2 Coating specification and evaluation

The requirements of this project is described as follows:

- Surface morphology should be inspected, including texture, cracks, holes etc., which are indication of non-uniformity and are unacceptable.
- Cross-section analysis should be performed to inspect film thickness.

Figure 7-1 shows the ideal coatings required for this project, and surface inspection locations are shown in Figure 7-2. Surface metallography of green coatings are performed at locations A, E, F, G and D. Fully processed coating thickness should be: fuel side: 25±5μm (Green~50±10 μm); edges: 15±5 μm (Green~30±10 μm). There should be no coatings on two air side seal surface, two D areas, two edges and fuel side. The coating specification is illustrated in Figure 7-3.

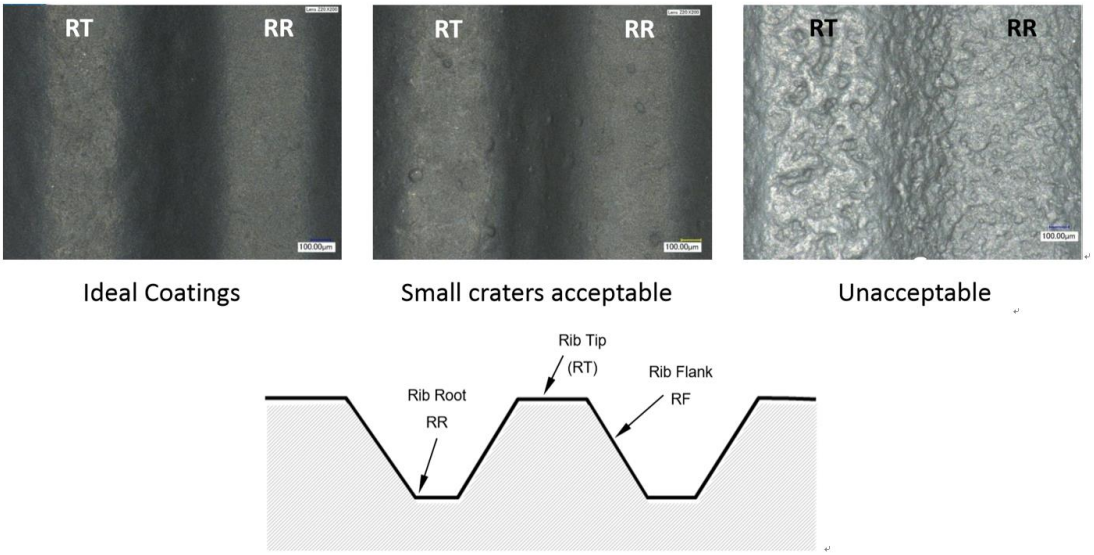


**Figure 7-1: Ideal coatings required for SOFC interconnects**

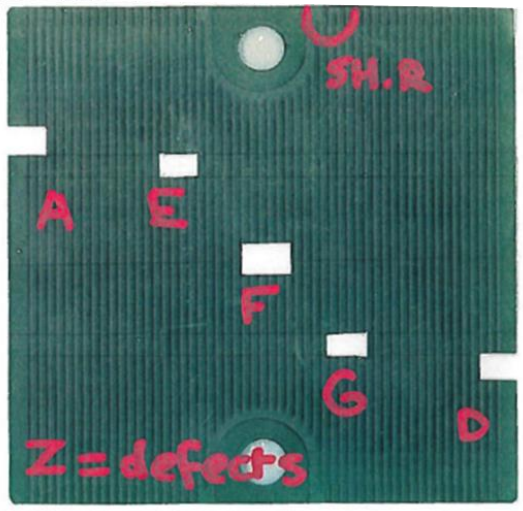


**Figure 7-2: Metallography locations**

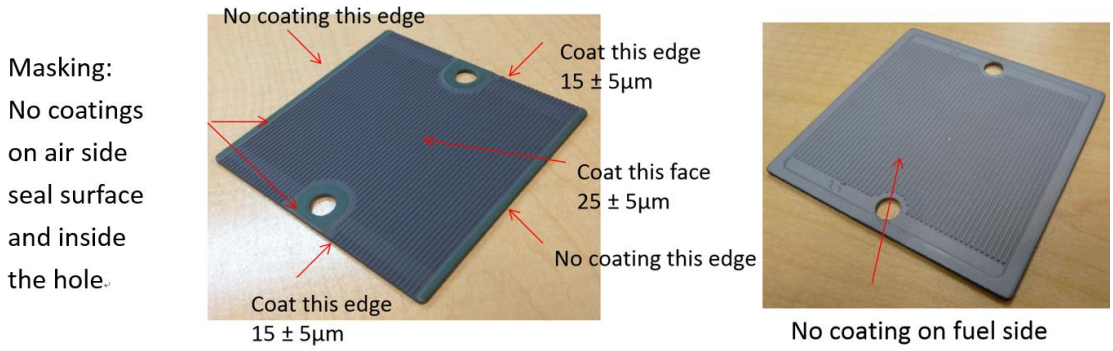


**Figure 7-3: Coating specification for SOFC interconnects**

The thickness of the coating is evaluated by scanning electron microscopy (SEM). The coated substrate is cut off and divided into 5 parts. 5 metallographic sections are taken at locations A, B, C, D, E (as shown in Figure 7-4), and cross-section analysis of coatings is performed along the red line. It should be noticed that front edge has one short rib near D area, which is not present at back edge.

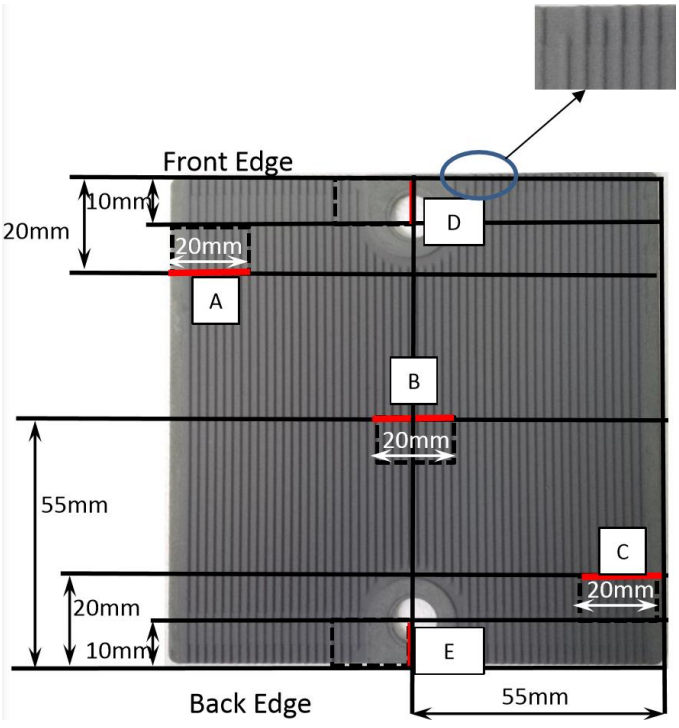


**Figure 7-4: Five sections of coating thickness evaluation**

## 7.3 Cold pressed powder coating

### 7.3.1 Formula and process

MCO-2 powder and polyester/TGIC-2 were at a mass ratio of 1:1, as shown in Table 7-1. The process is illustrated in Figure 4.2. The MCO-2 powder and polyester/TGIC-2 were blended and ground by a roll mill. After roll milling for 48 hours, the mean particle size of the mixture ($D_{50}$) was 5.33 μm. The slurry was air dried for 48 hours, compressed and pulverized to a powder of $D_{50}$=8.91 μm, $D_{10}$=2.2 μm, $D_{90}$=22.17 μm. Dry electrostatic spray under the conditions of 70 kV voltage and 30 μA charging current, which were the same with that of extruded power coating method. The produced powder coating was sprayed onto SOFC interconnect and was cured at 190 °C for 15 minutes in a convection oven.

**Table 7-1: Formula of cold pressed powder coating for SOFC interconnects**

| Materials | Mass ratio |
|---|---|
| MCO-2 | 1 |
| polyester/TGIC-2 | 1 |
| D.I. Water | 1 |

### 7.3.2 Results and discussion

The coated SOFC interconnect is shown in Figure 7-5. It was difficult to see the RT and RR on the coated side. The surface morphology was also examined, as shown in Figure 7-6. RR part of the SOFC interconnect was flooded and the grooves could not be observed. This phenomenon is attributed to too much air in the powder, which means that the powder is too loose, so the powder cannot form a continuous and compact film while curing. When being heated, the resins in the powder melt and merge together to form a film. But if there is too much air in the powder, the distance between resin particles is increased; as a result, resin particles cannot coalesce together or form a continuous and compact film.

**Figure 7-5: Visible appearance of SOFC interconnect by cold pressed powder coating**

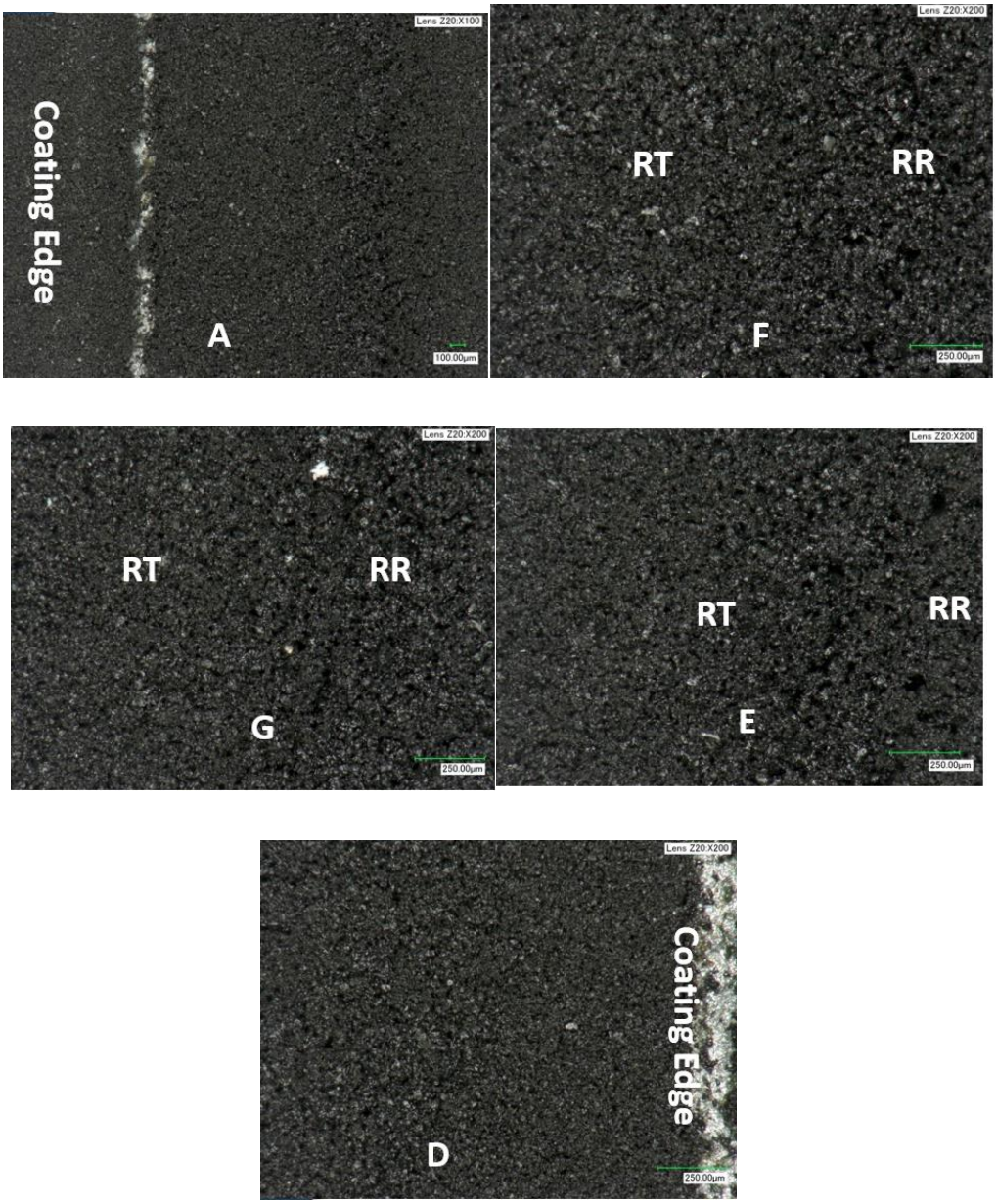


**Figure 7-6: Surface morphology at five locations**

The cross-section and EDS analysis were also conducted, as demonstrated in Figure 7-7. EDS mapping showed that the MCO powders were encapsulated in the resin and were large in size. The coating was mainly composed of resins, and MCO particles were dispersed. It may result in significant change in coating morphology after thermal treatment. Metallographs at location A, C, D and E looked similar and are included in appendix. Overall, this method requires significant optimization applied to SOFC interconnects.

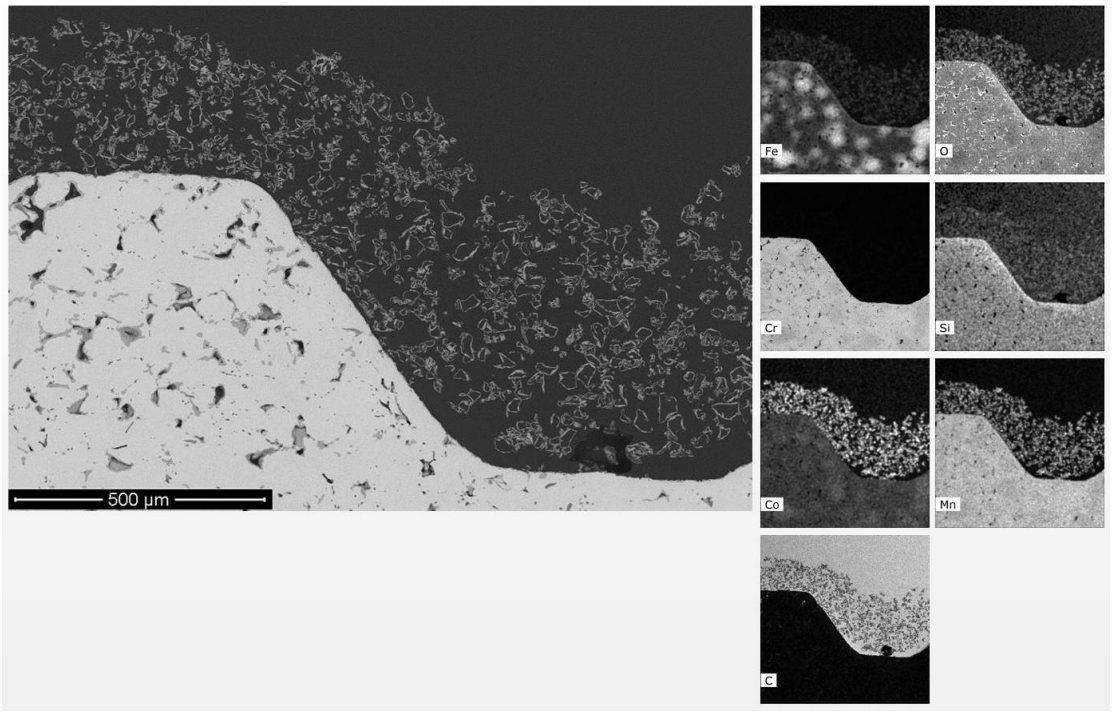


**Figure 7-7: Cross-section analysis at location B and EDS mapping**

## 7.4 Extruded powder coating

### 7.4.1 Formula and process

Based on the successful formula and process for coating aluminum panels by the method of extruded powder coating, this method was further applied in coating SOFC interconnects supplied by Stackpole International (SI). The formula is shown in Table 7-2. The properties of polyester/TGIC-2 is described in Table 4-1.

**Table 7-2: Formula of extruded powder coating for SOFC interconnects**

| Materials | Mass ratio |
|---|---|
| MCO-2 | 1 |
| polyester/TGIC-2 | 1 |

The process is demonstrated in Figure 7-8. MCO-2 powder and polyester/TFIC-2 resin were blended by a high shear mixer and then went through the extruder, forming chips. After extrusion, the chips were pulverized by a high shear grinder and were sieved by a 45 µm vibratory sieve. The mean particle size of the sieved powder was measured as 33 µm. The produced powder coating was then manually dry electrostatically sprayed at

25 °C, relative humidity 50% at 50 kV, with a 30 µA charging current. The powder output was set to be 60% and the total air volume was 6.0 $Nm^3/h$. After spraying, the SOFC interconnects were cured at 190 °C for 15 minutes in a convection oven.

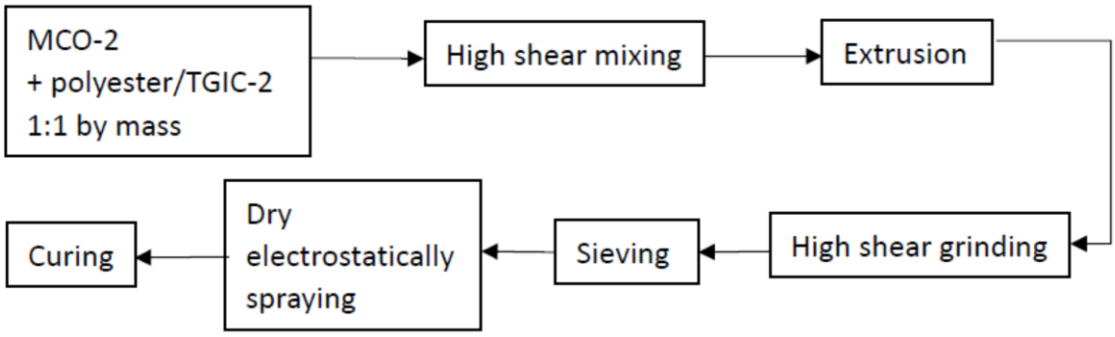


**Figure 7-8: Block diagram of extruded powder coating process**

## 7.4.2 Results and discussion

(1) Surface morphology

The coated SOFC interconnect is shown in Figure 7-9. It is obvious that RR was clearly visible and there were almost no coatings on the fuel side in comparison with cold pressed powder coating.

**Figure 7-9: Visible appearance of SOFC interconnect by extruded powder coating**

As shown in Figure 7-2, surface microscopic observation was performed at locations A, E, F, G and D. The surface morphology of extruded powder coating are shown in Figure 7-10. The film showed a good uniformity, but there were still some craters and holes. The RR parts of the SOFC interconnect were covered well and uniformly. However, the coating edges showed some defects, like section A and section D. When performing electrostatic spray, a current flow developed between the spry gun and the substrate. The current flow pulled the charged particles from the nozzle of the gun and carried them along to the substrate. The particles traveled directly to the area of the substrate which was closest to the gun, leading to less coating deposition in more complex areas and shapes, such as recesses and right angle bends etc. As a result, the coatings at the edges showed poor quality.

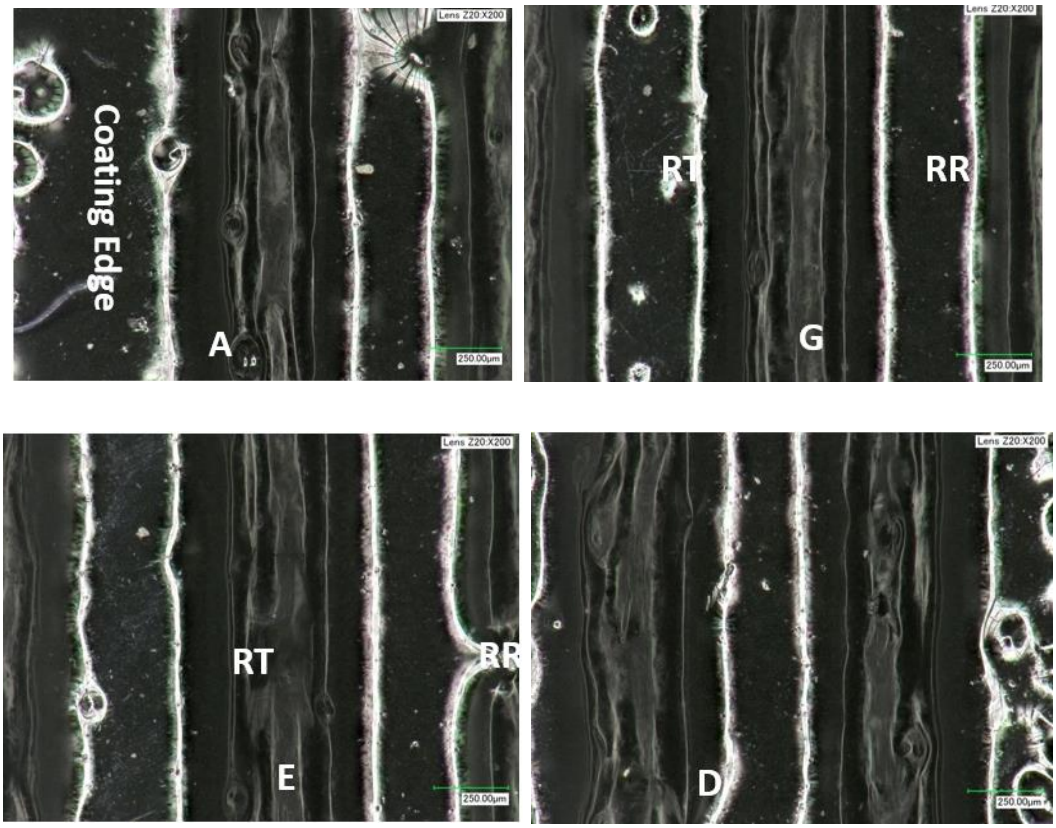


**Figure 7-10: Surface microscopy of SOFC interconnect by extruded powder coating**

(2) Cross-section analysis

Coating cross-section evaluation of extruded powder coatings was performed at locations A, B, C, D and E (as shown in Figure 7-4). The results are shown in Figure 7-11. From this figure, it can be observed that a few resins as black spots were visible inside the coatings, and at location B, the formation of the dark area at RT is due to the richness of resin. Some bigger black spots could also be observed at location C. Location D and Location E were at the edge of the SOFC interconnect and it shows that edge coatings were not continuous. The inferior quality of edge coatings may be due to the "Faraday Cage" effect. The particles are drawn to the outermost points of the substrate, leading to uneven coating.

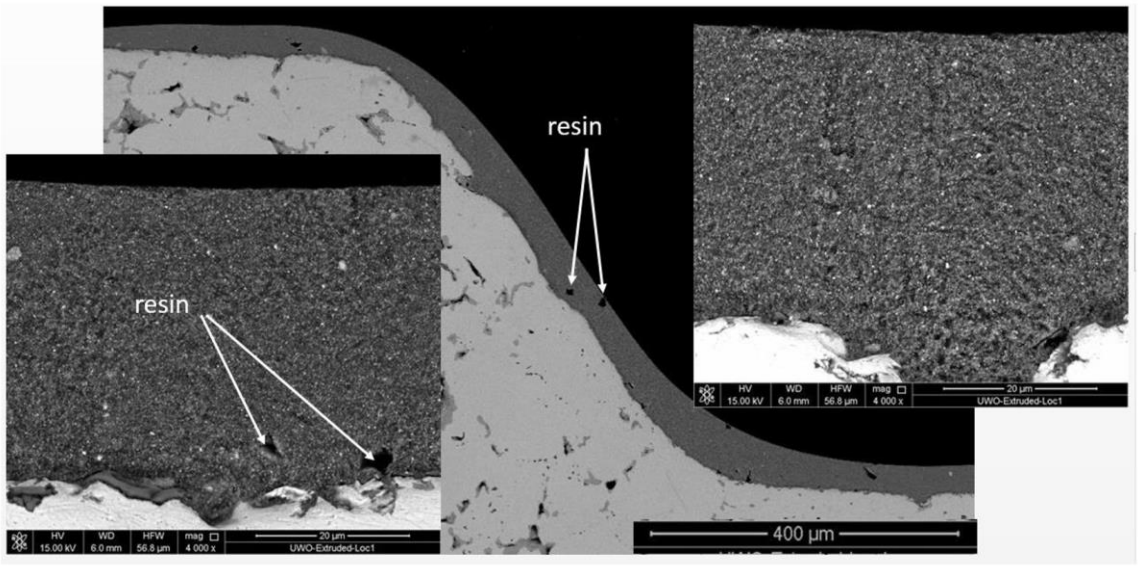


Location A

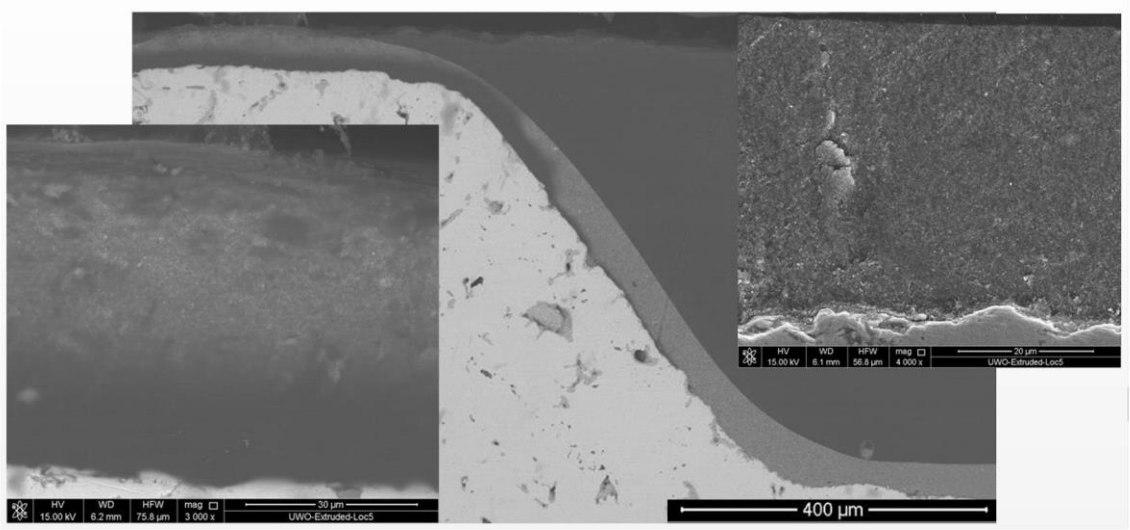


Location B

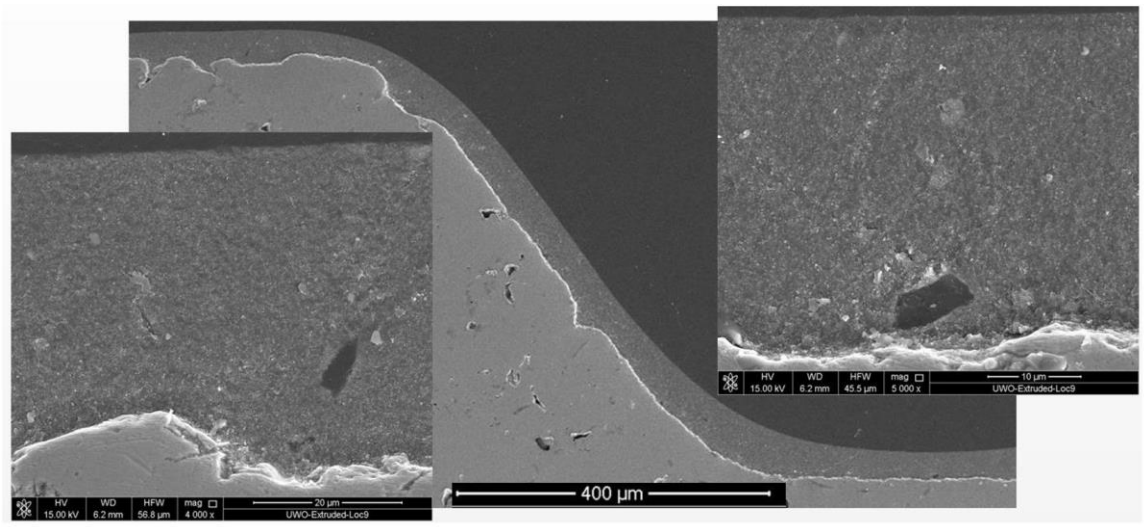


Location C

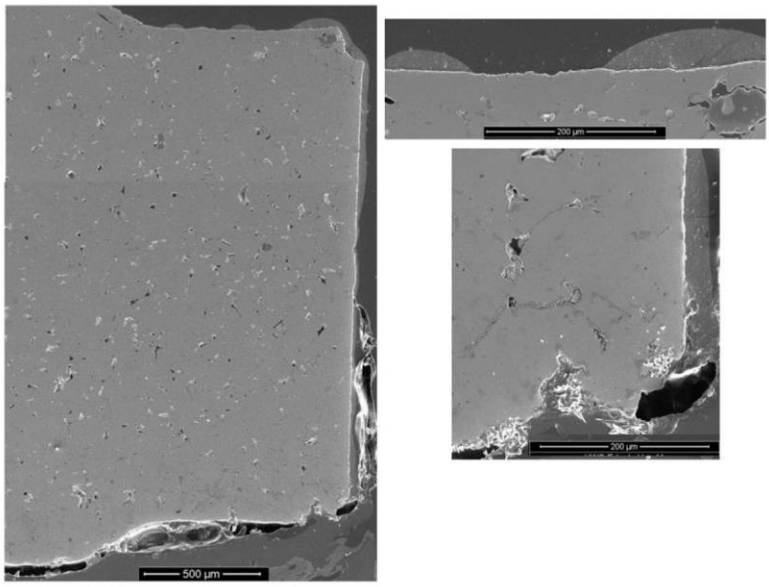


Location D

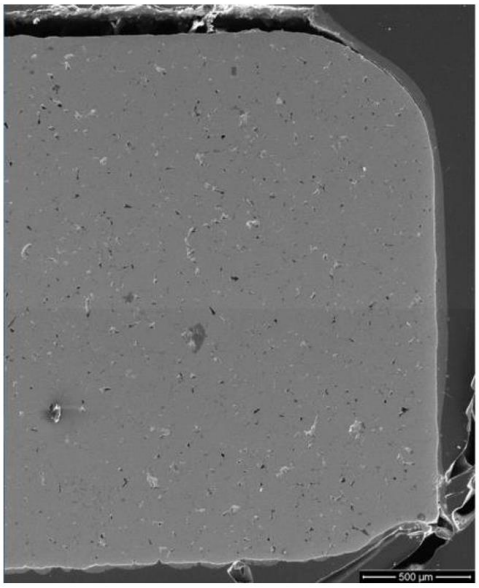


Location E

**Figure 7-11: Cross-section analysis at five locations**

The film thickness at each location is described in Table 7-3. The green coating thickness is fairly uniform. The difference in film thickness of three parts RT, RR and Flank is acceptable. The edges of location A and location D show relatively lower film thickness, which also demonstrate the Faraday Cage effect.

**Table 7-3: Film thicknesses at five locations**

| Location | | RT | RR | Flank |
|---|---|---|---|---|
| A | Edge (µm) | 20±4 | 53±4 | 60±5 |
| | Near Edge (µm) | 37.4±3 | 31.5±3.4 | 46.3±4.4 |
| B | | 48±4 | 45±2 | 48±6 |
| C | Edge (µm) | 50±2 | 39±5 | 45±6 |
| | Near Edge (µm) | 36±6 | 45±2 | 43±2 |
| D | | 29±3 | | |
| E | | 45±6 | | |

(3) Energy dispersive spectroscopy analysis

From the cross-section analysis, some dark spots inside the coatings were observed. Furthermore, energy dispersive spectroscopy (EDS) was conducted to analyze these dark spots. The results are shown in Figure 7-12. Three different parts A, B and C are shown in the images. Table 7-4 illustrates seven atomic percentages of the three parts. Figure 7-

13 exhibits EDS mapping of the substrate. EDS analysis showed dark rectangular spot (B) was predominantly composed of carbon-containing-resin. The gray spot (A) was mainly made of MCO-2 powder as the contents of oxygen, manganese and cobalt were the highest in it among the three parts, while part C which was the continuous film contained both resin and MCO-2 powder. It can be concluded from EDS mapping that carbon is predominantly present in the coating, which means that resin is the main component of the coating.

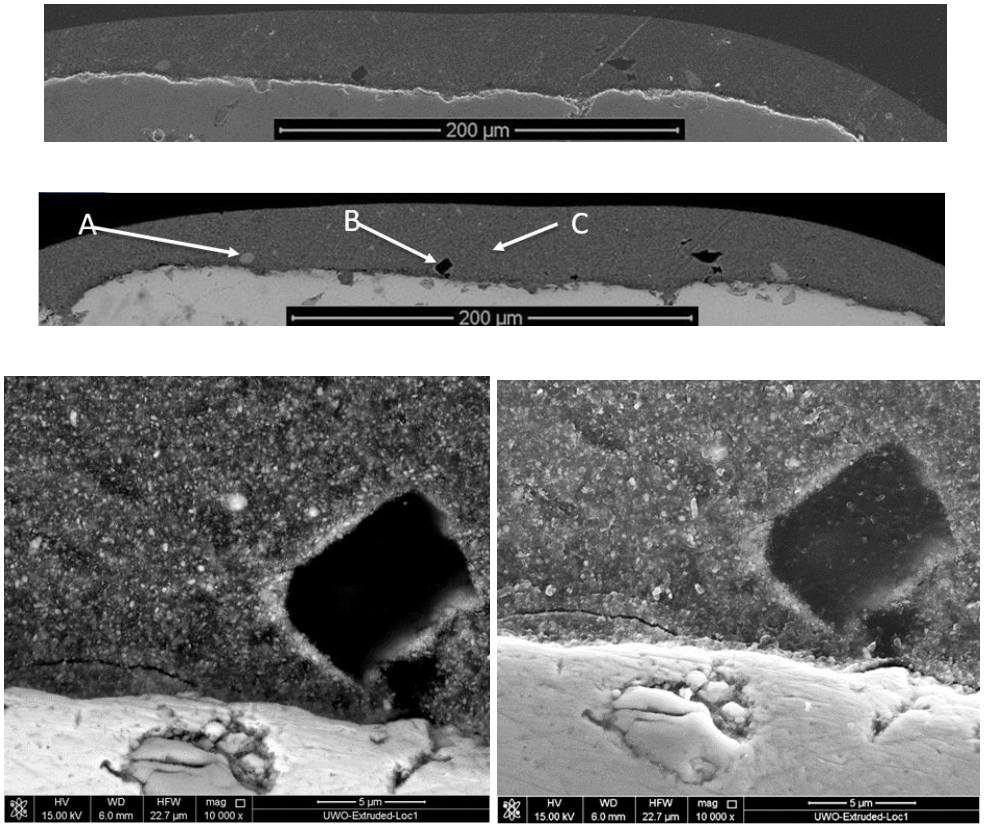


**Figure 7-12: EDS images**

**Table 7-4: Atomic percentages of A, B and C**

| Location | Atomic (%) | | | | | | |
|---|---|---|---|---|---|---|---|
| | C | O | Si | Cr | Mn | Fe | Co |
| A | 22.8 | 40.4 | 0.2 | 1.6 | 17.5 | 0.3 | 17.3 |
| B | 77.0 | 6.5 | 0.1 | 0.8 | 7.6 | 0.1 | 7.9 |
| C | 42.8 | 23.4 | 0.2 | 0.7 | 16.9 | 0.2 | 16.0 |

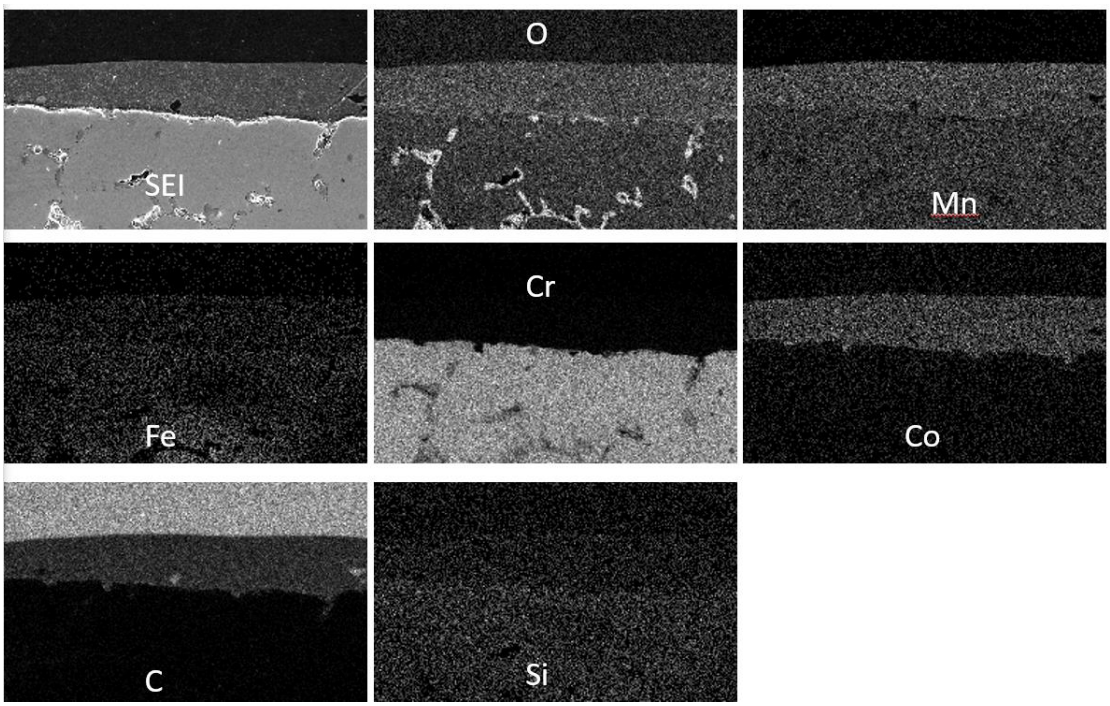


**Figure 7-13: EDS mapping**

(4) Resin burn-off

The SOFC interconnects was cut to two parts and one part was heated to 500ºC at 5 °C/min and kept for 1 hour then cooled to ambient at 5 °C/min. There was a significant change in coatings morphology after the thermal treatment (as shown in Figure 7-14). After sintering the polymer was burned off, resulting in the inadequate coverage of the substrate. It is due to the fact that too much resin (pigment/binder ratio is 1 by mass) used leads to increased porosity after firing. Moreover, some of the resin structure appear to be large in size. So the extruded powder coating method needs to be optimized for SOFC application.


**Figure 7-14: SOFC interconnect before (right) and after (left) sintering**

## 7.5 Conclusions

Two techniques including cold pressed powder coating and extruded powder coating were applied to SOFC interconnects. The conclusions are as follows:

(1) The SOFC interconnect by cold pressed powder coating was difficult to observe the RT and RR on the coated side. RR was almost flooded so its texture could not be observed. EDS mapping showed the MCO powders were encapsulated in the resin and were large in size. The film was not compacted and not continuous which requires significant optimization.

(2) The SOFC interconnects coated by extruded powder coating showed better quality. Cross-section analysis and EDS analysis were conducted for the film deposited by extruded powder coating. It was found that thickness of the green coating was fairly uniform, which is a key advantage of this technique. However, the coating at the edge was not continuous and a few resins as black spots were visible inside the coating. EDS analysis exhibited that dark spot was predominantly composed of polymer. Significant change in coating morphology was observed post-thermal treatment,

which is not favorable. These problems are mainly due to too much resin used in the formula (resin: MCO=1:1 by mass ratio), which leads to large size of resins appeared in the coating and increased porosity after firing. Extruded powder coating is promising but needs to be optimized for SOFC application.

# Chapter 8

# 8 Conclusions and recommendations

## 8.1 General conclusions

For SOFC interconnects, the current preferred coating is $Mn_{1.5}Co_{1.5}O_4$ spinel (MCO) applied by air-plasma spray (APS) method, which has transfer efficiency of only around 40% and the equipment cost is relatively high. Therefore, there is a need to develop a more economical alternative. Powder coating is a promising technology which has a potential to apply to SOFC interconnects, and it brings along many advantages including negligible emission, simple process and low cost.

This thesis focuses on an invention of new powder coating formulation and its preparation as SOFC interconnect coating. Based on different preparation methods, four coating techniques namely slurry powder coating, thermally compacted powder coating, cold pressed powder coating and extruded powder coating are studied. In addition, the optimization of the formulation has been accomplished to get a satisfactory coating film.

### 8.1.1 Slurry powder coating technique

An initial formula containing polyester/TGIC-2 resin and MCO powder mixed by 1:1 mass ratio was proposed. It was found that the quality of the coating was not desirable, with respect to film smoothness and substrate coverage. Severe cracking of the coatings on aluminum panels was observed, possibly due to too high pigment/binder ratio and poor dispersion of MCO powder in resins. A typical surfactant of which dosages were 0.05%, 0.1%, 0.5% and 1% was adopted to improve the wetting property and dispersion of MCO particles. The results showed that the surfactant had almost no effect on improving film quality.

A lower pigment/binder ratio (MCO: polyester/TGIC=1:2 by mass) was employed to investigate its effect on film quality. Although the pigment/binder ratio was significantly decreased, the same sever cracking was still observed, which might be mainly due to the surface tension, residual tension and melt viscosity. The difference of thermal expansion

coefficient between the film and the substrate resulted in film cracking. In addition, an appropriate surface tension and melt viscosity can create good levelling properties.

The effect of polyvinyl alcohol (PVA) on film forming was also studied. For the formula with MCO powder, polyester/TGIC and PVA mixed by mass ratio of 6:12:1, there was an improvement on film forming, although the film cracking phenomenon still existed. For the formula with MCO powder, polyester/TGIC and PVA mixed by mass ratio of 6:6:1, the cracking phenomenon disappeared, and the panel's visual appearance was much better than before, mainly attributing to the function of PVA, which has excellent film-forming property. However, the adhesion and hardness of the film were not very good, so further optimization of the formulation is necessary.

### 8.1.2 Thermally compacted and cold pressed powder coating techniques

For thermally compacted powder coating, a formula of D.E.R.$^{TM}$ 661 solid epoxy resin and MCO powder with 0.8 μm diameter ($D_{50}$) at mass ratio of 1:1 was proposed. The film obtained was fairly poor and had severe defects of non-uniformity, mainly due to too much air trapped in the powder, which resulted in the large distance between resin particles. As a result, resins could not merge together to form a continuous film.

For cold pressed powder coating, pressing was introduced in the process in order to let the air inside the powder escape and to compact the powder. A typical solid polyester resin was used to replace solid epoxy resin. It was found that this formula achieved a better film quality with respect to the continuity of the film. However, there were still some defects on the film, which are attributed to the incompatibility of particle sizes between resin and MCO powder. The cohesion and hardness of the film was not good, which is due to the lack of crosslinking reaction and can be solved by adding curing agent.

An optimized formula containing MCO powder of 6 μm ($D_{50}$) and polyester/TGIC was employed for cold pressed powder coating, but there was no improvement on the film quality because of the low curing temperature and the lack of high shear pressing. Increasing the curing temperature can promote more effective crosslinking reactions, leading to further enhancement of adhesion and hardness of the film. In addition,

particles under high shear press and high temperature can form a uniform structure, which benefits film-forming process. A further optimization of this method is necessary.

### 8.1.3 Extruded powder coating technique

Extrusion is a conventional process in powder coating industry. By utilizing extrusion process, ingredients can be well mixed into a relatively homogeneous material with uniform property due to the high shear-mixing characteristic of extruder, indicating good performance of produced powder with good film-forming ability and enhanced film quality.

The effects of voltages adopted for electrostatic spraying on film quality have also been evaluated. Three different voltages of 30 kV, 50 kV and 70 kV were employed and compared, among which 30 kV voltage was too low for powder deposited on the substrate and was not effective. The films deposited at 50 kV and 70 kV exhibited excellent adhesion, moderate hardness and high gloss intensity, due to the good mixing during extrusion process and the crosslinking reactions during curing process. Under optical microscopy, both films showed defects, including pinholes, seeds and inadequate coverage, which are caused by trace amount of contamination and the difference in surface tension.

From visual appearance of panel, the film electrostatically sprayed at 50 kV showed better smoothness than that sprayed at 70 kV. When electrostatic spraying at 70 kV, the film formed had more pinholes which is caused by a phenomenon called back ionization. This technique is promising and can be used for future application of SOFC interconnects.

### 8.1.4 Application of powder coating technology on SOFC interconnects

Two techniques including cold pressed powder coating and extruded powder coating were applied on SOFC interconnects. On the SOFC interconnect by cold pressed powder coating, it was difficult to observe the RT and RR on the coated side, where RR was almost flooded. EDS mapping showed the MCO powders were encapsulated in the resin

and were large in size. The film was not compacted and not continuous, as requires significant optimization.

The SOFC interconnects coated by extruded powder coating showed better quality. Cross-section analysis and EDS analysis were conducted for the film deposited by extruded powder coating. It was found that thickness of the green coating was fairly uniform, which is a key advantage of this technique. However, the coating at the edge was not continuous and a few resins as black spots were visible inside the coating. EDS analysis showed that the dark spot was predominantly composed of polymer. Significant change in coating morphology was observed after the thermal treatment, which was not allowed for SOFC interconnect coating. These problems are mainly due to too much resin used in the formula (resin: MCO=1:1 by mass ratio), which leads to increased porosity after firing and large size of resins appeared in the coating. Extruded powder coating is promising but needs to be optimized for SOFC application.

## 8.2 Recommendations

Powder coating technology is introduced to use on SOFC interconnect coating for the first time in research. Although different powder coating techniques and formulations have been studied, only extruded powder coating technique built a film with excellent adhesion, moderate hardness, uniform thickness and good visual appearance. However, issues regarding to large size resin existing in the film and the significant change in film morphology after-thermal treatment still need to be solved. The effects of various powder coating components, namely resins, curing agents, different types of additives, parameters of spray gun such as air flowrate and pressure, voltage etc. on the film quality should be further investigated.

# References


[1] Mah, Joelle CW, et al. Metallic interconnects for solid oxide fuel cell: A review on protective coating and deposition techniques. *International Journal of Hydrogen Energy*, 2016.

[2] Xiao, Jinhua, et al. Oxidation behavior of Cu-doped MnCo2O4 spinel coating on ferritic stainless steels for solid oxide fuel cell interconnects. *International Journal of Hydrogen Energy*, 2016, 41(22): 9611-9618.

[3] Ebrahimifar H, Zandrahimi M. Oxidation and electrical behavior of a ferritic stainless steel with a Mn–Co-based coating for SOFC interconnect applications. *Oxidation of Metals*, 2015 Oct 1, 84(3-4): 329-44.

[4] Xiaofang W, Wenqiang Z, Bo Y, Xuqiang G, Jingming X. Research Progress on the Interconnect Coating Technology for the SOFC/SOEC. *Rare Metal Materials and Engineering*. 2015 Jun 1, 44(6): 1555-60.

[5] Visser, J. Van der Waals and other cohesive forces affecting powder fluidization. *Powder technology*, 1989, 58(1), 1-10.

[6] B. Lestarquit. Geometry of a paint film: Basics revisited. *Prog. Org. Coatings*, 2016 Jan, vol. 90, pp. 200–221.

[7] Nix VG, Dodge JS. Rheology of powder coatings. *Journal of Paint Technology*, 1973 Jan 1, 45(586): 59-63.

[8] Rutledge GK, Alpert J, Ebisuzaki W. NOMADS: A climate and weather model archive at the National Oceanic and Atmospheric Administration. *Bulletin of the American Meteorological Society*, 2006 Mar 1, 87(3): 327.

[9] EIA U. Annual energy review 2011. *Energy Information Administration*. 2012 Sep.

[10] Hall T, McCrabb H, Wu J, Zhang H, Liu X, Taylor EJ. Electrodeposition of CoMn onto stainless steels interconnects for increased lifetimes in SOFCs. *ECS Transactions*, 2010 Oct 15, 28(30): 197-209.

[11] Chadran PR, Arjunan TV. A review of materials used for solid oxide fuel cell. *Int. J. Chem. Tech. Res.*, 2014, 7: 488-97.

[12] Stambouli AB, Traversa E. Solid oxide fuel cells (SOFCs): a review of an environmentally clean and efficient source of energy. *Renewable and Sustainable Energy Reviews*, 2002 Oct 31, 6(5): 433-55.

[13] Data from The International Fuel Cells, a Unitedd Techology Company. *Fuel Cells Review*. 2000.

[14] Gonzalez Cuenca MM. Novel anode materials for solid oxide fuel cells. *Twente University Press*, 2002.

[15] Carlson EJ, Sriramulu S, Teagan P, Yang Y. Cost modeling of SOFC Technology. *In First International Conference on Fuel Cell Development and Deployment*, 2004 Mar 10.

[16] Zhu WZ, Deevi SC. Development of interconnect materials for solid oxide fuel cells. *Materials Science and Engineering: A*, 2003 May 15, 348(1): 227-43.

[17] Yang Z, Weil KS, Paxton DM, Stevenson JW. Selection and evaluation of heat-resistant alloys for SOFC interconnect applications. *Journal of the Electrochemical Society*, 2003 Sep 1, 150(9): A1188-201.

[18] Piccardo P, Amendola R. SOFC's interconnects materials development. *In Proc. Internat. Workshop Advances and innovations in SOFCs* 2009.

[19] Schmidt VH. Electrical properties of lanthanum cromite based ceramics in hydrogen and oxidizing atmospheres of high temperature. Rept. No. DOE/ET/15415-1, *US Department of Energy, Washington DC*, 1981.

[20] Minh NQ, Takahashi T. Science and technology of ceramic fuel cells. *Elsevier*, 1995 Aug 15.

[21] Steele BC, Drake JA. Electrochemistry and Clean Energy. *Electrochemistry and Clean Energy*, 1994.

[22] Tolochko SP, Konyuk IF, Ivashkevich LS. *Neorg. Mater.*, 1980, 20: 1892.

[23] Tolochko SP, Kononyuk IF. Production and Electrical Properties of Solid Solutions $La_{1-x}Ca_xCr_yCo_{1-y}O_3$ ($0 \leq x \leq 0,3$; $0 < y \leq 1$). *Neorg. Mater.* 1986, 22(10): 1696-700.

[24] Zhuk PP, Vecher AA, Samokhval VV, Naumovich EN, Viskup AP. Properties of lanthanum chromium doped with iron. *Izv. Akad. Nauk SSSR, Neorg. Mater.* 1988, 24(1): 105-8.

[25] Kononyuk IF, Tolochko SP, Surmach NG. Preparation and electrical properties of $La_{1-x}Ca_xCr_{1-y}Ni_yO_3$ ($0 < or = x < or = 0.3$; $0 < or = y < or = 1$). *Izvestiya Akademii Nauk SSSR, Neorg. Mater.* 1986, 22(1): 98-102.

[26] Anderson HU, Murphy R, Humphrey K, et al. *The Rare Earths in Modern Science and Technology*, 1978.

[27] Armstrong TR, Simner SP, Hardy JS, Stevenson JW. Optimizing lanthanum chromite interconnects for solid oxide fuel cells. *Pacific Northwest National Laboratory (PNNL), Richland, WA (US)*, 1999 Aug 1.

[28] Armstrong TR, Stevenson JW, Pederson LR, Raney PE. Dimensional instability of doped lanthanum chromite. *Journal of The Electrochemical Society*, 1996 Sep 1, 143(9): 2919-25.

[29] Srilomsak S, Schilling DP, Anderson HU. Proceedings of the First International Symposium on Solid Oxide Fuel Cells. *USA: The Electrochemical Society*, 1989: 16-8.

[30] Yokokawa H, Sakai N, Kawada T, Dokiya M. Chemical thermodynamic considerations in sintering of $LaCrO_3$-based perovskites. *Journal of the Electrochemical Society*, 1991 Apr 1, 138(4): 1018-27.

[31] Samsonovin, GV. The Oxide Handbook, Plenum Press. *In: Turton, C.N., Turton, T.I. (Eds.)*, 1973, p.125.

[32] Urbanek, J, Miller, M, Schmidt, H et al. *In: Proceedings of Fourth European Solid Oxide Fuel Cell Forum. Lucerne, Switzerland*, 2000, 2: 503.

[33] Dulieu, D, Cotton, J, Greiner, H. *ln: Proceedings of Third European Solid Oxide Fuel Cell Forum. Nantes, France*, 1998, p.447.

[34] Zhu WZ, Deevi SC. A review on the status of anode materials for solid oxide fuel cells. *Materials Science and Engineering: A*, 2003 Dec 5, 362(1): 228-39.

[35] Fergus JW. Metallic interconnects for solid oxide fuel cells. *Materials Science and Engineering: A*, 2005 Apr 25, 397(1): 271-83.

[36] Jeffrey W.Fergus, Metallic interconnects for solid oxide fuel cells. *Mater. Sci. Eng.:A*, 2005, 397(1): 271–283.

[37] Zhenguo Yang, John S. Hardy, Matt S. Walker, Guanguang Xia, Steven P. Simner, Jeffry W. Stevenson. Structure and conductivity of thermally grown scales on ferritic Fe–Cr–Mn steel for SOFC interconnect applications. *J. Electrochem. Soc.*, 2004, 151 (11): A1825–A1831.

[38] Jong-Jin Choi, Jungho Ryu, Byung-Dong Hahn, Woon-Ha Yoon, Byoung-Kuk Lee, Dong-Soo Park. Dense spinel $MnCo_2O_4$ film coating by aerosol deposition on ferritic steel alloy for protection of chromic evaporation and low-conductivity scale formation. *J. Mater. Sci.*, 2009, 44(3): 843–848.

[39] Y. Liu. Performance evaluation of several commercial alloys in a reducing environment. *J. Power Sources*, 2008, 179(1): 286–291.

[40] Jong-Hee Kim ,Rak-Hyun Song, Sang-Hoon Hyun. Effect of slurry coated $LaSrMnO_3$ on the electrical property of Fe–Cr alloy for metallic interconnect of SOFC. *Solid State Ion.*, 2004, 174(1): 185–191.

[41] Junwei Wu, Chengming Li, Christopher Johnson, Xingbo Liu. Evaluation of SmCo and SmCoN magnetron sputtering coatings for SOFC interconnect applications. *J. Power Sources*, 2008, 175(2): 833–840.

[42] Weifeng Wei, Weixing Chen, G. Ivey Douglas. Oxidation resistance and electrical properties of anodically electrodeposited Mn–Co oxide coatings for solid oxide fuel cell interconnect applications. *J. Power Sources*, 2009, 186 (2): 428–434.

[43] Chunwen Sun, Rob Hui, Roller. Athode materials for solid oxide fuel cells: a review. *J. Solid State Electrochem.*, 2009, 14(7): 1125–1144.

[44] Balland A, Gannon P, Deibert M, Chevalier S, Caboche G, Fontana S. Investigation of $La_2O_3$ and/or $(Co,Mn)_3O_4$ deposits on Crofer22APU for the SOFC interconnect application. *Surface and Coatings Technology*, 2009 Jul 15, 203(20): 3291-6.

[45] Yang Z, Xia GG, Li XH, Stevenson JW. $(Mn,Co)_3O_4$ spinel coatings on ferritic stainless steels for SOFC interconnect applications. *International Journal of Hydrogen Energy*, 2007 Nov 30, 32(16): 3648-54.

[46] Changjing F, Kening S, Naiqing Z, Derui Z. Effects of protective coating prepared by atmospheric plasma spraying on planar SOFC interconnect. *Rare Metal Materials and Engineering*, 2006 Jul 1, 35(7): 1117.

[47] Konysheva E, Laatsch J, Wessel E, Tietz F, Christiansen N, Singheiser L, Hilpert K. Influence of different perovskite interlayers on the electrical conductivity between $La_{0.65}Sr_{0.3}MnO_3$ and Fe/Cr-based steels. *Solid State Ionics*, 2006 Mar 31, 177(9): 923-30.

[48] Pattarkine GV, Dasgupta N, Virkar AV. Oxygen transport resistant and electrically conductive perovskite coatings for solid oxide fuel cell interconnects. *Journal of The Electrochemical Society*, 2008 Oct 1, 155(10): B1036-46.

[49] Kunschert G, Schlichtherle S, Strauss GN, Kailer K. Ceramic PVD coatings as dense/thin barrier layers on interconnect components for SOFC applications. *ECS Transactions*, 2007 May 25, 7(1): 2407-16.

[50] Mikkelsen L, Chen M, Hendriksen PV, Persson Å, Pryds N, Rodrigo K. Deposition of $La_{0.8}Sr_{0.2}Cr_{0.97}V_{0.03}O_3$ and $MnCr_2O_4$ thin films on ferritic alloy for solid oxide fuel cell application. *Surface and Coatings Technology*, 2007 Dec 15, 202(4): 1262-6.

[51] Hui Zhang, Zhaolin Zhan, Xingbo Liu. Electrophoretic deposition of $(Mn,Co)_3O_4$ spinel coating for solid oxide fuel cell interconnects. *J. Power Sources*, 2011, 196(19): 8041–8047.

[52] Zhenguo Yang, Guan-Guang Xia, Xiao-Hong Li, Jeffry W.Stevenson, $(Mn,Co)_3O_4$ spinel coatings on ferritic stainless steels for SOFC interconnect applications. *Int. J. Hydrog. Energy*, 2007, 32 (16): 3648–3654.

[53] Petric A, Ling H. Electrical conductivity and thermal expansion of spinels at elevated temperatures. *Journal of the American Ceramic Society*, 2007 May 1, 90(5): 1515-20.

[54] Kiefer, T, et al. *Proceedings of the 26th Risø International Symposium on Materials Science: Solid State Electrochemistry*, 2005, pp. 261-266.

[55] Choi JP, Weil KS, Chou YM, Stevenson JW, Yang ZG. Development of MnCoO coating with new aluminizing process for planar SOFC stacks. *International Journal of Hydrogen Energy*, 2011 Apr 30, 36(7): 4549-56.

[56] Chen X, Hou PY, Jacobson CP, Visco SJ, De Jonghe LC. Protective coating on stainless steel interconnect for SOFCs: oxidation kinetics and electrical properties. *Solid State Ionics*, 2005 Feb 14, 176(5): 425-33.

[57] Yang Z, Xia GG, Li XH, Stevenson JW. $(Mn,Co)_3O_4$ spinel coatings on ferritic stainless steels for SOFC interconnect applications. *International Journal of Hydrogen Energy*, 2007 Nov 30, 32(16): 3648-54.

[58] Mirzaei M, Simchi A, Faghihi-Sani MA, Yazdanyar A. Electrophoretic deposition and sintering of a nanostructured manganese–cobalt spinel coating for solid oxide fuel cell interconnects. *Ceramics International*, 2016 May 1, 42(6): 6648-56.

[59] Laxmidhar Besra, Meilin Liu. A review on fundamentals and applications of electrophoretic deposition (EPD). *Prog. Mater. Sci.*, 2007, 52 (1):1–61.

[60] M. Zarabian, A.Yazdan Yar,S. Vafaeenezhad, M. A. FaghihiSani, A. Simchi., Electrophoretic deposition of functionally-graded NiO–YSZ composite films. *J. Eur. Ceram. Soc.*, 2013, 33(10): 1815–1823.

[61] Yanjie Xu, Zhaoyin Wen, Shaorong Wang, Tinglian Wen. Cu doped Mn–Co spinel protective coating on ferritic stainless steels for SOFC interconnect applications. *Solid State Ion.*, 2011, 192 (1): 561–564.

[62] Andre LG, Prette, Marco Cologna, Vincenzo Sglavo, Rishi Raj. Flash sintering of $Co_2MnO_4$ spinel for solid oxide fuel cell applications. *J. Power Sources*, 2011, 196(4): 2061–2065.

[63] Yuchao Fang, Chaoling Wu, Xiaobo Duan, Shaorong Wang, Yungui Chen. High-temperature oxidation process analysis of $MnCo_2O_4$ coating on Fe-Cr alloy. *Int. J. Hydrog. Energy*, 2011, 36(9): 5611–5616.

[64] Piccardo P, Gannon P, Chevalier S, Viviani M, Barbucci A, Caboche G, Amendola R, Fontana S. ASR evaluation of different kinds of coatings on a ferritic stainless steel as SOFC interconnects. *Surface and Coatings Technology*, 2007 Dec 15, 202(4): 1221-5.

[65] Chevalier S, Bonnet G, Larpin JP. Metal-organic chemical vapor deposition of $Cr_2O_3$ and $Nd_2O_3$ coatings: oxide growth kinetics and characterization. *Applied Surface Science*, 2000 Oct 23, 167(3): 125-33.

[66] Houngninou C, Chevalier S, Larpin JP. Synthesis and characterization of pack cemented aluminide coatings on metals. *Applied Surface Science*, 2004 Sep 15, 236(1): 256-69.

[67] Bertrand GL, Caboche G, Dufour LC. Low-pressure-MOCVD LaMnO $3\pm\delta$ very thin films on YSZ (100) optimized for studies of the triple phase boundary. *Solid State Ionics*, 2000 Apr 30, 129(1): 219-35.

[68] Cabouro G, Caboche G, Chevalier S, Piccardo P. Opportunity of metallic interconnects for ITSOFC: Reactivity and electrical property. *Journal of Power Sources*, 2006 May 19, 156(1): 39-44.

[69] Piccardo P, Chevalier S, Molins R, Viviani M, Caboche G, Barbucci A, Sennour M, Amendola R. Metallic interconnects for SOFC: Characterization of their corrosion resistance in hydrogen/water atmosphere and at the operating temperatures of differently coated metallic alloys. *Surface and Coatings Technology*, 2006 Dec 20, 201(7): 4471-5.

[70] Fontana S, Amendola R, Chevalier S, Piccardo P, Caboche G, Viviani M, Molins R, Sennour M. Metallic interconnects for SOFC: Characterisation of corrosion resistance and conductivity evaluation at operating temperature of differently coated alloys. *Journal of Power Sources*, 2007 Sep 27, 171(2): 652-62.

[71] Chu CL, Lee J, Lee TH, Cheng YN. Oxidation behavior of metallic interconnect coated with La–Sr–Mn film by screen painting and plasma sputtering. *International Journal of Hydrogen Energy*, 2009 Jan 31, 34(1): 422-34.

[72] Lim DP, Lim DS, Oh JS, Lyo IW. Influence of post-treatments on the contact resistance of plasma-sprayed $La_{0.8}Sr_{0.2}Mn_{O3}$ coating on SOFC metallic interconnector. *Surface and Coatings Technology*, 2005 Nov 2, 200(5): 1248-51.

[73] Nie HW, Wen TL, Tu HY. Protection coatings for planar solid oxide fuel cell interconnect prepared by plasma spraying. *Materials Research Bulletin*, 2003 Sep 2, 38(9): 1531-6.

[74] Qu W, Jian L, Hill JM, Ivey DG. Electrical and microstructural characterization of spinel phases as potential coatings for SOFC metallic interconnects. *Journal of Power Sources*, 2006 Jan 23, 153(1): 114-24.

[75] Vargas MJ, Zahid M, Tietz F, Aslanides A. Use of SOFC metallic interconnect coated with spinel protective layers using the APS technology. *ECS Transactions*, 2007 May 25, 7(1): 2399-405.

[76] Han SJ, Pala Z, Sampath S. Plasma sprayed manganese–cobalt spinel coatings: Process sensitivity on phase, electrical and protective performance. *Journal of Power Sources*, 2016 Feb 1, 304: 234-43.

[77] Liuyin X. Preparation and formulation of powder coating for application of enamelled wire, 2013. Master thesis, University of Western Ontario.

[78] Jing F. Study on powder coating particles and development of new powder coating application methods, 2010. Master thesis, University of Western Ontario.

[79] Harold C, Beachell, PF, Janet H. A study of the oxidative degradation of polyvinyl formal. *Journal of Polymer Science*, 1951, 7(4); 353-376.

[80] Richart D. Powder Coating Process, in: Kirk-Othmer Encyclopedia of Chemical Technology, *John Wiley & Sons*, 2001, published online, 7: 35-68.

[81] Bocchi, GJ. Join with PCI to improve powder coating community, *Products Finishing*, 2006, 70(6): 73-74.

[82] Spyrou E. Powder Coatings: Chemistry and Technology. *Vincentz Network*, 2012.

[83] Misev TA. Powder Coating: Chemistry and Technology, *John Wiley & Sons*, New York, 1991.

[84] Mleziva, J, Hanzlik, V, Kinel, J, Miklas, Z. Poliesteri, Tehnika, Sofia, 1969, p.90.

[85] Eastman Kodak Co., EP 0.070.118 , 1981.

[86] Meng X, Zhang H, Zhu J. Characterization of particle size evolution of the deposited layer during electrostatic powder coating processes. *Powder Technology*, 2009, 195(3): 264-70.

[87] Schellenberger S, Entenmann M, Hennemann A, Thometzek P. TECHNIK-Effektpigmente-Schmelzvorgang unter der Lupe. *Farbe und Lack*. 2007, 113(4): 130-5.

[88] Dullaert K, Steeman P, Bolks J. A mechanistic study of the effect of pigment loading on the appearance of powder coatings: The effect of surface topography on the optical properties of powder coatings: Modelling and experimental results. *Progress in Organic Coatings*, 2011 Apr 30, 70(4): 205-12.

[89] Miller E. Users Guide to Powder Coatings, p.35, *Society of Manufacturing Engineers*, Dearborn Michigan, 1985.

[90] Hughes, JF. In Electrostatic Powder Coating, *Research Studies Press Ltd.*, Letchworth, Hertfordshire, 1984, p.1

[91] Hughes JF, Athwal CS, Coventry PF. Implications of ion-wind and back-ionisation on precipitator performance. *In Electrostatics' 83*. Conference Series No. 66. 1983 (pp. 167-72). Institute of Physics.

[92] Sing S, Bright AW. *IEEE/IAS Conf. Proc*., 1977, 29G, p. 729.

[93] Sing S, Bright AW. *IEEE/IAS Conf. Proc*., 1978, 3F, p. 105.

[94] Sing S, Hughes JF, Bright AW. *Inst. Phys. Conf. Ser*., 1979, No. 48, p. 17.

[95] Mayr MB, Barringer SA. Corona compared with triboelectric charging for electrostatic powder coating. *J. Food Sci. (JFS) E: Food Eng. Phys. Prop*, 2006, 71:171-177.

[96] Kleber W, Makin B. Trboelectric powder coating: a practicle approach for industrial use. *Particul. Sci. Technol*, 1998, 16: 43-53.

[97] Trigwell S, Biris AS, Sims RA, Mazumder MK. Effects of powder velocity and contact materials on tribocharging of polymer powders for powder coating applications. *Particul. Sci. Technol*, 2008, 26: 145-157.

[98] M. L. Maniar, D. S. Kalonia, and A. P. Simonelli. Determination of specific rate constants of specific oligomers during polyester hydrolysis. *J. Pharm. Sci.*, 1991, vol. 80, no. 8, pp. 778–782.

[99] ASTM standard D5767, Standard Test Method for Distinctness of Image.

[100] ASTM standard D523, Standard Test Method for Specular Gloss.

[101] ASTM standard E430, Standard Test Method for Haze.

[102] ASTM standard D3359-09e2, Standard Test Method for measuring adhesion by tape test.

[103] ASTM standard D3363-92a, Standard Test Method for measuring hardness by pencil hardness tester.

[104] Du Z, Wen S, Wang J, Yin C, Yu D, Luo J. The Review of Powder Coatings. *Journal of Materials Science and Chemical Engineering*, 2016 Mar 9, 4(03): 54..

[105] Prasad LK, McGinity JW, Williams RO. Electrostatic powder coating: Principles and pharmaceutical applications. *International journal of pharmaceutics*, 2016 May 30, 505(1): 289-302.

[106] Orchard SE. The flow of paint coatings: a hydrodynamic analysis. *Progress in organic coatings*, 1994 May 1, 23(4): 341-50.

[107] Walz, G, and Kraft, K. *Proceedings of 41$^{th}$ International Conference on Organic Coatings Science and Technology*, Athens, 1978, p.56.

[108] Zhifeng Z, Kun Q. Effects of the molecular structure of polyvinyl alcohol on the adhesion to fibre substrates. *Fibres & textiles in Eastern Europe*, 2007, 1 (60): 82-5.

[109] Liberto NP. Users Guide to Powder Coating, 4th Edition. *Society of Manufacturing Engineers*, 2003.

[110] Jing F. Characterization of fine powders and development of processes for powder coatings, 2013. Ph.D. thesis, University of Western Ontario.

[111] Bocchi GJ. Join with PCI to improve powder coating community. *Products Finishing*, 2006, 70(6): 73-74.

[112] Bruno Fawer. Cure dynamics of powder coating, retrieved from powdercc.com/images/pdf/Cure%20Dynamics.pdf.

[113] Allexandria Va. Powder coating-The complete finisher's handbook. Chapter 12.

[114] Charlie, M. Continuous Mixing of Solid Dosage Forms via Hot-Melt Extrusion. *Pharmaceutical Technology*, 2008, 32(10): 76-86.

[115] Particle Sciences, Hot Melt Extrusion, Technical Brief, 2011, 3.

# Appendices

## Appendix I: ASTM D3359-09, Standard Test Methods for Measuring Adhesion by Tape Test

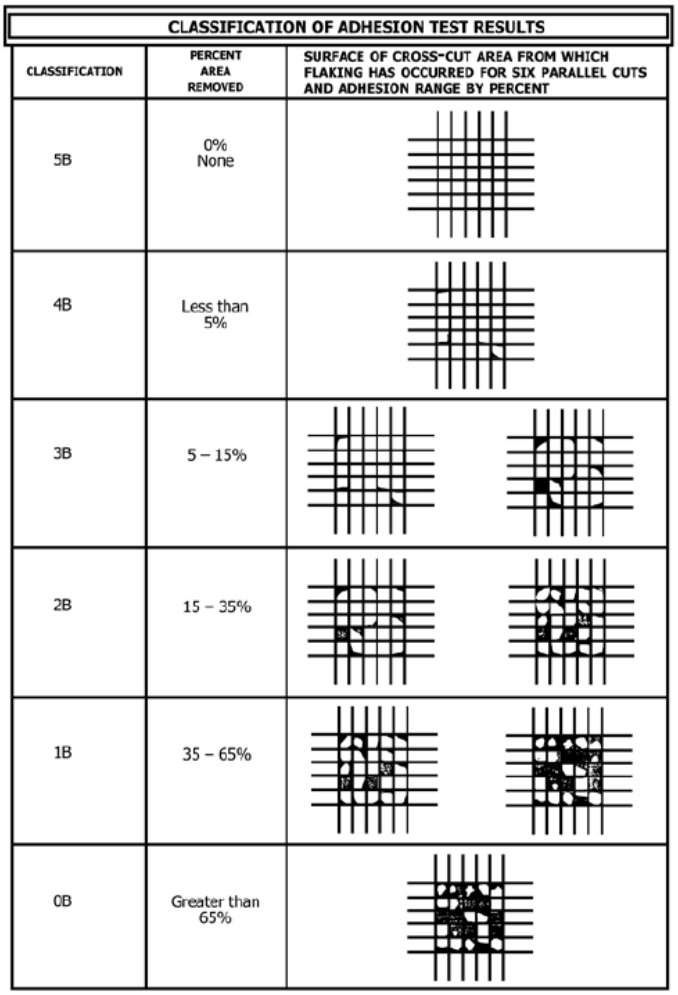

| CLASSIFICATION OF ADHESION TEST RESULTS | | |
|---|---|---|
| CLASSIFICATION | PERCENT AREA REMOVED | SURFACE OF CROSS-CUT AREA FROM WHICH FLAKING HAS OCCURRED FOR SIX PARALLEL CUTS AND ADHESION RANGE BY PERCENT |
| 5B | 0% None | |
| 4B | Less than 5% | |
| 3B | 5 – 15% | |
| 2B | 15 – 35% | |
| 1B | 35 – 65% | |
| 0B | Greater than 65% | |

**Figure A-1: Classification of adhesion test results according to ASTM D3359**

**Appendix II: ASTM D3363-92, Standard Test Methods for Measuring Hardness by Pencil Test**

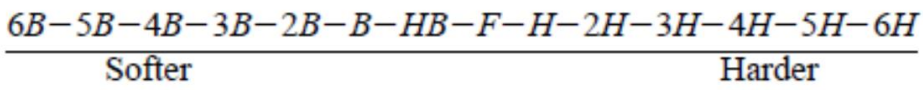


**Figure A-2: Classification of hardness test results according to ASTM D3363**

**Appendix III: Cross-section analysis for SOFC interconnect by cold pressed powder coating**

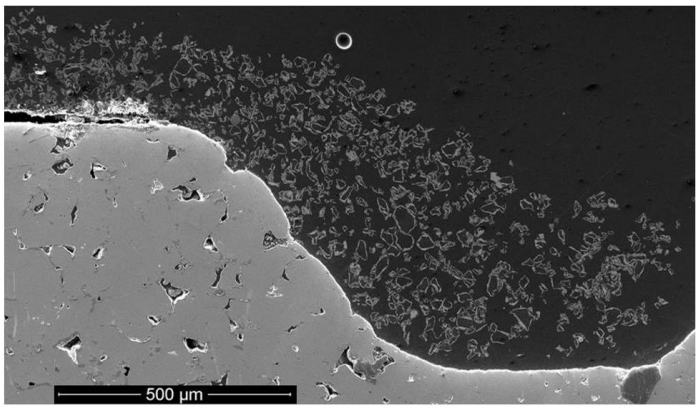


**Location A**

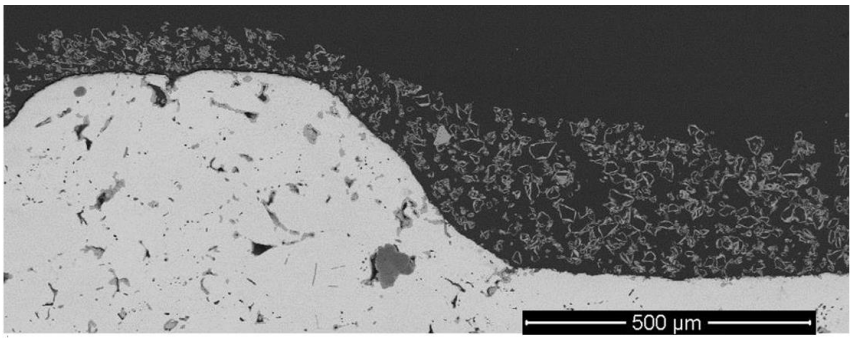


**Location C**

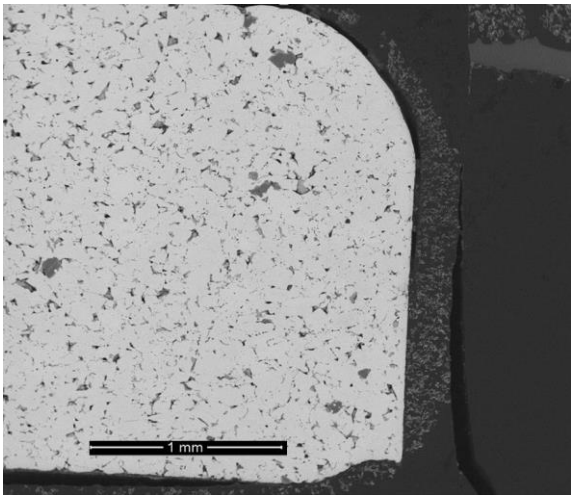


**Location D**

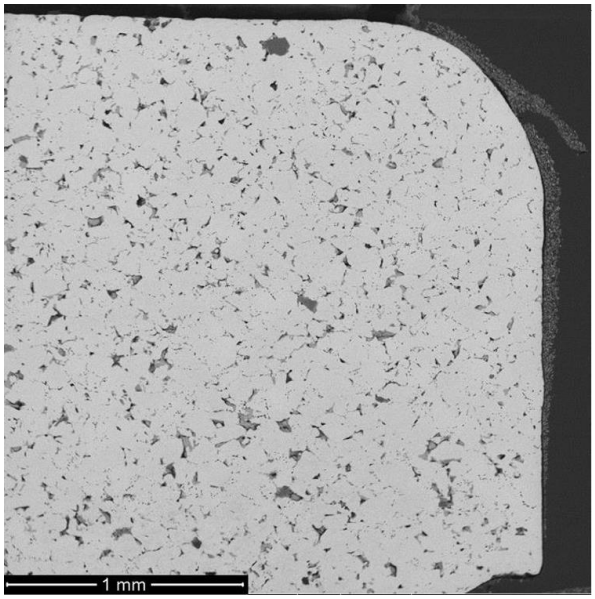


**Location E**

**Figure A-3: Cross-section analysis at location A, C, D and E**

# Curriculum Vitae

## Profile

**Name:** Yandazi Zhou

**Gender:** Female

**Date of Birth:** August 14, 1991

## Education and Qualification

**Master of Engineering Science** 05.2015-08.2016 University of Western Ontario
Formulation and process of powder coating for solid oxide fuel cell interconnects

**Master of Engineering** (Chemical Engineering) 09.2013-06.2016 China University of Petroleum
Fundamental study on fluidization behavior of fine and ultrafine powder

**Bachelor of Engineering** (Chemical Engineering) 09.2009-06.2013 China University of Petroleum
Research on fluid thermal conversion reaction of liaohe vacuum residue

## Awards and Honors

“First-Class Graduate Student Scholarship” in 2014

“Excellent Bachelor Thesis” in 2013

“First-Class Scholarship” in 2010, 2011, 2013

“Technological Innovation Excellent Student” in 2010